TECHNICAL NOTE R-136

TECHNICAL NOTE R-136

AD 613047

A COMPARATIVE ANALYSIS OF THE PERFORMANCE CAPABILITIES OF VARIOUS TYPES OF ELECTROSTATIC PROPULSION ENGINES

by Dr. A. Lucile Cox

COPY 2 OF 3
HARD COPY $. 4.00
MICROFICHE $. 0.75
108p

February 1965

DDC
RECEIVED
APR 6 1965
DDC-IRA A

RESEARCH LABORATORIES
BROWN ENGINEERING COMPANY, INC.
HUNTSVILLE, ALABAMA

ARCHIVE COPY

TECHNICAL NOTE R-136

A COMPARATIVE ANALYSIS OF THE PERFORMANCE CAPABILITIES OF VARIOUS TYPES OF ELECTROSTATIC PROPULSION ENGINES

By

Dr. A. Lucile Cox

February, 1965

RESEARCH LABORATORIES
BROWN ENGINEERING COMPANY, INC.

ABSTRACT

The operating characteristics of three types of atomic ion engines and three types of colloidal ion engines are evaluated. The major theoretical factors which will limit payload capacity are brought out for each type of engine. Total propulsion system masses for the production of ten pounds of thrust for 2, 000 hours and for 10, 000 hours of engine operation are compared. Examination of the payload capacities of the various engines for several lunar and planetary missions shows that the colloidal ion engines have a superior payload capacity for lunar missions and may be competitive with atomic ion engines for planetary missions. The specific mass of the power supply system is shown to be a much more dominant factor in determining the payload capacities of the atomic ion engines than for the colloidal ion engines.

Approved

Raymond C. Watson, Jr.
Raymond C. Watson, Jr.
Director of Research

BLANK PAGE

TABLE OF CONTENTS

TABLE OF CONTENTS (Continued)

LIST OF FIGURES

LIST OF FIGURES (Continued)

LIST OF TABLES

LIST OF SYMBOLS

A_b	Cross-sectional area of ion beam, cm^2
A_e	Cross-sectional area of engine, cm^2
A_{fs}	Cross-sectional area of the feed system manifold, cm^2
a	Fraction of propellant mass to represent tankage mass
B	Intercept in breakdown equation
d	Electrode gap distance, cm
d_{cs}	Breakdown limited electrode gap distance for a cesium coated electrode, m
d_m	Breakdown limited electrode gap distance, m
F	Thrust, lb-f
G	Ratio of thrust to initial vehicle mass, earth gravity units
g	Acceleration due to gravity, cm/sec^2
I	Current, amp
I_s	Specific impulse, sec
j	Current density, amp/cm^2
M_e	Mass of engine, lb
M_f	Mass of propellant, lb
M_{fs}	Mass of feed system, lb
M_i	Total initial vehicle mass, lb
M_p	Mass of power supply system, lb
M_{pay}	Payload mass, lb

LIST OF SYMBOLS (Continued)

M_{tot}	Total propulsion system mass, lb
$M_{tot_{10}}$	Total propulsion system mass for a 10 lb-f level, lb
$\left(\frac{M_f}{F}\right)_{10000}$	Propellant mass per pound of thrust for 10,000 hr operation, lb/lb-f-10,000 hr
P_b	Beam power, watts
P_e	Electric power from power supply system, kwe
P_{in}	Total power required by the engine, watts
$P_{e\,10}$	Total electric power required for a 10 lb-f level, kwe
q/m	Particle charge-to-mass ratio, coul/kg
s	Slope in breakdown equation
t	Engine operating time, hr
t_{fs}	Thickness of feed system structural material, cm
u	Exhaust velocity, cm/sec
V	Voltage, v
V_{net}	Net accelerating voltage (=V in simple accel engines, =0.25 V in 4:1 accel-decel engines), v
x	Average energy required to produce one utilized ion, ev
y	Fractional power loss due to poor beam collimation
z	Fractional power loss in electrical atomization colloidal ion engine due to variation of the particle charge-to-mass ratios and ion losses without appreciable acceleration

LIST OF SYMBOLS (Continued)

Greek Symbols

β	Ratio of surface electric field to applied voltage
ϵ_o	Permittivity of empty space
η	Power efficiency
η_f	Propellant efficiency
ϕ	Surface work function, ev
Δv	Velocity increment which a vehicle must achieve, cm/sec

BLANK PAGE

INTRODUCTION

Recent analytical treatments of electric thrustor systems have indicated that the weights of the power supply systems may severely limit the payload capabilities of the electric thrustors[1,2]. The weight of the power supply system is a major factor in missions conducted with the thrustor operating at a high specific impulse. For lunar missions at specific impulse values less than 4000 sec, however, the effect of the weight of the power supply system is less significant. Such missions are seldom examined for electrostatic thrustors because of the increased engine weights and low power efficiencies of the particular electrostatic engines which have been most intensively studied. The colloidal ion engines, which should theoretically have low engine weights and perform efficiently at specific impulse values less than 4000 sec, have not been accorded sufficient study to make their characteristics definite. It nevertheless is important to have in mind the probable capabilities of these engines, particularly the possibility of large payload ratios for lunar freighter missions even with power supply system specific weights as high as 40 lb/kwe. In addition, it should be pointed out that colloidal ion engines may be capable of performing missions at high specific impulse values with almost the same payload capacity as the atomic ion engines. The colloidal ion engine, therefore, may be capable of serving as a generally applicable thrustor for lunar and planetary missions.

The present analysis is concerned only with electrostatic propulsion systems. The characteristics of the more promising types of electrostatic engines are examined on the basis of limitations inherent in the engine concepts and on such experimental data as are available. The effects of these characteristics on the weights of the components of the thrustor systems is then examined. Finally, the performance capabilities of thrustor systems employing the various engines are estimated. Since the propellant particles in the colloidal ion thrustors can theoretically be produced with

a specific particle charge-to-mass ratio, over a rather wide range, the effect of particle charge-to-mass ratio on system weight and performance is examined.

Although the results of this study are necessarily tentative, the trends should be valid. Earlier attempts at a comparative analysis of the various electrostatic propulsion concepts were, of course, even more vague and lacking in detail[3-5]. This examination of the different types of electrostatic propulsion engines should indicate more clearly the most promising areas for research in electrostatic propulsion and the most serious basic defects of the various concepts.

TYPES OF ELECTROSTATIC PROPULSION ENGINES

The two general types of electrostatic propulsion engines considered in this study are the atomic ion engines (propellant ion mass < 300 amu) and the colloidal ion engines (propellant ion mass > 1000 amu). Molecular ion engines (propellant ion mass ≈ 300-1000 amu) have not been examined in detail since it appears that molecules suff' iently heavy for propulsion would undergo considerable fragmentation as a result of the heat, radiation or electrom bombardment employed in vaporizing and ionizing the propellant.

Performance parameters were calculated, however, for each of the colloidal ion engine concepts at the charge-to-mass ratio of 10^5 coul/kg (equivalent to 1000 amu/electronic charge). It is doubtful that such propellant particles can be efficiently and reliably produced by any of the colloidal ion concepts, but the inclusion of these particles helps indicate the trends produced by various factors.

As much effort has been devoted to the development of the atomic ion engines, their capabilities and characteristics can be rather well delineated and are not likely to change appreciably with further development unless some new atomic ion engine concept is evolved. The major improvements in these engines will be in increasing their reliability and lifetime.

Although the hardware designs of the colloidal ion engines are not necessarily more complex than those of the atomic ion engines, the processes and conditions which must be established for their successful operation are generally complex and interdependent. For this reason, and also because comparatively little effort has been devoted to these engines, considerable improvement in performance may result from further research and development of the colloidal ion engines. There are, however, some basic theoretical limitations inherent in some of the colloidal ion engine concepts. Furthermore, because of the lack of effort on the colloidal ion engine concepts, some of the processes involved in their operation have not

been studied experimentally in detail and are simply assumed to operate as desired. Thus, it is possible that some of these engines will not even approximate the estimated performance until much more effort has been accorded to their development.

Atomic Ion Engines

The two basic types of atomic ion engines, based on the method of ionization employed, are the surface contact engine and the bombardment engine. In the surface contact engine, cesium is superior to all other substances as the propellant material primarily because of its low ionization potential. Although the bombardment engine has been studied with various elements as the propellant material, the mercury ion shows certain performance advantages because of its relatively low charge-to-mass ratio ($Hg^+ = 5 \times 10^5$ coul/kg compared with $Cs^+ = 7.5 \times 10^5$ coul/kg). Although inferior to mercury on the basis of the performance capabilities of the propellant ions, cesium may show a lower power consumption for ionization when used as the propellant in a bombardment ion engine. This factor would be of more importance in missions requiring a low specific impulse since more ions must be produced for operation at a given thrust level. On the other hand, the mercury ion, being heavier, provides more thrust per ion, so fewer ions are required for a given thrust level if the propellant material is mercury rather than cesium. Thus, the effect of the choice of propellant material in the bombardment engine tends to be cancelled. In the following comparative analysis, cesium is the propellant material employed in the surface contact engines and mercury is the propellant for the bombardment ion engines.

The design of the engine, particularly as regards beam focussing, can affect the engine performance capabilities. Further improvement of this factor, however, will probably be more important in extending electrode lifetime than in increasing the payload capacity of a thrustor system. To indicate the magnitudes of performance improvement which might be achieved

by better electrode designs, a cesium surface contact ion engine with the ion emitter in a sastrugi geometry was included as a separate engine. It was assumed that this design factor affects the thrustor component weights by making it possible to reduce the engine area relative to the beam area in comparison with the button or slit type of engine geometries. Although the effect of this improved geometry appears small, it may significantly improve the payload capability of the atomic ion engine in the specific impule range around 3000 sec. In this regime, the weight of the engine and feed system of the atomic ion thrustors becomes comparable with the weights of the propellant and the power supply system, thereby enabling the engine geometry to affect the payload capacity appreciably.

Simple accelerators and accel-decel accelerators with a 4:1 accel-decel ratio were represented for all engine types. Generally, atomic ion engines with accel-decel accelerators show better performance than with simple accelerators, whereas the reverse is true for the colloidal ion engines. Higher accel-decel ratios were not considered because of the increasing defocussing effect of such geometries.

Condensation Colloidal Ion Engines

The condensation colloidal ion source must produce a condensable vapor and condense it into fine particles. The particles must become charged either by condensation on an ion or by a charging process after particle formation. In this type of colloidal ion source, the conditions of temperature and pressure must be carefully controlled throughout the condensation process to achieve particle growth to uniform sizes.

In most types of ion engines, the vapor will be produced by boiling the propellant material using the waste heat from the power supply system. The propellant vapor for one type of condensation colloidal ion engine, however, could be produced by means of a chemical reaction, such as a combustion reaction, which generates sufficient heat to release the reaction

product as a vapor. The need for propellant efficiency makes it necessary to consider only reactions which produce a single stable product, and excess gas or vapor used as a reactant must be carefully limited. If the reaction produces much heat, as in the case of combustion, some ions will form in the reaction products and serve as nuclei for the condensation process, directly producing charged colloidal particles.

One basic difficulty in the condensation colloidal ion sources is the need for elimination of the heat of condensation from the growing particles. This cooling can be accomplished by excess propellant vapor or another gas, but this coolant should be at a relatively low temperature to be effective. The excess heat released by combination chemical processes which form stable products (heat of formation), would hinder condensation and result in much uncondensed propellant material.

Condensation colloidal ion sources usually employ expansion through nozzles to produce the supersaturated vapor needed for condensation to colloidal particles. To take care of the excess heat produced in a reaction, a high expansion area ratio could be employed. This approach, however, is not likely to greatly increase the proportion of material condensing because of the lessening density of the vapor, which reduces the collision rate of the molecules. It can be shown[6] that most of the condensation (about 25% condensed) in a supersaturated vapor expanding under equilibrium conditions occurs before the area ratio of the expansion reaches 2:1 for mass flow rates about as high as could be utilized for propulsion. At an area ratio of 5:1, approximately 33% of the vapor could condense under equilibrium conditions, and a 10:1 area ratio would permit only about 36% of the material to condense. The higher temperature resulting from a reaction would render propellant efficiency too low to be useful for propulsion purposes and would make it difficult to achieve uniform growth. The reaction type of condensation colloidal ion source has, therefore, not been examined in this study.

As was pointed out, a vapor with no excess heat, saturated at the throat and expanding through a nozzle could achieve only about 37% condensation. Since the flow density in a condensation colloidal ion engine with a single propellant material is dependent upon the required particle charge-to-mass ratio, under space charge limitations, the propellant efficiency of such engines decreases as the charge-to-mass ratio increases. To avoid low propellant efficiency, a coolant gas of low molecular weight, such as hydrogen, could be mixed with the condensable vapor. This technique provides for practically complete condensation of the condensable substance and the uncondensed molecules constitute only a small percentage (5%-10%) of the total weight of the propellant material.

Two basic types of condensation colloidal ion sources have been examined parametrically in this study. The differences in the two devices stem mainly from the nucleation and ionization processes. In the ionic nucleation method, ions are produced in the vapor before it passes the throat of the nozzle. This technique lowers ion efficiency since it allows appreciable recombination and ion losses at the walls. However, only a low degree of ionization is required in the colloidal ion source, so the power efficiency of the engine should be better than can be achieved with atomic ion engines. In addition, the power efficiency increases as the net accelerating voltage is increased. Since the colloidal ion engine can, in contrast to atomic ion engines, operate at high voltages ($\geqq$ 10 kv) in a specific impulse range favorable for missions to the moon and nearer planets, this type engine should facilitate the development of efficient, light weight propulsion systems.

The presence of ions at the onset of the vapor expansion provides a means of controlling the flow and particle growth processes. These ions serve as nuclei for the condensation; therefore, particle growth can start very close to the throat and equilibrum conditions should be approached throughout the expansion. This should favor uniformity of particle growth. In addition, the ions can be slowed preferentially with respect to the uncharged

vapor by means of electrostatic fields. Slowing of the charged particles allows them to experience a sufficient number of sticking and cooling collisions to achieve the required growth within a short distance from the throat (≈ 1 cm). This factor keeps the engine weight low and maintains good beam collimation. In this region of the device, the beam contains electrons as well as the positively charged colloidal ions, so space charge forces are not a problem.

As a result of kinetic energy exchanges, the flow leaving the nozzle should consist of a highly directed inner core of the heavy particles with the light gas partially randomized. The collimation of the colloidal ion beam would be destroyed if the flow were permitted to undergo a shock. By use of the skimmer nozzle technique[7], however, most of the randomized gas can be removed from the central flow and only very minor shocks will occur in the residual gas present in the central beam. A small potential difference between the nozzle and the skimmer is employed to remove the electrons from the flow and present to the accelerator a well-collimated beam of colloidal ions with only a very low residual gas density. The small positive potential (relative to the nozzle) applied to the skimmer serves to ensure power efficiency in the accelerator by rejecting those particles with high charge-to-mass ratios, which can greatly reduce the power efficiency of colloidal ion thrustors[8]. Particles with too high a charge-to-mass ratio would have too little momentum to pass this potential barrier. This factor, together with the control of particle charge-to-mass ratio provided by the field near the throat of the nozzle, should enable the ionic nucleation colloidal ion source to produce any desired particle charge-to-mass ratio with very little distribution of the charge-to-mass ratio.

To avoid the formation of uncharged colloids, which would reduce propellant efficiency, the condensable propellant material should be incapable of undergoing neutral nucleation. Mercury or cadmium are reasonably easy to vaporize and have such large surface tensions that neutral nucleation should not be appreciable under the required operating conditions.

The details of the design and operation of an ionic nucleation condensation colloidal ion engine with a mixed propellant of cadmium and hydrogen are being presented in a separate report. The analysis in that report, together with data obtained from experiments[6, 9] with this type of engine, using mercury alone as the propellant material, provide the basis for the values employed in the calculations for the present evaluation. The experimental studies have shown the ability of this concept to produce particles with charge-to-mass ratios ranging from 5×10^2 coul/kg to 1.25×10^4 coul/kg. In some experiments, space charge limited currents of particles with charge-to-mass ratios between 7×10^3 coul/kg and 10^4 coul/kg were indicated, and the effects of the potentials applied to control the charge-to-mass ratios were demonstrated. With a 20 kv accelerator, a small engine produced 0.18 millipounds thrust.

The neutral nucleation condensation colloidal ion source employs propellant materials which can readily undergo neutral nucleation. Condensation and growth then take place rapidly in a shock region in the expanding flow. The resultant colloidal particles are ionized, usually by means of a corona, electrons are trapped and the colloidal ions are accelerated[10-12]. In the past experiments, the colloidal ions were negatively charged. This fact may present a problem in neutralization in an actual engine.

Because of the shock, the entire flow will be considerably randomized. The particle beam will not be well collimated and the uncondensed material cannot be efffectively removed from the colloidal ions. This gas will tend to promote breakdown in the accelerator. The published experimental results indicate difficulties in producing a sufficiently dense beam of particles suitable for propulsion, presumably because the nucleation rate is too slow under flow conditions which could produce particles with charge-to-mass ratios greater than 100 coul/kg. The propellant material employed in these experiments was mercurous chloride, and it is expected that other materials could partially alleviate this problem. The use of an admixture of hydrogen to increase the propellant efficiency might

have an adverse effect on the rate of nucleation and growth. Therefore, the evaluation of this type of engine was based on the utilization of mercurous chloride alone as the propellant material but with the assumption that higher nucleation rates and higher charge-to-mass ratios will result from further effort.

Electrical Atomization Colloidal Ion Engines

Although the operation of an electrical atomization colloidal ion source is comparatively simple, the details of the mechanism involved seem to be rather complex. Basically, a high field is employed to overcome the forces holding a liquid together, and colloidal fragments of the liquid are ejected in a charged condition from the main body of the liquid. These droplets generally are multicharged, in contrast to the propellant particles produced in the condensation colloidal ion sources. Because of this multicharged condition, the particle charge-to-mass ratios cannot exceed some value, dependent on the properties of the propellant material, or the particle will be unstable and undergo further change. Thus, the properties of the propellant material, the electrode designs and the field must be carefully planned and controlled to achieve stable operation of the source. This type of source appears to be capable of operating in several distinct modes[13]. A high voltage mode produces particles with very high charge-to-mass ratios, including dimer and trimer ions. Another mode produces particles with charge-to-mass ratios of about 200 coul/kg to 700 coul/kg. Unless particle charge-to-mass ratios of 10^3 - 10^4 coul/kg can be produced in a stable mode, the heavier particles will need a second acceleration stage for most propulsion applications. However, attempts at further acceleration may produce changes in charge-to-mass ratios of the multicharged particles.

In its simplest form, the electrical atomization colloidal ion source consists of a hollow needle with an extracting electrode nearby. The needle should have a very fine point to enhance the field. A large number of these

needles are needed to produce a sufficient current of particles for propulsion purposes, and certain spatial limitations must be observed in arrays of needles to avoid degradation of the field at the needle tip. Other design approaches have been examined for use with the electrical atomization principal, but their complexity would probably reduce the reliability of the device and increase the engine weight.

Although a variety of propellant materials, including metals, organic compounds and inorganic compounds, have been studied in the electrical atomization source, most of the recent work has utilized glycerol. To obtain good performance with glycerol, it is necessary to increase its conductivity by adding a salt soluble in glycerol. Although the past experiments have provided currents less than 10^{-5} amp per needle, further study with other propellant materials is expected to increase the current obtained from each needle. The present evaluation assumes a propellant material with the properties of glycerol but a higher overall current density than can now be obtained with an array of needles. It is also assumed that the device can be developed to operate stably and produce particles of any specified charge-to-mass ratio from 2×10^2 coul/kg to 10^4 coul/kg. Evaluations for particles with 10^5 coul/kg are included.

Powder Dispersal Colloidal Ion Engines

The dispersal and charging of powders to produce a colloidal ion propellant has been considered in some detail by various workers during the past seven years. This concept involves the interdependent problems of particle deagglomeration and charging. An analysis, supported by experimental investigations, indicated that the power required to deagglomerate and charge powders by electron bombardment would be prohibitively high for the charge-to-mass ratio range of interest[14]. It was thought that fine carbon powders might be able to achieve usable charge-to-mass ratios by charge absorption because their porous nature presents

a high ratio of surface area to mass. Experiments with this method, however, have not been encouraging[15]. Therefore, no powder dispersal colloidal ion engines have been considered in the present evaluation.

ENGINE CHARACTERISTICS

Breakdown Limitations

More experimental information is needed to understand and evaluate the breakdown limitations for the various types of electrostatic engines. Such studies, however, may still be premature for colloidal ion engines since their operating conditions have not been firmly defined. A recent experimental study indicates that the conditions of engine operation may have considerable effect on breakdown[16]. In the surface contact engines, a partial coating of cesium on the electrodes reduces the field which can be tolerated in a vacuum, because the cesium lowers the work function of the electrode surface.

The Fowler-Nordheim concept of field emission seems to provide a good representation of the effects leading to breakdown. Employing this relation, but including the effect of surface work function as delineated by Strayer, et. al., leads to the following equation:

$$I = B\ V^2 \exp\left(-2.3\ s\ \frac{10^4}{V}\right) \tag{1}$$

where

- I - current in amps,
- B - intercept $\approx 5 \times 10^{-7}$,
- V - voltage in volts,
- s - slope $= -\ 2.96 \times 10^3\ \phi^{3/2} \times \frac{0.951}{\beta}$,
- ϕ - surface work function, and
- β - ratio of surface electric field to applied voltage.

For a pure tungsten surface and assuming that the field can be represented as $\frac{V}{d}$, the above relation gives the following equation:

$$\log^{*} I = -\ 6.301 + 2 \log V + 2.7 \times 10^8 \frac{d_m}{V} \tag{2}$$

* log represents log to the base 10.

where

d_m - the gap distance in meters,

V - voltage in volts, and

I - current in amps.

Assuming that a current of 1.6×10^{-19} amp is sufficient to initiate breakdown yields the following relation between gap distance and breakdown voltage:

$$d_m = 4.6 \times 10^{-8}\, V + 7.4 \times 10^{-9}\, V \log V \quad . \tag{3}$$

At larger distances, such as would be employed in high voltage colloidal ion accelerators, the magnitude of the voltage is likely to be more important than the field. It appears that impinging electrons of energies in excess of a few hundred kev cause a more rapid increase of charge carriers in the gap as the voltage is increased above this level. This phenomenon has been considered by Cranberg[17] and can be represented by the following equation:

$$d_m = 1.11 \times 10^{-13}\, V^2 \quad . \tag{4}$$

This latter effect seems more limiting at voltages greater than 7×10^5 V, whereas the effect of work function is more stringent at lower voltages. Adding Equations 3 and 4 provides the following relation which is generally applicable for uncoated tungsten electrodes:

$$d_m = 4.6 \times 10^{-8}\, V + 7.4 \times 10^{-9}\, V \log V + 1.11 \times 10^{-13}\, V^2 \quad . \tag{5}$$

This equation gives a conservative estimate in the range from 10^5 V to 5×10^6 V, since both terms are significant in this regime. Equation 5 was employed to calculate the breakdown limits for the mercury bombardment engine and the condensation colloidal ion engines. These results are presented numerically in Tables IA and IB and graphically in Figure 1.

It was assumed that a cesium coating will form on electrodes in surface contact engines and reduce the work function to 2 ev. This assumption yields the following equation to represent the breakdown

limitations of the surface contact engines:

$$d_{Cs} = 6.5 \times 10^{-8} V + 1.041 \times 10^{-8} V \log V + 1.11 \times 10^{-13} V^2 \quad . \qquad (6)$$

Minimum gap distances calculated from this equation are shown in Table IA and Figure 1.

A different breakdown law was assumed for the electrical atomization colloidal ion engine. In this type of engine, the particles are charged by the field effect. Since the processes involved in this method are not completely understood, the factors controlling breakdown cannot be positively identified. For the purpose of the present analysis, the views of Olendzkaya[18] on breakdown with liquid particles charged by a field effect between electrodes were followed. According to this concept, the main factor governing breakdown is the field strength between the electrodes enhanced by polarization forces. The field strength on the surface of a sphere is proportional to the change density, but the charge on a sphere charged by the field effect in a simple geometry is proportional to the field between the electrodes and the square of the particle radius. Thus, the field strength at the surface of the particle is determined directly by the field between the electrodes. This simple viewpoint is directly applicable only for flat electrodes and a uniform field. Although results obtained with this geometry are not expected to accurately represent the effects prevailing in the needle geometry of the electrical atomization colloidal ion source, Olendzkaya's results for mercury drops were employed to calculate the breakdown limitations for the electrical atomization engine. Adding Cranberg's relation (Equation 4), to extend the breakdown effect to higher voltages, gives the following equation:

$$d_m = 4 \times 10^{-7} V + 1.11 \times 10^{-13} V^2 \quad . \qquad (7)$$

This equation was employed to calculate the breakdown limited gap distances presented in Table IC and Figure 1 for the electrical atomization colloidal ion engine.

Space Charge Limitations

Child's law, given in the following equation, was employed to calculate the space charge limited current densities for all types of engines under consideration:

$$j = \frac{4}{9} \varepsilon_0 \left(\frac{2q}{m}\right)^{\frac{1}{2}} \frac{V^{3/2}}{d^2} = 5.4 \times 10^{-12} \left(\frac{q}{m}\right)^{\frac{1}{2}} \frac{V^{3/2}}{d^2} \tag{8}$$

where

j - current density in amp/cm^2,

ε_0 - permittivity of empty space,

$\frac{q}{m}$ - particle charge-to-mass ratio in coul/kg, and

d - breakdown limited gap distance in cm.

The results of the space charge limit calculations are given, as functions of the accel potential, in Tables IA, IB and IC and in Figure 2.

Since the net accelerating voltage determines the exhaust velocity for particles of a given charge-to-mass ratio, the exhaust velocity or specific impulse can be related to the voltage by the following equation:

$$I_s = \frac{u}{g} = \frac{\sqrt{2}}{g} \left(\frac{q}{m}\right)^{\frac{1}{2}} V_{net}^{\frac{1}{2}} = 0.1441 \left(\frac{q}{m}\right)^{\frac{1}{2}} V_{net}^{\frac{1}{2}} \tag{9}$$

where

I_s - specific impulse in sec,

u - exhaust velocity in cm/sec,

g - acceleration due to gravity = 980 in cm/sec^2, and

V_{net} - net accelerating voltage in volts.

V_{net} equals V in straight accel engines or = 0.25 V in 4:1 accel-decel engines. Specific impulse values computed from the above equation are presented as functions of accel potential in Tables IA, IB and IC and in Figure 3.

Since current density and specific impulse are both dependent on the accel potential, they can be related to each other as shown in Figure 4. Figure 2 shows maximum current densities for the atomic ion engines and the condensation colloidal ion engines at potentials between 2×10^4 v and 3×10^4 v and at 5.5×10^3 v for electrical atomization engines. However, the range of specific impulses best suited for missions to the moon, as discussed in a subsequent section, is 1000 sec - 4000 sec and high current densities at specific impulse values greater than 4000 sec cannot be efficiently utilized in lunar missions. Thus, Figure 4 illustrates a basic argument for utilizing colloidal ion engines rather than atomic ion engines for lunar missions. On the basis of maximum current density, condensation colloidal ion engines producing propellant ions with particle charge-to-mass ratios around 3×10^3 to 2×10^4 coul/kg appear to be best suited for lunar missions. Figure 5 is a simplified representation of Figure 4 to show the capabilities of the different types of electrostatic propulsion engines over the whole range of particle charge-to-mass ratios which the given engine type is assumed to produce. Engines producing particles with charge-to-mass ratios of 10^5 coul/kg are regarded as distinct from the true colloidal ion engines. The poor showing of the electrical atomization engine in these graphs is primarily due to the breakdown limitation assumed for this type of engine.

If the acceleration of the ions is regarded as ideal (i. e., no ion losses and only parallel ion trajectories), the power density in the beam can be computed simply as the product of current density and voltage:

$$\frac{P_b}{A_b} = j\,V \tag{10}$$

where

P_b - ideal beam power in watts, and

A_b - cross sectional area of ion beam in cm^2 .

The power densities as functions of specific impulse and particle charge-to-mass ratio are given in Tables IA, IB and IC and in Figure 6. For a given type of engine, the range of possible power densities is depicted in Figure 7.

As a result of the foregoing considerations, the ideal thrust density can be calculated as a function of voltage as follows:

$$\frac{F}{A_b} = \left(\frac{2j^2 V_{net}}{q/m}\right)^{\frac{1}{2}} = \frac{7.63\times10^{-12}\, V^{3/2}\, V_{net}^{\frac{1}{2}}}{d^2}, \ \frac{\text{Newtons}}{\text{cm}^2} = \frac{1.74\times10^{-12}\, V^{3/2}\, V_{net}^{\frac{1}{2}}}{d^2}, \frac{\text{lb-f}}{\text{cm}^2} \tag{11}$$

where

F - thrust in lb-f/cm^2.

Thus, the thrust densities are basically dependent on the breakdown limitations. These results are given in Tables IA, IB and IC. As functions of specific impulse, however, the thrust densities also vary with particle charge-to-mass ratios, as shown in Figure 8. Figure 9 is the simplified version of Figure 8 to represent the overall thrust density capabilities of each type of engine.

Equations 10 and 11 provide a general relation between specific impulse and the ratio of thrust to beam power. The results are the same for all engines at a given specific impulse. As shown in Tables IA, IB and IC and in Figure 10, the thrust per unit of beam power increases with decrease in specific impulse. This fact is one of the fundamental reasons favoring the use of low specific impulses, since the power supply system in many mission applications will be the major weight factor in the overall thrustor system.

Power Efficiency

Since the weight of the power supply system is highly significant in determining the performance capabilities of the various electrostatic propulsion engines, the power efficiencies of the different engines will have

a strong bearing on their payload capacities for many missions. The ideal beam power, represented as P_b in the preceding section, does not include power utilized for ionizing the propellant material or power losses, such as result from poor beam collimation. These factors have been estimated and incorporated into equations to represent the power efficiency for each type of electrostatic propulsion engine. The general representation for power efficiency is shown by Equation 12.

$$\eta = \frac{P_b}{P_{in}} = \frac{j\,V_{net}}{j\,V_{net} + xj + yj\,V_{net}} = \frac{1}{1 + x/V_{net} + y} \tag{12}$$

where

η - power efficiency of engine,

P_{in} - power required by the engine to produce a given beam power in watts,

x - average energy required to produce one utilized ion, and

y - estimated power loss due to poor beam collimation.

For the surface contact engine, beam collimation should be good, so the factor, y, was regarded as negligible for this case. From reports of studies of the surface contact engine[19, 20], it was assumed that the average energy required to create each ion which reaches the accelerator is 1000 ev/ion. Therefore, Equation 13 represents the power efficiency of the surface contact engine.

$$\eta = \frac{1}{1 + 1000/V_{net}} \quad . \tag{13}$$

The estimates obtained from this equation are given in Table IA and Figure 11.

For the mercury bombardment engine the average energy required to produce one utilized ion was estimated as 800 ev/ion, and a 4% loss in thrust production was assumed for the y factor in Equation 12[21, 22]. Thus, the efficiency of the bombardment ion engine is estimated from the following equation:

$$\eta = \frac{1}{1.04 + 800/V_{net}} \quad . \tag{14}$$

Results obtained from Equation 14 are shown in Table IA and Figure 11.

Since the operation of the colloidal ion engines is still undergoing research investigation, the efficiency estimates will be less accurate than for the atomic ion engines. Although the two types of condensation colloidal ion engines will probably show very different power efficiencies after they have reached the development stage, for the purpose of the present study, these engines were considered to have the power efficiencies given by the following equation:

$$\eta = \frac{0.9}{1 + 5\times 10^3/V_{net}} \quad . \tag{15}$$

The factor 0.9 in the numerator represents inefficiency in the accelerator resulting from a distribution of particle charge-to-mass ratios[8]. There are reasons to regard this estimate as conservative for both condensation colloidal ion engines. Experimental results with the neutral nucleation source have indicated a factor of 0.986 or higher[10], while the ionic nucleation engine incorporates techniques specifically planned to ensure that virtually all particles reaching the acceleration region are within a given selected range of particle charge-to-mass ratios. The estimate of 5000 ev/ion for the ionization process may be a good estimate for the ionic nucleation engine but is probably high for the neutral nucleation engine. However, the shock, which accompanies condensation in the neutral nucleation engine, will impair beam collimation thereby contributing to ion losses before the accelerator and power losses in the accelerator. Since the ionic nucleation colloidal ion source should produce a highly collimated beam, it should incur little loss from these causes. The efficiency estimates for the condensation engines are regarded here as identical and are presented in Table IB and Figure 11.

The following equation was employed to simulate the power efficiency of the electrical atomization colloidal ion engine:

$$\eta = \frac{1}{z + y} = \frac{1}{1.333 + 0.075} = 0.71 \quad . \tag{16}$$

Experimental studies of this source have indicated that light ions (charge-to-mass ratios appreciably greater than the average charge-to-mass ratio) constitute 5% to 10% of the total ion current. In addition, the inherent poor collimation of this source will, as in the case of the neutral nucleation engine, cause ion losses with and without significant losses in accelerator power. The term z in Equation 16 represents the losses due to variation of the particle charge-to-mass ratios and ion losses without large accelerator power loss. The term y, as in Equation 12, represents accelerator power losses due to poor beam collimation. The values assigned for z and y in Equation 16 are based on recent experimental results[13]. The estimated power efficiency of the electrical atomization engine is presented in Table IC and Figure 11.

The product of the estimated power efficiency and the ratio of thrust to ideal beam power (F/P_b) gives the thrust in pounds-force per watt of power obtained from the power supply system (F/P_{in}). These values are given in Tables IA, IB and IC and in Figure 12. From these results, the input power required to produce a thrust level of ten pounds of thrust was calculated and presented for each of the engines in Tables IA, IB and IC and in Figure 13. It is evident from these results that inability to develop light-weight power supplies is a much more serious deterrent for missions in the higher specific impulse range. It is also clear that the power requirements of the atomic ion engines are greater than those of the colloidal ion engines at lower specific impulse values; that is, specific impulse values less than 4000 sec.

Propellant Efficiency

Another engine characteristic which can have a significant effect on the total weight of a thrustor system is the efficiency of propellant utilization. The surface contact engines were assumed to have a propellant efficiency, η_f of 0.97[20]. An estimate of 0.93 was assigned as the propellant efficiency of the mercury bombardment engine[22].

The propellant efficiency of the ionic nucleation condensation colloidal ion engine is assumed equal to the weight percentage of condensable material in the mixed propellant flow. It has been estimated that 5% to 10% by weight of hydrogen in the propellant mixture should suffice for cooling the colloidal ions during condensation of the condensable portion of the propellant mixture. The propellant efficiency of the ionic nucleation engine, therefore, should be 0.90 to 0.95. In the present calculations the propellant efficiency was assumed to be 0.90.

In the case of the neutral nucleation condensation colloidal ion engine, the propellant efficiency is regarded as being a function of the particle charge-to-mass ratio. An empirical relation was set up to conform with existing experimental data and the theories of the dependence of nucleation and growth rates on the mass flow density[10-12]. The empirical equation relating propellant efficiency and particle charge-to-mass ratio in the neutral nucleation engine is:

$$\eta_f = \frac{2.5}{(q/m)^{1/3}} \quad . \tag{17}$$

There is, however, still some question about the ability of the required low flow densities to achieve a sufficient nucleation rate. The low propellant efficiency of this type of engine is a major hindrance to its achievement of a high payload capacity. It does not, however, appear feasible to collect and recirculate the uncondensed propellant, since the expansion renders the material very diffuse and the shock dissipates the directed kinetic energy of the flow. Furthermore, recirculation of that portion of the unused propellant which could be collected would entail additional power requirement and equipment weight.

The propellant losses in the electrical atomization colloidal ion engine stem mainly from the distribution of particle charge-to-mass ratios and the poor collimation of the beam. The values representing these factors in Equation 16 for the power efficiency of this engine are: $z = 1.333$ for the

losses due to the distribution of charge-to-mass ratios and ion losses due to poor collimation and y = 0.075 for the power loss due to poor collimation in the accelerator. Since the latter value is greater for light ions, y should be less when representing propellant material losses in the accelerator. If y = 0.05, the propellant efficiency of the electrical atomization engine will be 0.723.

BLANK PAGE

THRUSTOR COMPONENTS

The characteristics of the electrostatic propulsion engines largely determine the masses of the components of a thrustor system. The thrustor system is here considered to be composed of a power supply system, an engine, propellant, propellant tanks, a propellant feed system and support structures.

Propellant

The mass of propellant required for a given mission depends upon the mission specifications as well as the engine characteristics. In order to make a generalized comparison of the propellant requirements of the various engines, an engine operating period of 10,000 hours was arbitrarily selected. The mass of propellant ejected per unit area of the beam depends upon the space charge limited current density, j, and the particle charge-to-mass ratio according to the following equation:

$$\left(\frac{M_f}{A_b}\right)_{10,000} = \frac{j}{\eta_f\, q/m} = 7.94\times10^7 \frac{j}{\eta_f\, q/m} \quad \frac{\text{lb}}{10,000 \text{ hrs - cm}^2} \tag{18}$$

where

η_f - propellant efficiency,

A_b - beam area in cm^2, and

M_f - propellant mass required for 10,000 hrs operation in pounds.

The ten thousand hour propellant mass flow densities calculated from Equation 18 are presented in Tables IIA, IIB1, IIB2 and IIC.

A more important parameter is the total mass of propellant which must be ejected by each type of engine in producing a pound of thrust for 10,000 hours. This value is readily calculated as follows:

$$\frac{M_f}{F} = \frac{M_f/A_b}{F/A_b}, \quad \frac{\text{lb}}{\text{lb-f}} \quad . \tag{19}$$

The results of this calculation are given in Tables IIA, IIB1, IIB2 and IIC and in Figure 14. The severe weight handicap incurred by the low propellant efficiency of the neutral nucleation condensation colloidal ion engine is obvious in Figure 14.

<u>Engine</u>

The mass of the engine is dependent on the design of the ion source and accelerator. Since there is considerable latitude in design development, the equations representing these factors are not rigorous. The ratio of the actual ion source area to the beam area is a particularly signficant design feature. However, other factors may also be important in some regimes of operation. The electrode gap distance will make insulating support mass appreciable at very high voltages. Also, the various engine components may be heavier for one type of engine than for another.

A recent report[20] describing a modular array of slit sources was utilized as the model for one type of surface contact engine. This same geometry was also applied to the condensation colloidal ion engines. The effect of the accelerator voltage on beam spreading must be considered as well as the size of the various structures. The following equation was used to estimate the area of the engine for the strip type of surface contact engine and for the condensation colloidal ion engines:

$$\frac{A_e}{A_b} = \left(\frac{3.33 \times 10^4}{V} + 1.37\right)(1 + 0.167) = \frac{3.88 \times 10^4}{V} + 1.6 \qquad (20)$$

where A_e is the cross sectional area of engine in cm^2. The terms in the first set of parentheses represent the effect of voltage on beam spreading and the size of the accelerator structure relative to the beam. The term 0.167 in the second set of parentheses accounts for structures at the ends of the slits and connections between units. The estimated area ratios are given in Tables IIA, IIB1 and IIB2. Since the area ratios are functions of voltage only, the values do not change with particle charge-to-mass ratio.

Another model, the sastrugi geometry[23], was also examined for use as a surface contact engine design. Beam spreading in this engine was assumed to be lower than in the strip source. The equation used to calculate the relative engine area for this design is

$$\frac{A_e}{A_b} = \frac{2.5 \times 10^4}{V} + 1.6 \quad . \tag{21}$$

This is probably an optimistic estimate, but it can serve to indicate the ultimate magnitudes of improvement in performance which can be achieved by special designs. The engine area ratios calculated from Equation 20 are presented in Table IIA.

The bombardment ion engine is generally operated below space charge limits to achieve a satisfactory lifetime; however, the beam area corresponding to a space charge limited beam was assumed for the present analysis. This type of engine is cylindrical in shape, so the term for end effects is not needed. The accelerator for the bombardment ion engine is a plate with an arrangement of circular holes for the ion beam to pass through[22]. In the following equation the first term includes the holes and the areas between the holes while the second term corresponds to the peripheral structure around the main ion source area:

$$\frac{A_e}{A_b} = \frac{25 \times 10^4}{V} + 5 \quad . \tag{22}$$

In the electrical atomization colloidal ion engine, the problem of interference of the fields around the individual needle tips sets a minimum distance between units. This distance, however, is dependent on voltage. Recent experimental studies with arrays of needles indicate very high ratios of engine areas to beam areas since an average area of approximately 2.57 cm^2 is required for each needle in an array. If new propellant materials can deliver higher currents from each needle without increased beam spreading, a competitive engine mass may be possible for this type of colloidal ion source. Assuming each needle can produce 10^{-4} amp but

keeping the requirement for 2.57 cm^2 per needle leads to the following approximation:

$$\frac{A_e}{A_b} = \frac{10^5}{V} + 1.33 \quad . \tag{23}$$

Here the second term represents the peripheral area required for a circular array. Values calculated from Equation 23 are shown in Table IIC.

The masses of the engines are approximated on the basis of their cross sectional areas and lengths together with some assumed effective density of the structures. For both the strip geometry and the sastrugi modification of the surface contact engine, the following equation was used to estimate engine mass for simple accel engines:

$$\frac{M_e}{A_b} = (0.03 + 0.0005d)\,\frac{A_e}{A_b} \tag{24}$$

where M_e is the mass of the engine in lbs. The first term in parentheses represents the effective density of one square centimeter of an engine with a low voltage accelerator and the second term adds mass for higher voltages which necessitate longer accelerators. To include the added mass due to the decel electrode in accel-decel engines, a mass corresponding to an area density of 0.005 lb/cm^2 multiplied by the voltage dependent term in the area ratio equation (Equation 20 for the strip engine and Equation 21 for the sastrugi geometry) was added. The results are given in Table IIA.

The bon rdment engine should weigh less per unit source area than the surface contact engines with their heavy porous ionizers, so the following modification of Equation 24 was employed to estimate the mass of the bombardment ion engine:

$$\frac{M_e}{A_b} = (0.0265 + 0.0005d)\,\frac{A_e}{A_b} \quad . \tag{25}$$

The added mass for accel-decel engines was calculated, as in the case of the surface contact engines, as the product of the area density factor

0.005 lb/cm^2 and the voltage dependent term of Equation 22. The results are given in Table IIA.

The condensation colloidal ion engines require superheaters and feed chambers as well as the expansion nozzles. Although the nozzle used in the ionic nucleation engine is quite short, the skimmer will increase the engine mass. The masses for both condensation colloidal ion engines were approximated from the following equation:

$$\frac{M_e}{A_b} = (0.04 + 0.0005d)\frac{A_e}{A_b} \quad . \tag{26}$$

The corresponding accel-decel engine masses were increased by adding the product of 0.005 lb/cm^2 and the voltage dependent term from Equation 20. The results are given in Tables IIB1 and IIB2.

Since the electrical atomization engine consists of the needles, the extracting-accelerating electrode and a neutralizer, the weight should be comparatively low. The engine mass for this type of source was calculated from the following equation:

$$\frac{M_e}{A_b} = (0.02 + 0.0005d)\frac{A_e}{A_b} \quad . \tag{27}$$

An additive term of the product of 0.005 lb/cm^2 and the voltage dependent term from Equation 23 was added to the calculated simple accel engine masses to estimate the masses of the corresponding accel-decel engines. The results of these mass calculations are presented in Table IIC.

A more significant engine mass parameter than M_e/A_b is the engine mass required to produce one pound of thrust

$$\frac{M_e}{F} = \frac{M_e/A_b}{F/A_b} \quad . \tag{28}$$

Values of this parameter are given in Tables IIA, IIB1, IIB2 and IIC and in Figure 15. A simplified form of Figure 15 is shown in Figure 16 to indicate the overall range of values for each engine type. These results

show that engine mass should not be a very significant portion of the total thrust system mass for any engines except in cases in which the atomic ion engines or the hypothetical molecular ion engines are used at specific impulses less than 4000 sec.

Another parameter of interest in comparing the different engines is the engine area required to produce one pound of thrust. Values of this parameter were calculated from the following relation and listed in Tables IIA, IIB1, IIB2 and IIC:

$$\frac{A_e}{F} = \frac{A_e/A_b}{F/A_b} \quad . \tag{29}$$

Feed System

The main mass of the feed system for large electrostatic propulsion engines is the mass of a manifold to distribute the propellant material over the full cross sectional area of the engine. Thus, the cross sectional area of the manifold was taken to be equal to the cross sectional area of the engine. The mass of the feed system can therefore be approximated as the product of the engine area, the thickness of the material from which the feed system is fabricated and the density of this material. Stainless steel with a density of 0.01695 lb/cm^3 was assumed as the structural material for the feed system. The thickness of the manifold was calculated from the following equation which provides for protection against micrometeoroid penetration:

$$t_{fs} = 0.0088\,(A_{fs})^{0.3} = 0.0088\,(A_e)^{0.3} \tag{30}$$

where

t_{fs} - thickness of the feed system structure in cm, and

A_{fs} - cross sectional area of the feed system manifold.

For a generalized system, a thrust level of 10 lb-f was assumed to permit calculation of the thickness of the manifold. On the basis of the preceding discussion, the following equation estimates the feed system mass per unit of thrust:

$$\frac{M_{fs}}{F} = 0.017 \times 0.0088 \left(10\frac{A_e}{F}\right)^{0.3} \frac{A_e}{F} = 3 \times 10^{-4} \left(\frac{A_e}{F}\right)^{1.3} \tag{31}$$

where M_{fs} is the mass of the feed system in lbs. This equation was employed directly to calculate the feed system masses for the atomic ion engines, the neutral nucleation condensation colloidal ion engine and the electrical atomization colloidal ion engine. The bombardment ion engine may not require dispersal of propellant over the whole source area from a feed manifold, but a large thrust system will require some type of manifold to feed the individual modules. The mass estimate for this engine's feed system, however, may be excessive. Since the ionic nucleation condensation colloidal ion engine utilizes a mixture of two propellant materials, the feed system masses for this type of engine, as calculated from Equation 31 were arbitrarily multiplied by a factor of 1.5. The results of the feed system mass calculations are presented in Tables IIA, IIB1, IIB2 and IIC.

Support Structure

It is assumed that the mass of the power supply system includes any support structure required for this component. The support structure for the propellant tanks is included with the calculation of the mass of the propellant and tanks. Therefore, the mass of the support structure for the engine unit is formulated only on the basis of the masses of the engine and feed system. To include miscellaneous support structures, the comparatively large value of 10% of the total mass of the engine and feed system was taken as the support structure mass.

Considering the engine, the feed system and the accompanying support structure as a unit, the mass of this engine system unit for one pound of thrust was calculated by multiplying the sum of the engine and feed system masses per pound of thrust by 1.1. The resultant values are given in Tables IIA, IIB1, IIB2 and IIC.

Propellant Tanks

The masses of the propellant tanks were computed as the product of a constant for each propellant material and the mass of propellant material. The constants employed in these calculations were based on more complex calculations of tank weights with consideration for micrometeoroid protection and on estimates in the literature[2, 24]. These specific calculations utilize the volume of the propellant and a tank shape suitable for that volume. The tanks were taken to be composed of aluminum, but a steel liner was assumed for use when mercury is the propellant material. The generalized tank mass, given as percentage of propellant mass, is 5% for cesium, 2% for mercury, 2% for me-curous chloride used in the neutral nucleation colloidal ion engine, 8% for glycerol used in the electrical atomization colloidal ion engine, 2% for the cadmium used in the ionic nucleation colloidal ion engine and 20% for the hydrogen used in this latter engine.

Although the 20% figure for the hydrogen used in the ionic nucleation condensation colloidal ion engine is large compared to the other figures, its effect is not too significant since only 10% of the mass of the propellant is hydrogen. Values of 15%[2] and 20%[24] of the mass of hydrogen are given as tankage estimates in the literature, and the more conservative value was employed in the present study. Together with the cadmium tankage, this estimate for hydrogen provides a composite value of 3.8% of total propellant mass for the tankage needed for the ionic nucleation colloidal ion engine.

In calculation of a thrustor system mass, including the engine, feed system, propellant, tankage and support structures, a 10% support structure mass was assumed for the tanks with the propellant. This value added to the mass of the required power supply system would constitute the total propulsion system mass. Since the propellant mass and therefore the tankage and its support mass, depend upon the thrust level and the total time of engine operation, comparative calculations are not very meaningful unless

they are based on specific mission requirements. The significance of the propellant and tankage mass factors is demonstrated more clearly in a subsequent section on mission capabilities.

Power Supply System

The power supply system consists of a heat source, conversion equipment, shielding, controls and power conditioning, if required. Power conditioning will not be necessary for the propulsion power if a high voltage electrostatic generator is incorporated into the conversion equipment.

As in the case of the electrostatic propulsion engines, several types of each of these components may be considered, and many of these components are still in a research stage. Furthermore, the various components are interdependent. If a manned mission is planned, the mass of the radiation shield may be the dominant mass in the entire thrustor system. However, the mass of the required shield depends strongly on shield design, the type of reactor employed and the efficiency of the conversion system[25]. In view of the many variable factors involved in the power supply system, a simplified approach to the mass of the power supply system has been assumed for the present study. As a companion to the present analysis, a study entitled "A Comparative Analysis of Various Power Supply Systems for Use with Electrostatic Propulsion Engines" has been initiated to examine the power supply systems in detail.

For purposes of comparison and to get some estimates of the probable effects of the specific mass of the power supply system on overall propulsion system masses and payload capcities, four values of power supply specific mass were considered. These values are 10 lb/kwe, 20 lb/kwe, 30 lb/kwe and 40 lb/kwe. The lowest value is probably optimistic, but it should be possible to develop a reliable space power supply system with a specific mass less than 40 lb/kwe, if all components are specifically planned for space operation.

BLANK PAGE

MISSION CAPABILITIES

Two methods have been employed to compare the mission capabilities of the different electrostatic propulsion systems. The first method simply compares the total masses of the propulsion systems for a given operating time and thrust level. The other technique is less general but takes cognizance of the vital requirements of missions by comparing the payload capacities of the various propulsion systems for specified missions.

General Comparison of Total System Masses

The masses of the engine, feed system, engine unit support structure and power supply system are regarded as functions of thrust level, but not of operating time. A thrust level of 10 lb-f was assumed for these general comparisons. The mass of the propellant and the correlated masses of the propellant tanks and tank supports vary with operating time as well as with thrust level. Two values of operating time, 10,000 hr and 2,000 hr, were chosen to provide examples for this general comparison. These general calculations do not examine the ability of the propulsion systems to actually accomplish a mission. It may be noted, however, that 2,000 hours is in the range of operating times required for round trip earth orbit to moon orbit missions and 10,000 hours is in the operating time range of some round trip missions from earth orbit to Mars orbit and one way missions from earth orbit to Jupiter orbit.

The total propulsion system masses were calculated for each of the four arbitrarily chosen values of the specific mass of the power supply using the following equation:

$$M_{tot} = M_p + 1.1\ F\left(\frac{M_e}{F} + \frac{M_{fs}}{F}\right) + 1.1\ (1+a)\ F\left(\frac{M_f}{F}\right)$$

$$M_{tot_{10}} = P_{e_{10}} \times \left(\frac{M_p}{P_e}\right) + 11\left(\frac{M_e}{F} + \frac{M_{fs}}{F}\right) + 11\ (1+a)\left(\frac{M_f}{F}\right)_{10,000} \times \frac{t}{10^4} \qquad (32)$$

where

$M_{tot_{10}}$ - total propulsion system mass for 10 pounds of thrust in pounds,

M_p - mass of the power supply system in pounds,

a - fraction of propellant mass to represent tankage mass,

$P_{e_{10}}$ - electric power required for a 10 lb-f level in kwe,

$\frac{M_p}{P_e}$ - specific mass of power supply system in lb/kwe,

$\left(\frac{M_f}{F}\right)_{10,000}$ - propellant mass per pound of thrust for 10,000 hr operation in lb/lb-f - 10,000 hr, and

t - operating time in hr.

The results of these calculations are presented in Tables IIIA, IIIB1, IIIB2, IIIC, IVA, IVB1, IVB2 and IVC and in Figures 17, 18, 19 and 20. Only the extreme values of 10 lb/kwe and 40 lb/kwe for the specific mass of the power supply system were illustrated graphically.

The results show clearly that the ionic nucleation condensation colloidal ion propulsion system and the electrical atomization colloidal ion propulsion system have the lowest total mass weights at specific impulse values less than 3200 sec. Furthermore, the total mass of the ionic nucleation propulsion system appears to be less than or approximately equal to that of any other system up to a specific impulse of 14,410 sec. This is the specific impulse corresponding to particles of 10^4 coul/kg accelerated through a million volts. Although higher voltages were not examined in this study, they would probably incur such weight penalties in the accelerator to avoid breakdown that performance would decrease more rapidly than extrapolations would indicate.

Comparison of Figures 17 and 18 shows that the effect of the greater power supply specific mass is small for specific impulse values less than 4000 sec and negligible below 2000 sec in the case of 10,000 hours of engine operation. The specific mass of the power plant has a greater effect in

cases of 2,000 hours of engine operation. However, the total system masses are all lower for the shorter operating time, and significantly lower at specific impulse values less than 20,000 sec.

Mission Examples

The specific mission calculations were based on the theoretical equations which consider the translation of the exhaust velocity to vehicle velocity and the energy required to carry the vehicle through a planned trajectory.[26] These relations were modified to utilize the parameters calculated in this analysis and to incorporate the propellant inefficiency as well as the power inefficiency. The equations which must be satisfied to determine the payload capacity of a given engine performing a mission are the following:

$$\log\left(1 - G\frac{M_f}{F}\right) = -\frac{\Delta v}{2.26 \times 10^3 I_s} \tag{33}$$

$$t = \frac{\frac{M_f}{F} \times 10^4}{(M_f/F)_{10,000}} \tag{34}$$

$$\frac{M_{pay}}{M_i} = 1 - G\left[\frac{M_f}{F} + 2.78 \times 10^{-8}\left(\frac{M_{tot}}{F} - \frac{M_f}{F}\right) I_s \left(\frac{M_f}{F}\right)_{10,000}\right] \tag{35}$$

where

$G = \dfrac{F}{M_i}$ - ratio of thrust to initial vehicle mass;

Δv - velocity increment which the vehicle must achieve in cm/sec;

M_{pay} - payload mass in lb;

M_i - total initial vehicle mass in lb .

By means of Equation 33, the mass of propellant which must be ejected per pound of thrust is computed for a specific mission defined in terms of G, Δv, and I_s. The engine operating time is then calculated from Equation 34 by relation to the 10,000 hour values of propellant mass per pound of thrust listed in Tables IIA, IIB1, IIB2, and IIC and presented graphically in Figure 14. Calculation of the value of $(M_{tot}/F - M_f/F)$ in Equation 35 presents a problem, since the difference between M_{tot}/F and M_f/F may be smaller than the significance of the estimated values for the two quantities. Therefore, it is generally best to calculate $(M_{tot}/F - M_b/F)$ from the following modification of Equation 32:

$$\frac{M_{tot}}{F} - \frac{M_f}{F} = 1.1\left(\frac{M_e + M_{fs}}{F}\right) + 0.1\,P_{10}\,\frac{M_p}{P_e} + (0.1 + 1.1a)\frac{M_f}{F} \quad . \qquad (36)$$

The payload capacities and engine operating times are presented in Table V for lunar, Martian, and Jupiter missions. Power supply system specific masses of 10 lb/kwe and 40 lb/kwe were considered. An extra engine weight penalty was added in the cases of colloidal ions of low charge-to-mass ratios accelerated through potentials greater than 1000 kv. Accel-decel accelerator systems were employed for the atomic ion engines, but not for the colloidal ion engines. The results show the superiority of the colloidal ion engines for the lunar missions. It is also evident that the ionic nucleation condensation colloidal ion engine could be competitive with the atomic ion engines for the longer range missions, as represented by the mission to Jupiter. Thus, if developed to the performance capability of which it is theoretically capable, the ionic nucleation colloidal ion engine could serve in a generally applicable propulsion system for low thrust missions. Furthermore, good payload ratios can be delivered by this type of engine on lunar missions even with a power supply specific mass of 40 lb/kwe.

The missions considered in this study are constant thrust missions. Some payload increase can be secured by operating a variable thrust program. The colloidal ion engines could theoretically accomplish such programs by either of two different techniques. The particle charge-to-mass ratio could be varied or the accelerating potential could be varied. The latter technique is also feasible for the atomic ion engines.

BLANK PAGE

CONCLUSIONS

This evaluation of electrostatic propulsion engines shows the effects of fundamental limitations of the various types of engines on their payload capabilities. A major limitation to the performance of the atomic ion engines is a reduction in power efficiency which accompanies decreasing specific impulse values. This problem will set a severe restriction on the mission capabilities of these engines unless power supply systems can be developed with specific masses approaching 10 lb/kwe. In addition, the masses of the atomic ion engines become quite large at specific impulse values less than 4,000 sec because of their low values of mass ejected per unit area of the exhaust beam. For these reasons the atomic ion engine systems do not appear to be competitive for lunar missions. Although differences among the three types of atomic ion engines are cited, the differences in performance are slight except in the region of rapid change in engine mass, just under 4,000 sec specific impulse.

The colloidal ion engines are still in a research stage. The fundamental problems of the colloidal ion engines rather than experimental difficulties involved in their current laboratory investigations have been considered in this analysis. While the results of such an analysis cannot be exact, the general effects and tendencies are believed to be valid. Therefore, these engines should achieve a performance approaching that indicated by this analysis if sufficient effort is devoted to studying them.

Unless some means can be found to reduce the propellant inefficiency of the neutral nucleation condensation colloidal ion engine, its performance will be poorer than that of the other colloidal ion engines. When operating with comparatively heavy particles

($q/m \leq 10^3$ coul/kg) and high voltages, the neutral nucleation engine can achieve useful payloads in lunar missions. It would therefore be better for such applications than the atomic ion engines but would not be suitable for planetary missions. Unless power supply systems with specific masses less than 40 lb/kwe can be developed, payloads carried by the neutral nucleation engine will probably be too low for practical use.

The ionic nucleation condensation colloidal ion engine was planned to allow only a certain small propellant weight loss (5%-10%) in the form of a noncondensable gas included to facilitate condensation of virtually all of the condensable propellant. In addition, the engine design incorporates features that reduce power losses which are incurred by poorly collimated beams or beams with a wide distribution of particle charge-to-mass ratios. The ionic nucleation engine therefore should achieve the highest payloads in lunar missions and should be competitive with atomic ion engines in planetary missions. With propellant particles with charge-to-mass ratios of 10^4 coul/kg, the ionic nucleation engine should be generally applicable for missions best performed at specific impulse values from 1400 sec to 14,000 sec. The payload capacity of an ionic nucleation engine system would be reduced, particularly at the higher specific impulse values, unless power supply systems with low specific masses can be developed. However, this type of propulsion system should still be capable of carrying useful payloads even with power supply system specific masses of 40 lb/kwe.

The performance of the electrical atomization engine is expected to suffer from a fundamental restriction of its space charge limited current density as a result of its breakdown characteristics. This factor, together with the spatial requirements to avoid field interference

among the individual colloidal ion sources, cause engine masses to be generally heavier than for the condensation colloidal ion engines or the atomic ion engines. In addition, the electrical atomization engine suffers from an inherent poor beam collimation and some distribution of charge-to-mass ratios, which factors affect both propellant efficiency and power efficiency. None of these difficulties has a very large effect on the performance capability of the electrical atomization engine, but the additive effects reduce payload capacity in comparison with the ionic nucleation condensation colloidal ion engine. The performance of the electrical atomization engine should be superior to that of the neutral nucleation condensation colloidal ion engine for any mission and to that of the atomic ion engines for lunar missions.

ILLUSTRATIONS

LEGEND FOR GRAPHS

C ——— Condensation colloidal ion engines

E — — — Electrical atomization colloidal ion engines

S ------ Surface contact ion engines

B —·— Bombardment ion engines

INC ——— Ionic nucleation condensation colloidal ion engines

NNC—···— Neutral nucleation condensation colloidal ion engines

SS —·····—Sastrugi surface contact ion engines

CS ······· Strip surface contact ion engine

Suffixes denote particle charge-to-mass ratios for colloidal ion engines (no suffix shows no difference).

5 - 10^5 coul/kg

4 - 10^4 coul/kg

3 - 10^3 coul/kg

2 - 2×10^2 coul/kg

Prefixed denote type of accelerator (no prefix shows no difference).

a - simple accel

d - accel-decel

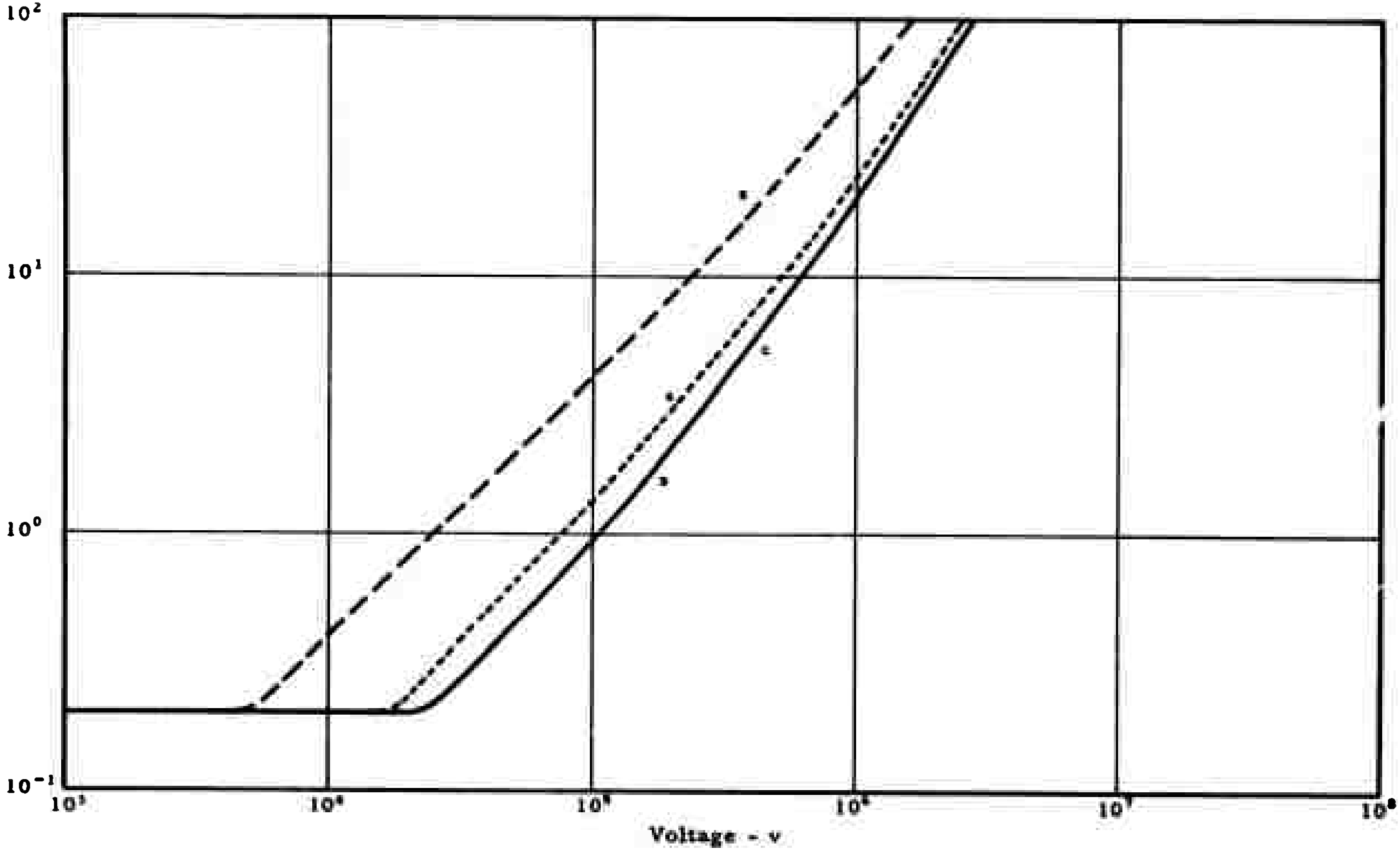

Figure 1. Breakdown Limitations

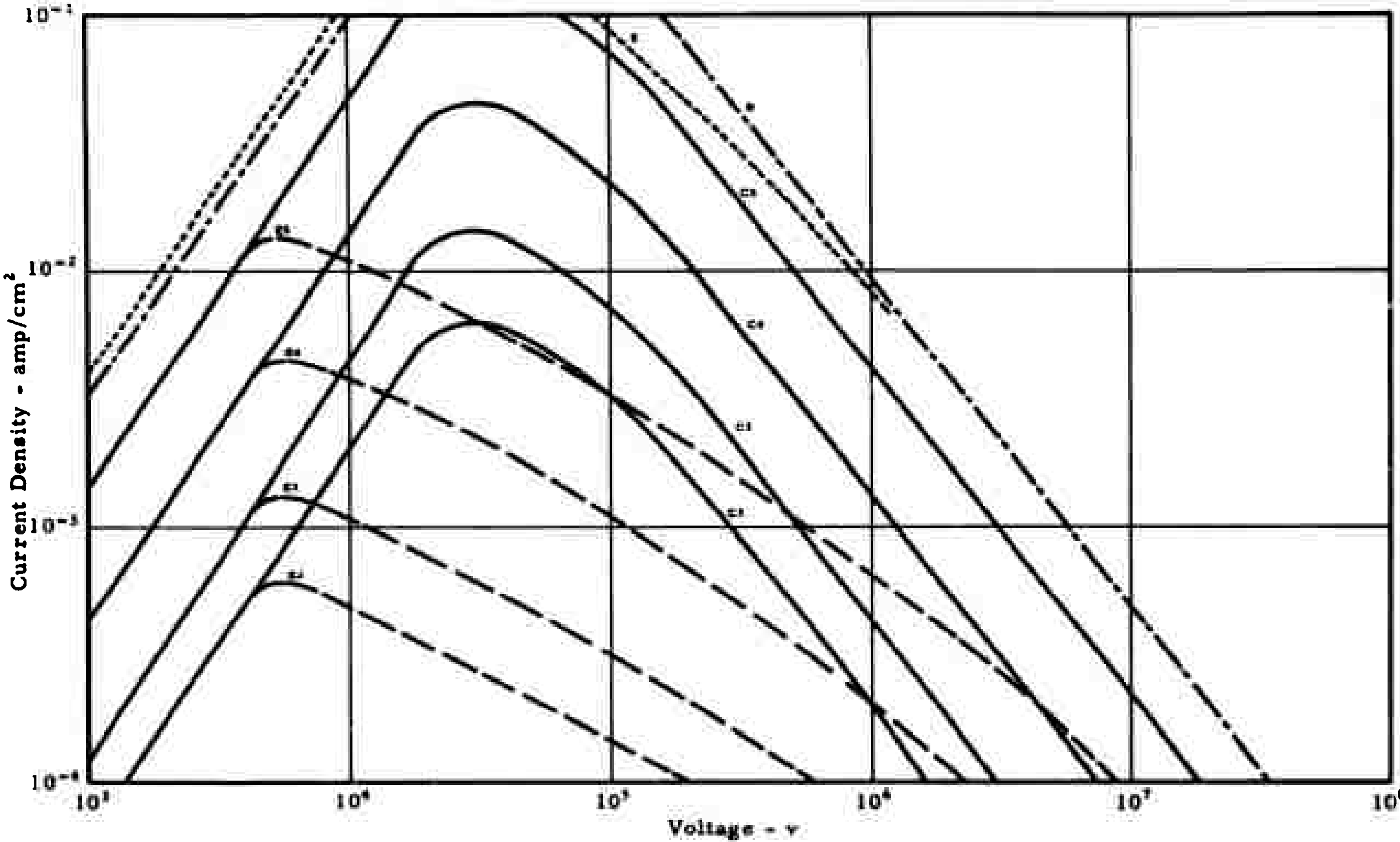

Figure 2. Space Charge Limitations

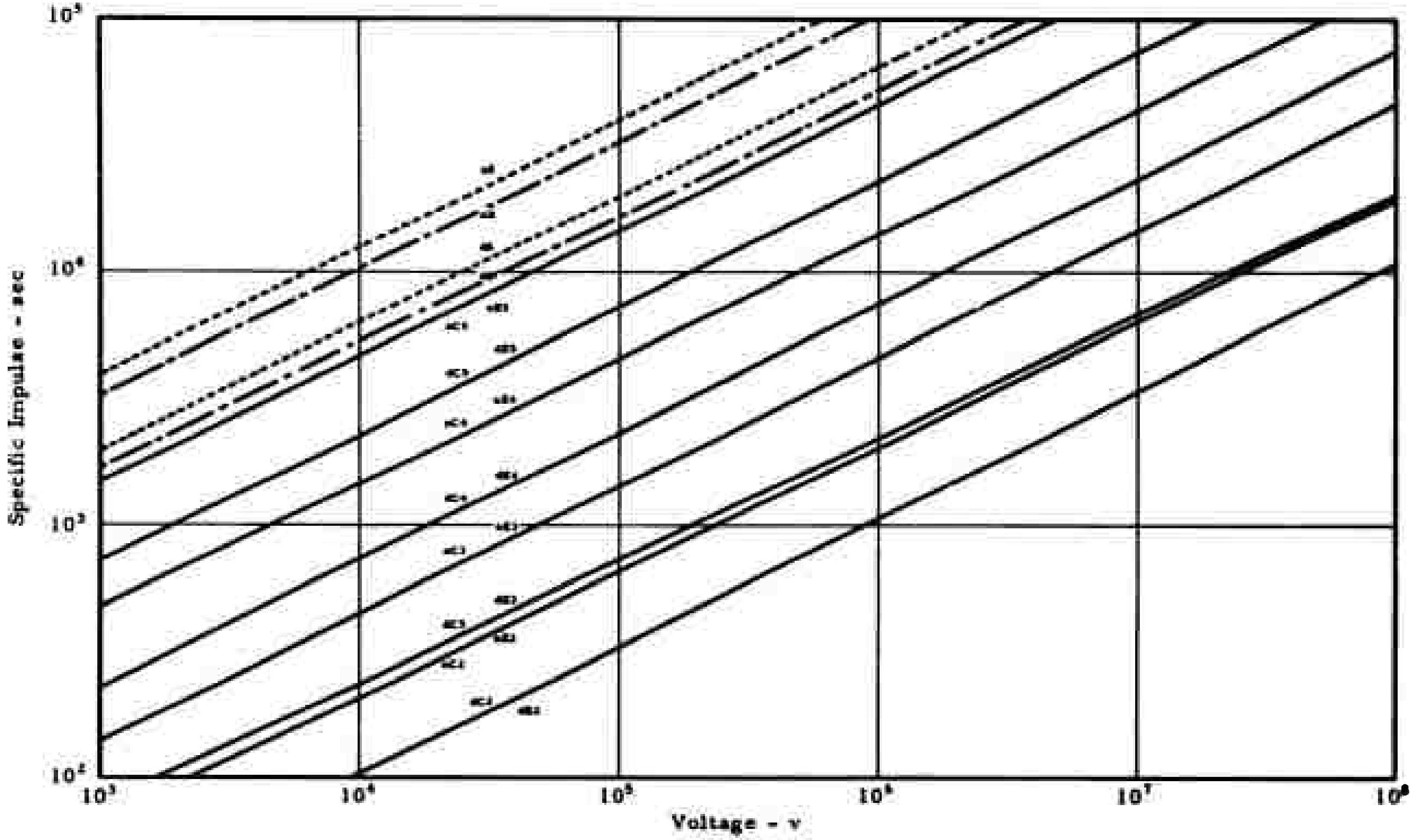

Figure 3. Dependence of Specific Impulse on Accel Voltage

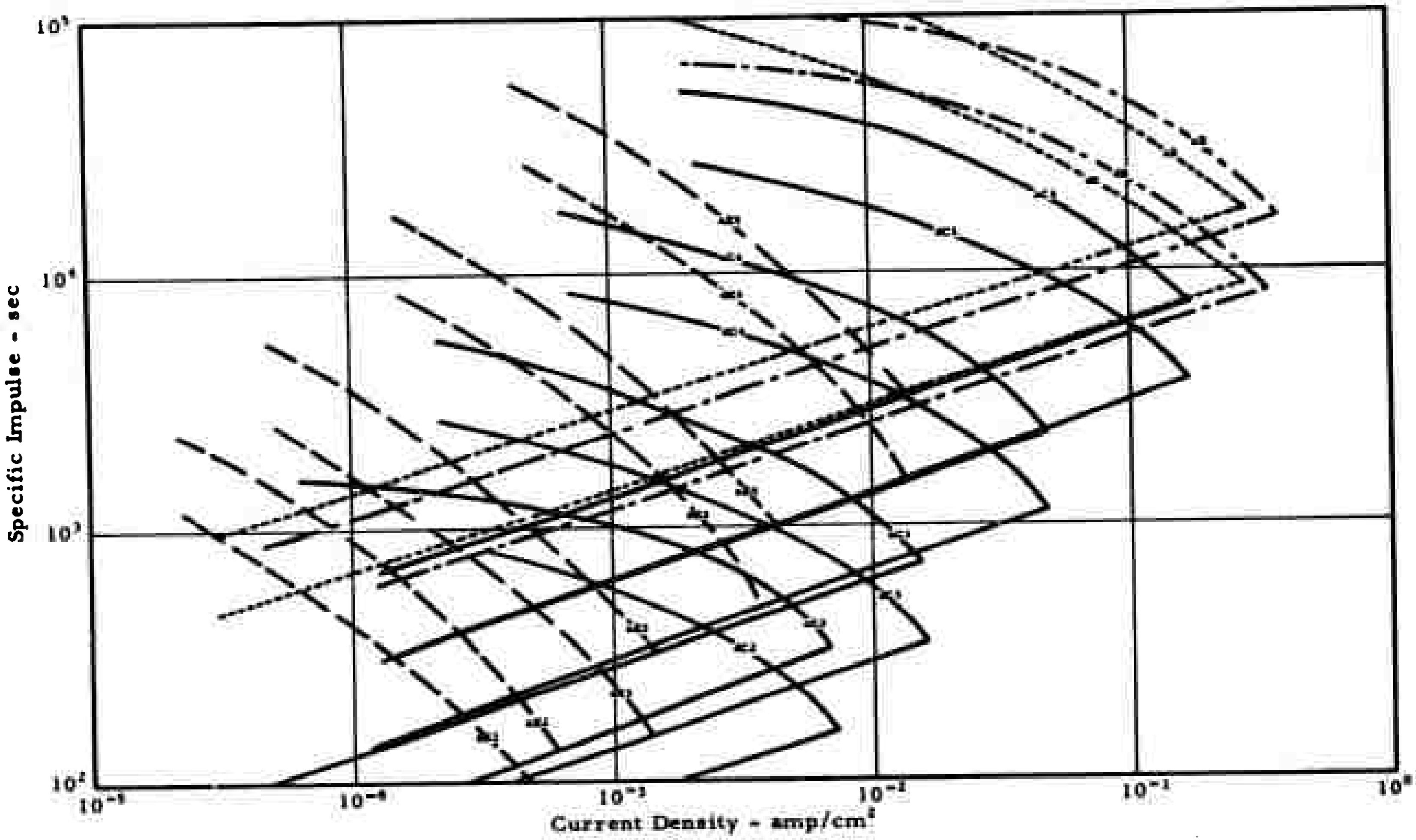

Figure 4. Relation Between Specific Impulse and Current Density

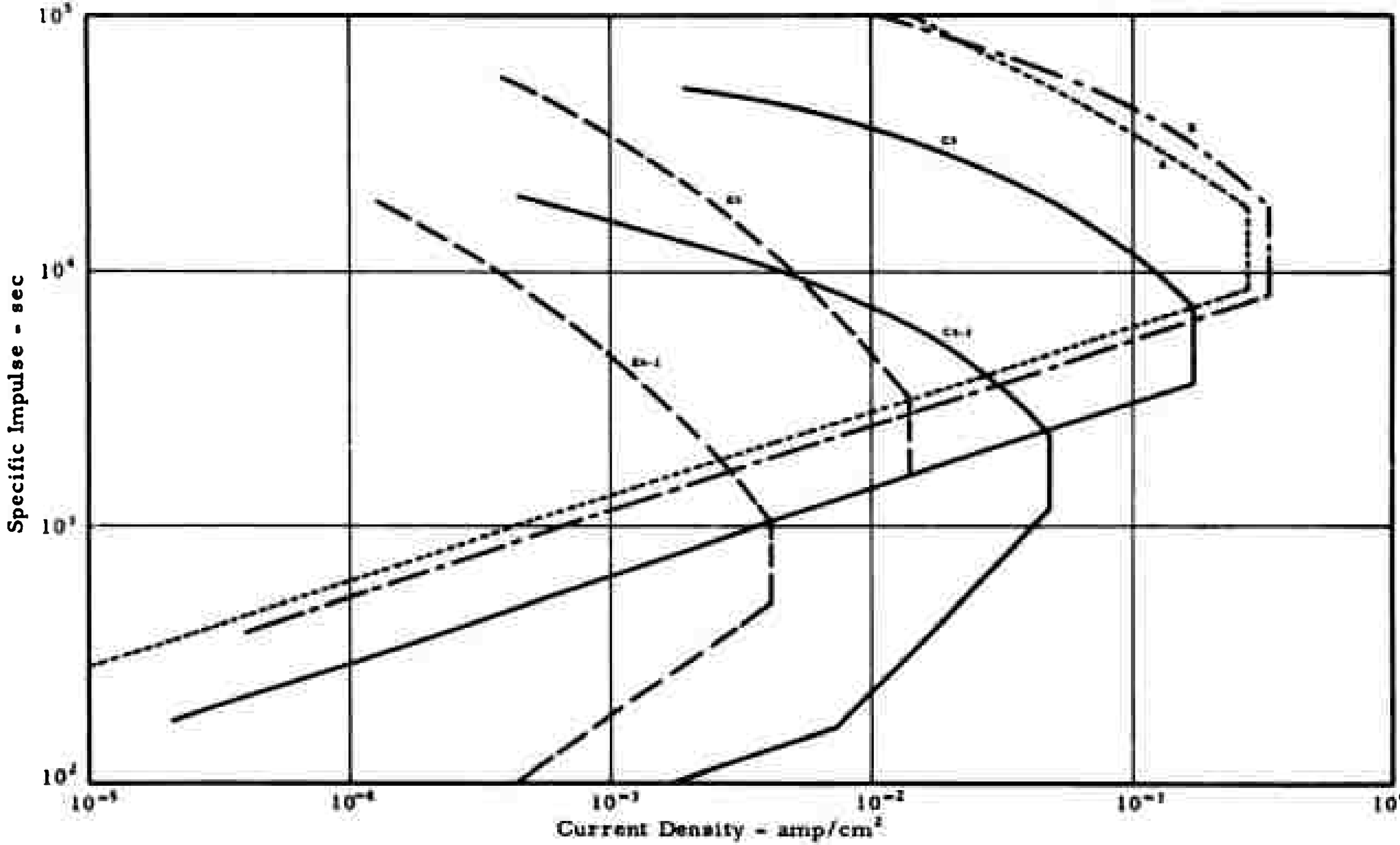

Figure 5. Overall Relations Between Specific Impulse and Current Density for Specific Engine Types

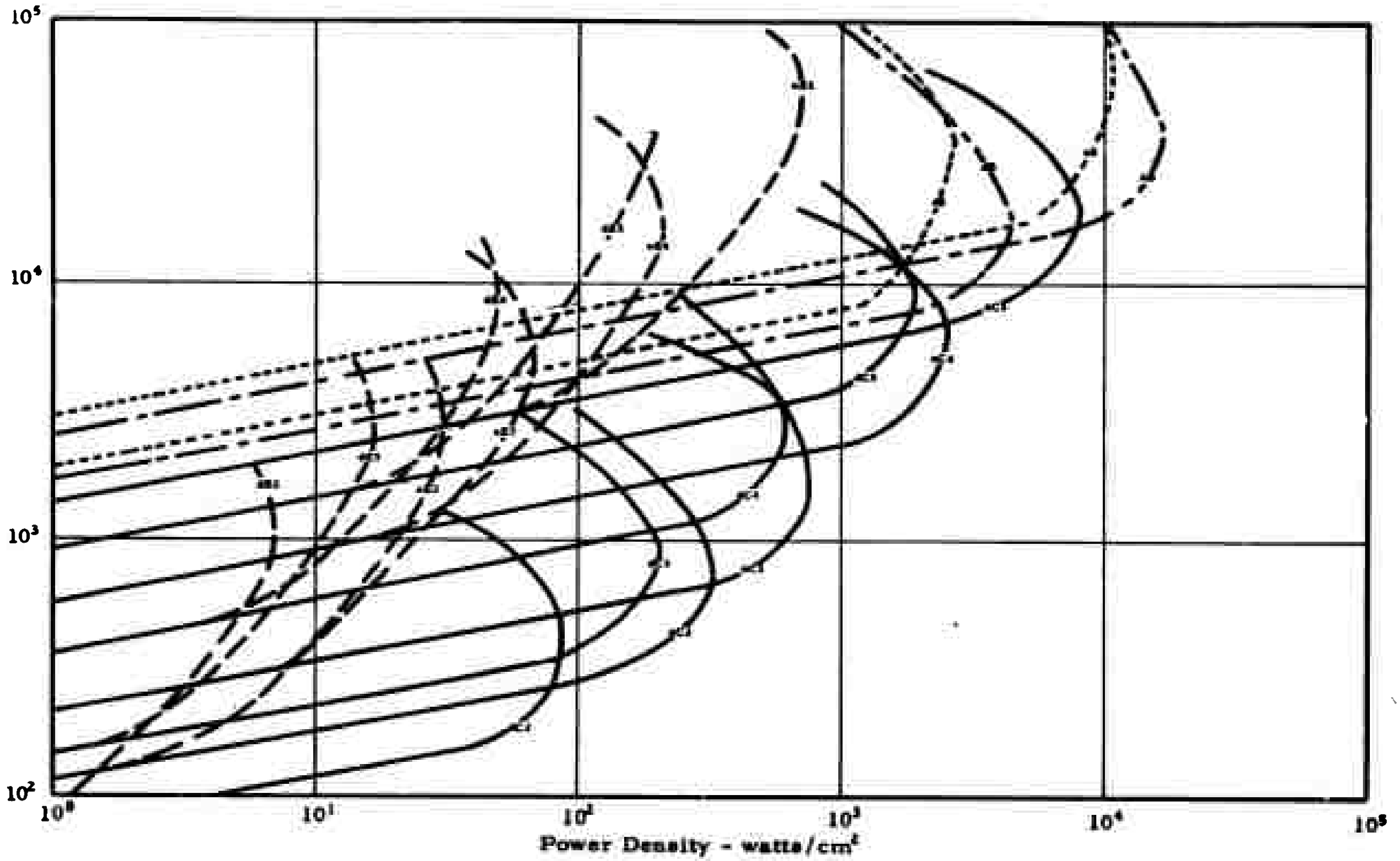

Figure 6. Relation Between Specific Impulse and Ideal Beam Power Density

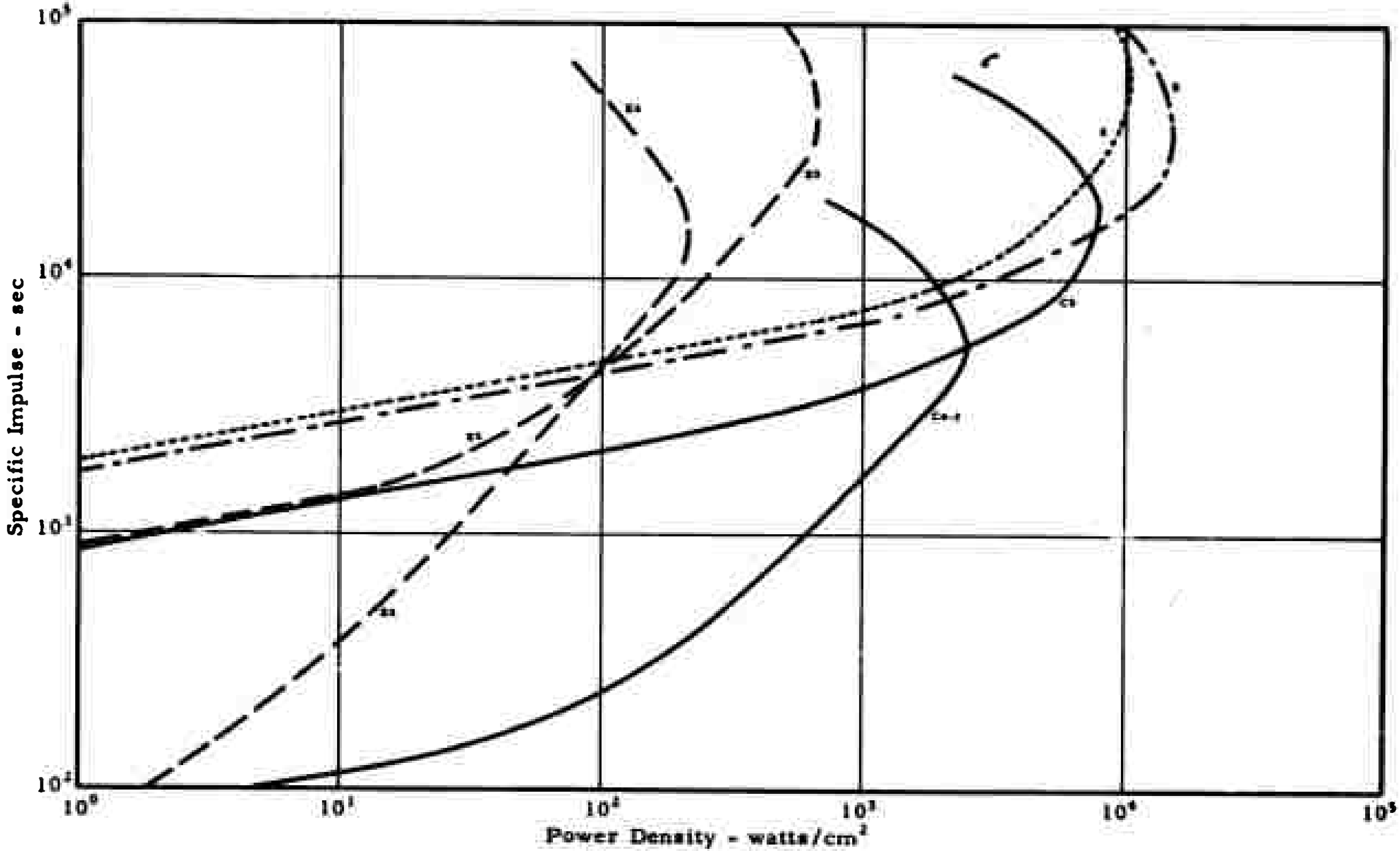

Figure 7. Overall Relations Between Specific Impulse and Ideal Power Density for Specific Engine Types

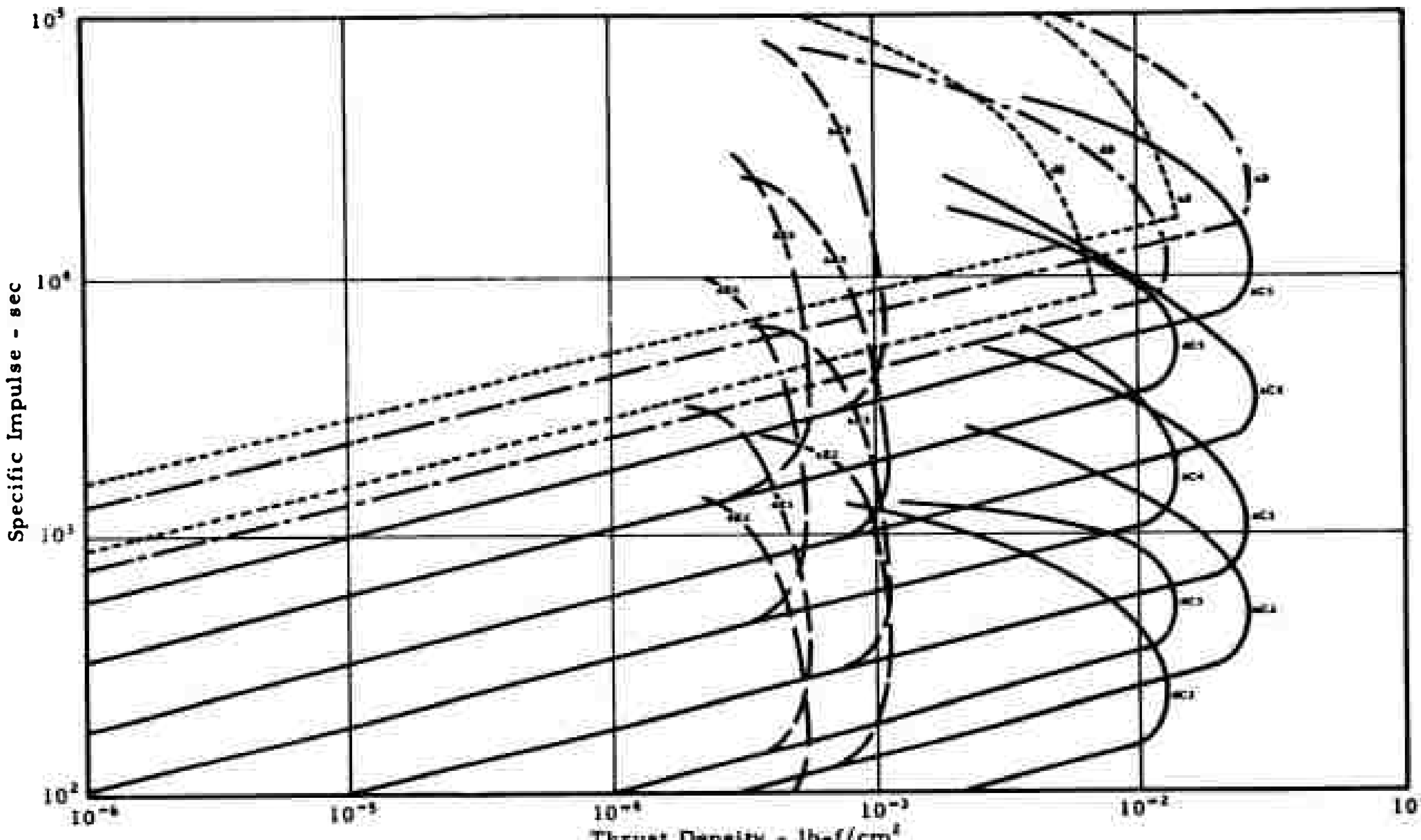

Figure 6. Relations Between Thrust Density and Specific Impulse

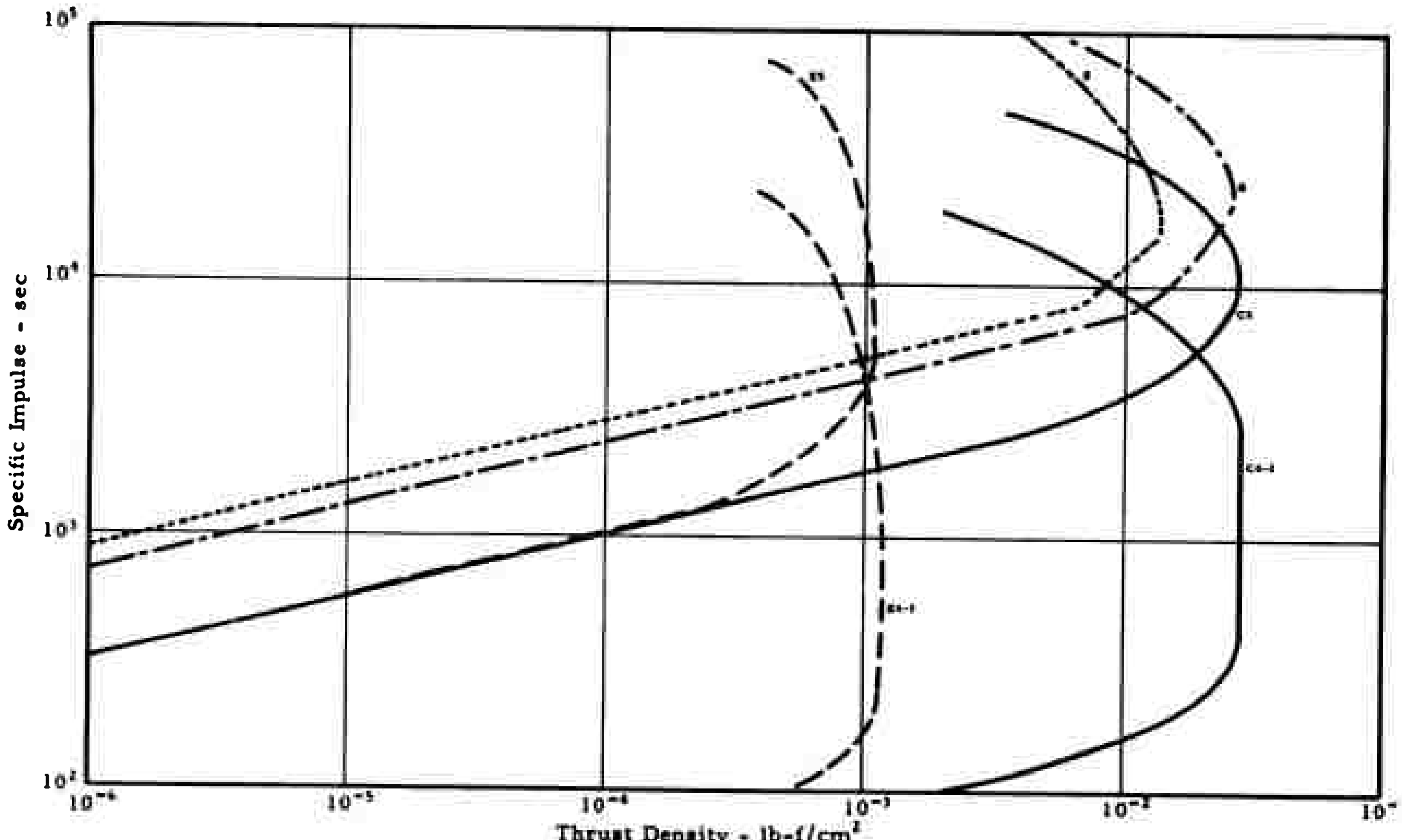

Figure 9. Overall Relations Between Specific Impulse and Thrust Density for Specific Engine Types

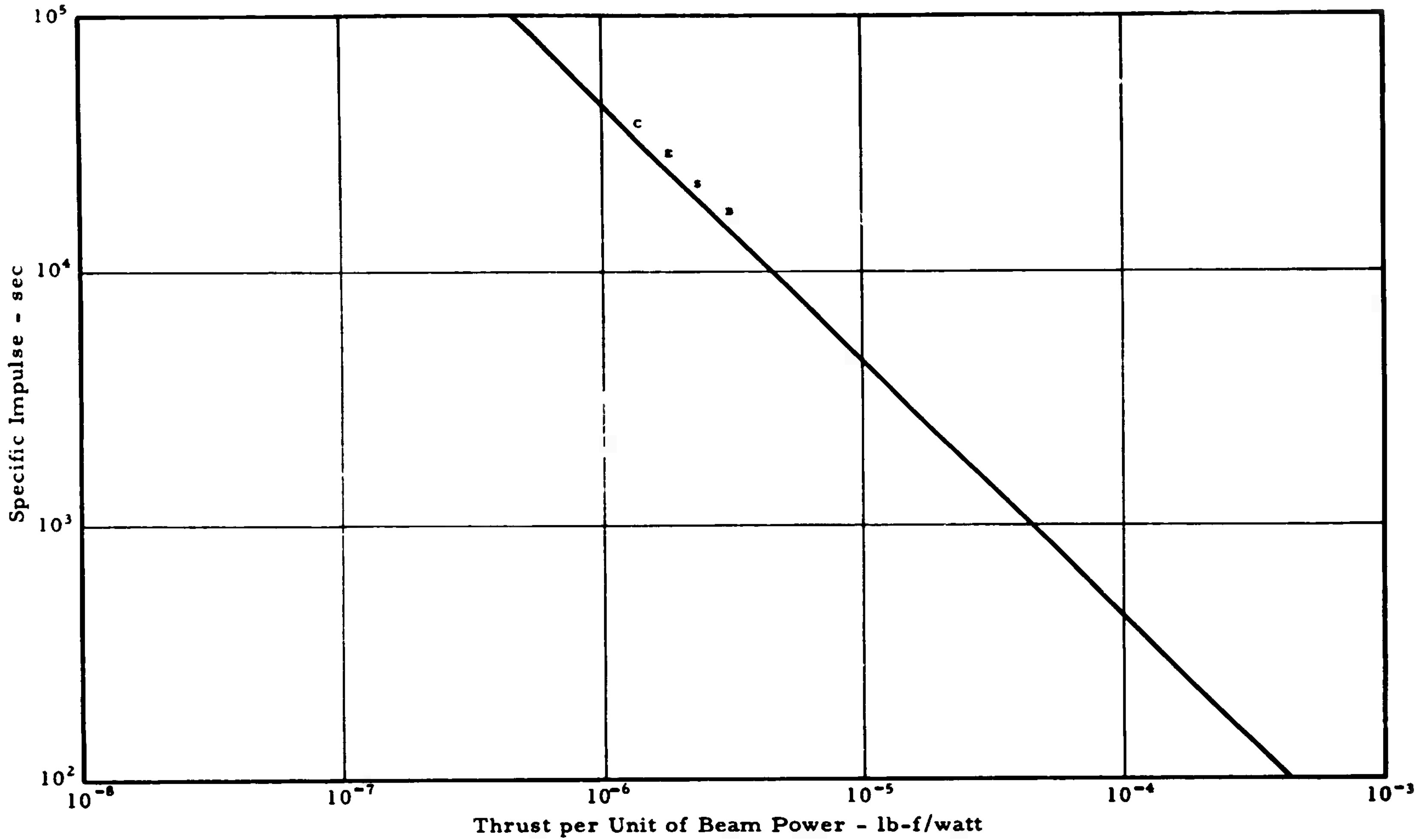

Figure 10. Relation Between Specific Impulse and Thrust-to-Beam Power Ratio

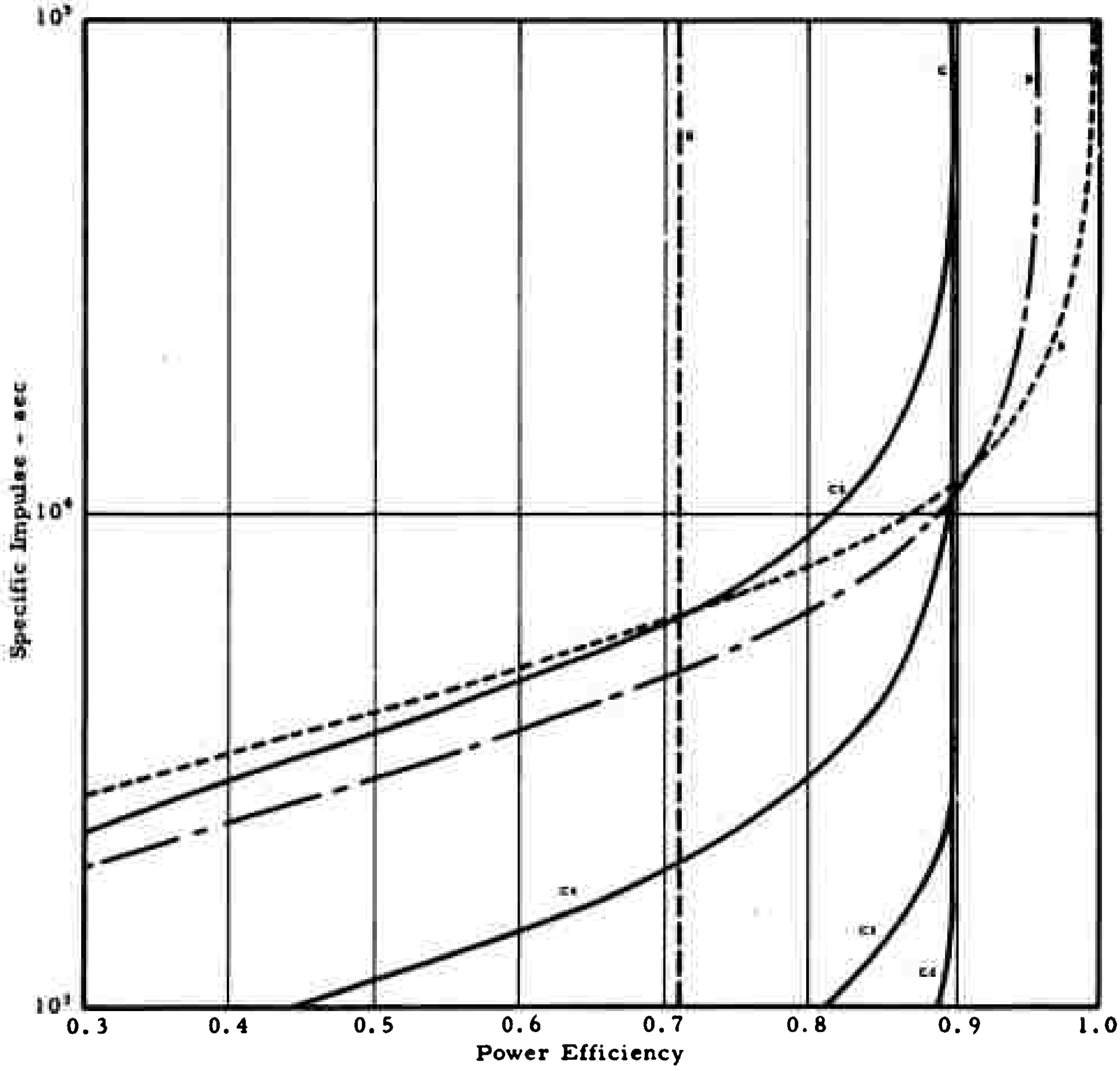

Figure 11. Relation Between Power Efficiency and Specific Impulse

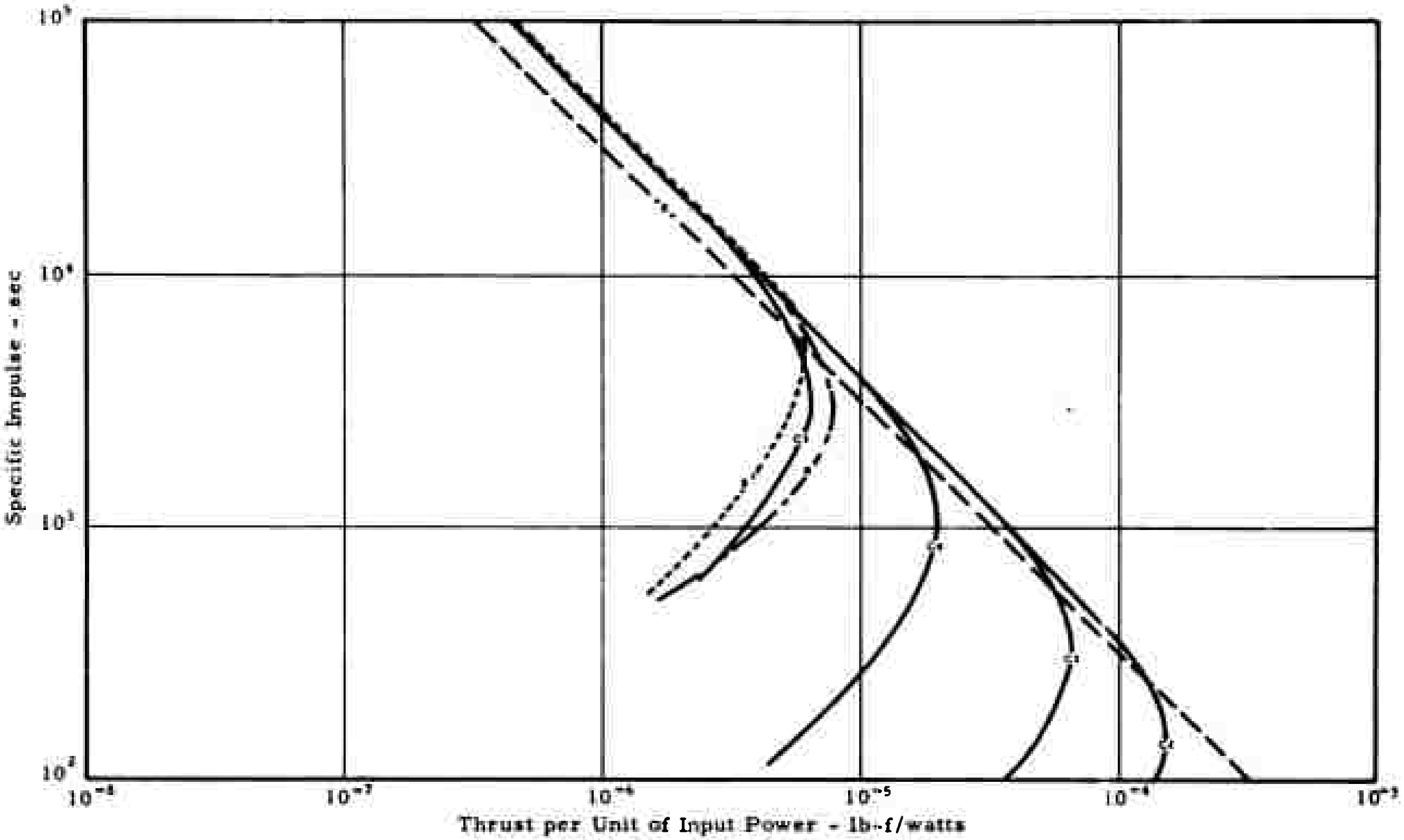

Figure 12. Relation Between Specific Impulse and Thrust-to-Input Power Ratio

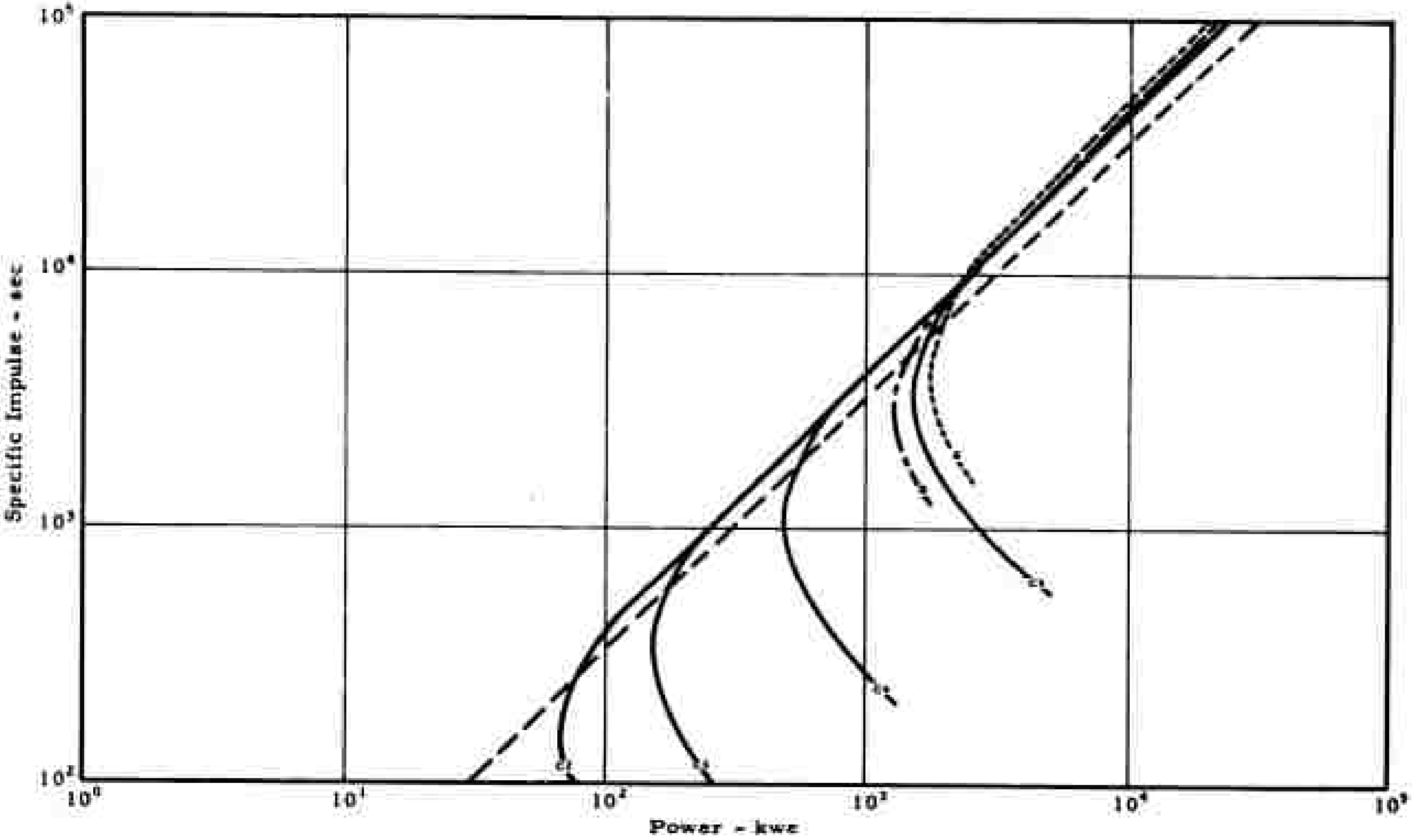

Figure 13. Input Power Requirement for Ten Pounds of Thrust

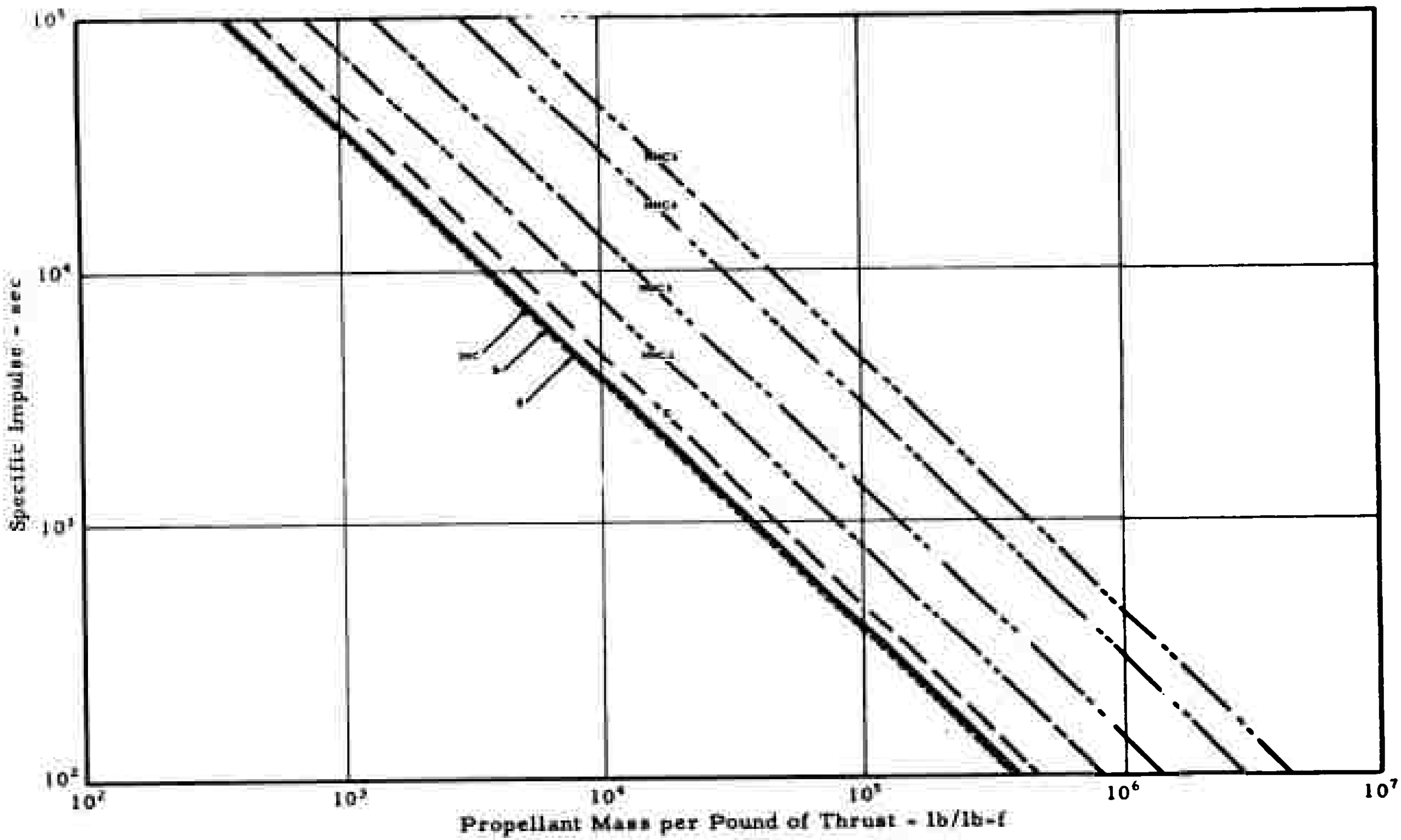

Figure 14. Ten Thousand Hour Propellant Mass Requirements for One Pound of Thrust

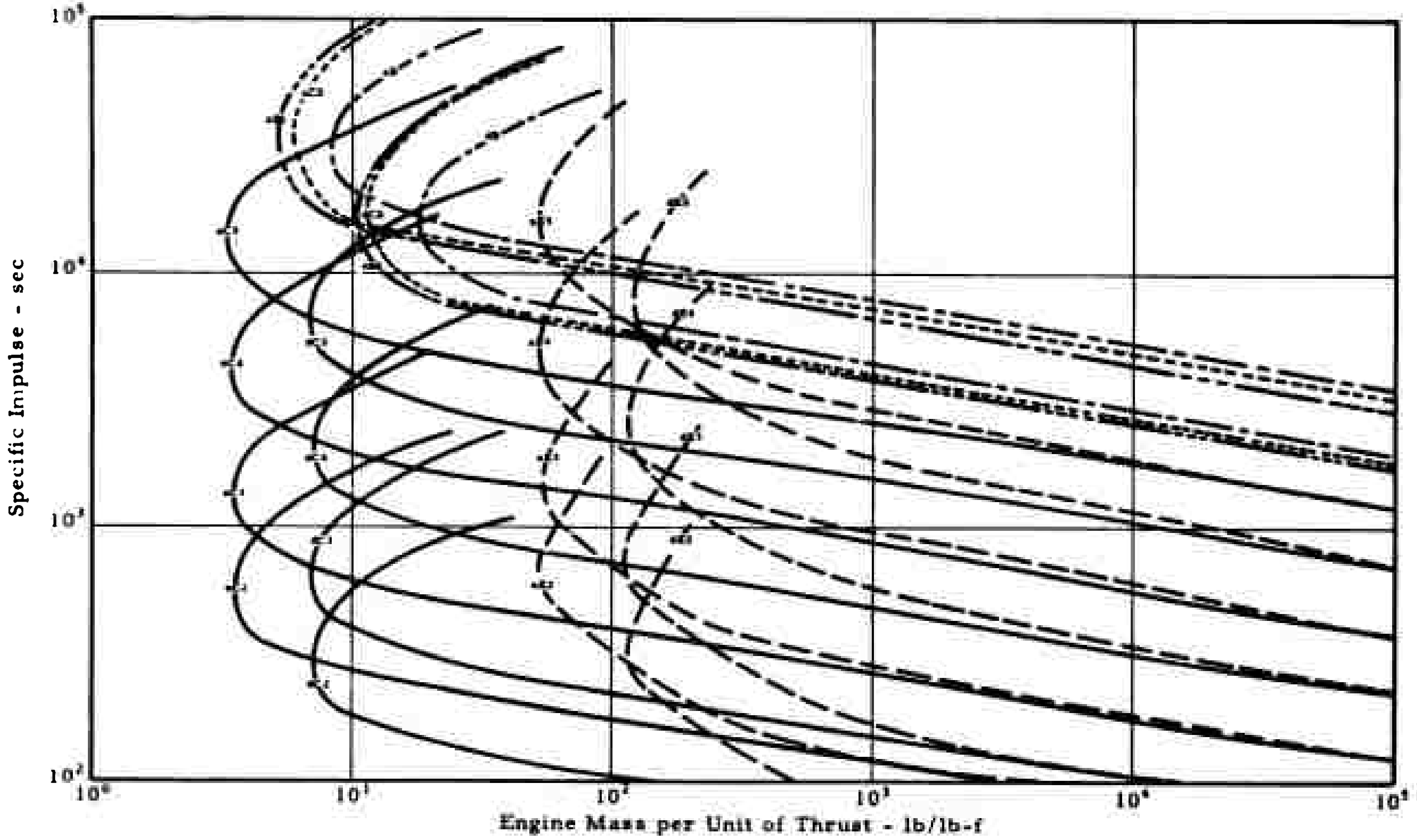

Figure 15. Relation Between Specific Impulse and Engine Mass per Pound of Thrust

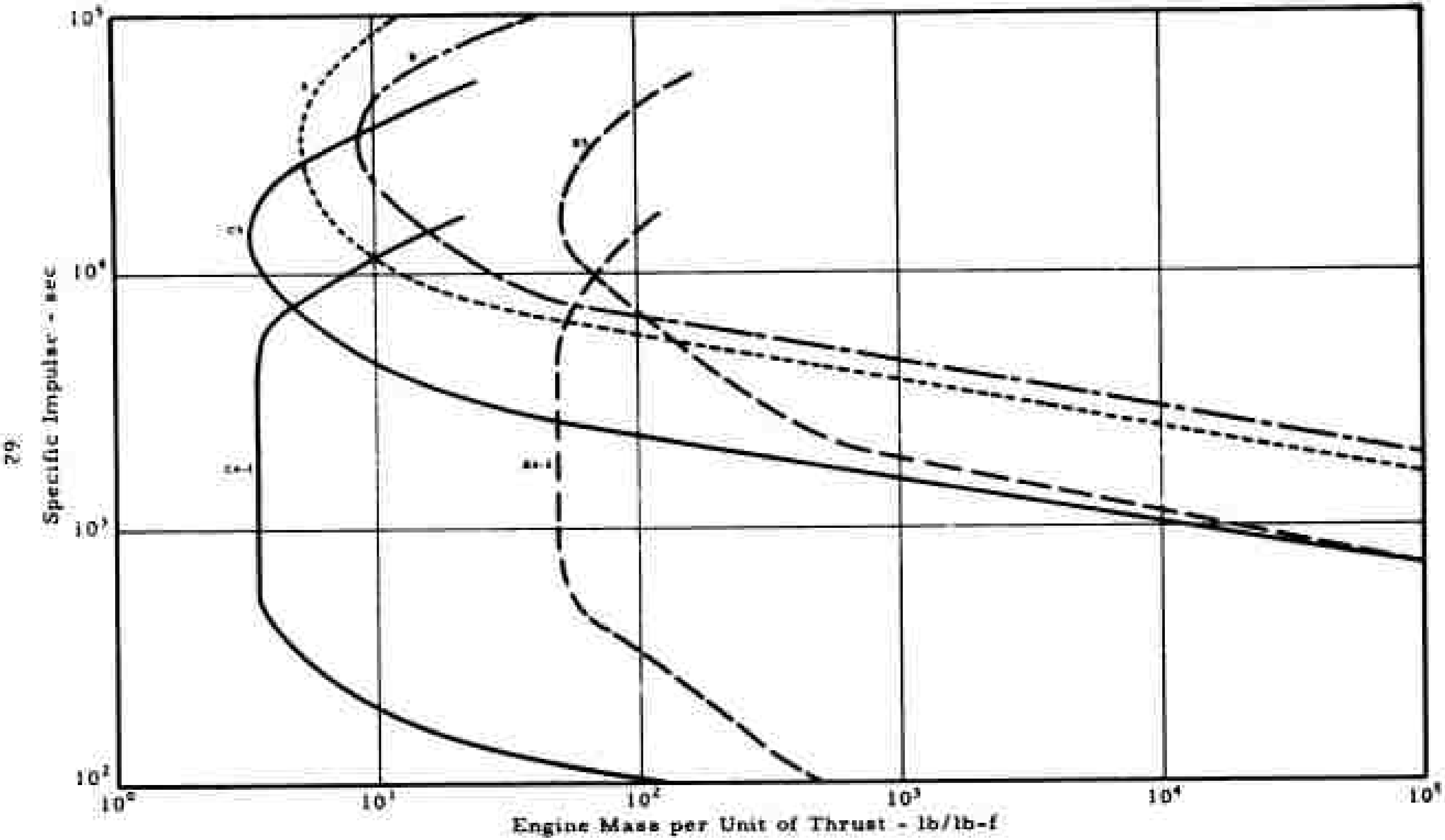

Figure 16. General Engine Mass Requirements per Pound of Thrust for Each Engine Type

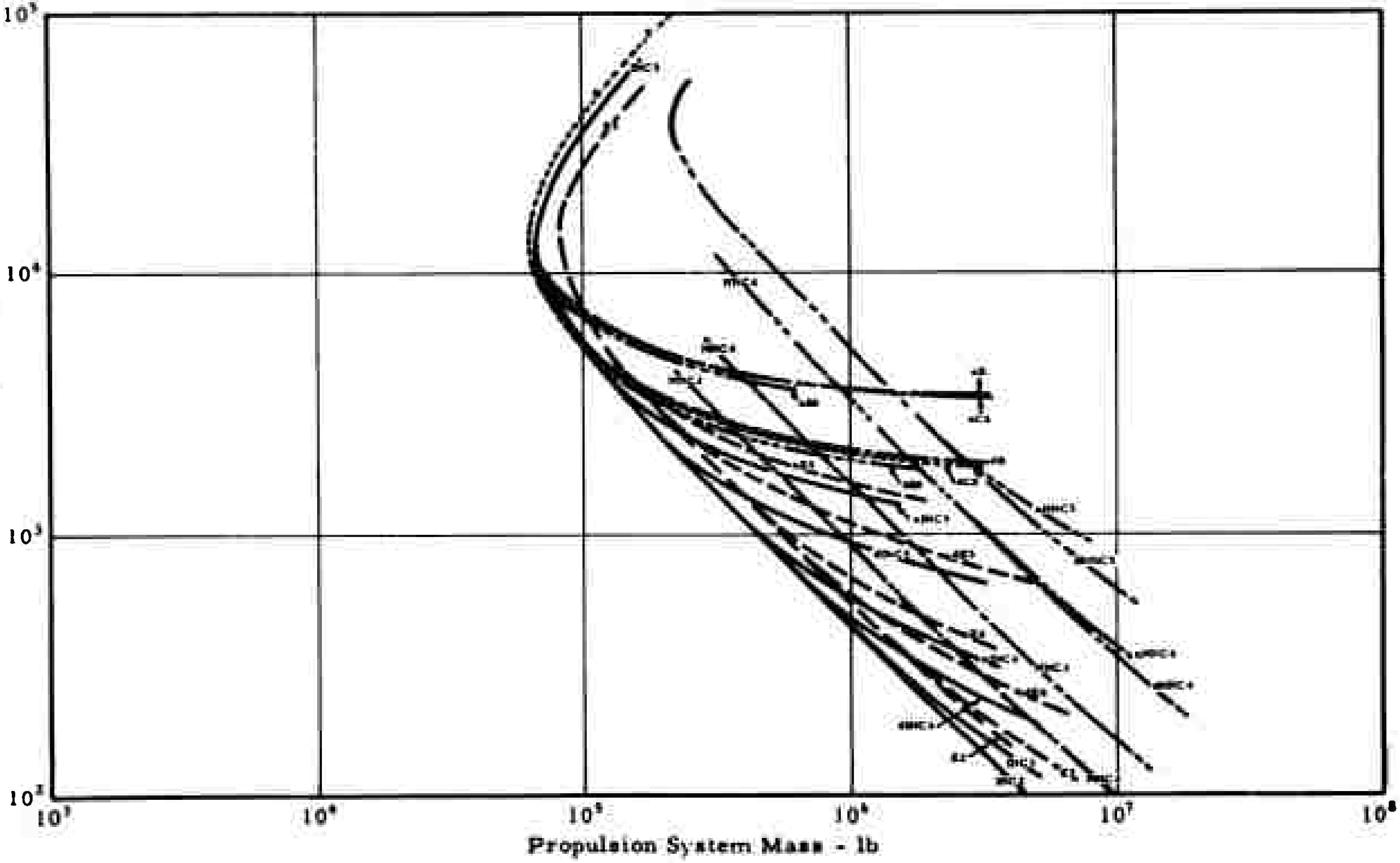

Figure 17. Total Propulsion System Mass for 10 lb-f and 10,000 hr with Power Supply Specific Mass = 10 lb/kwe

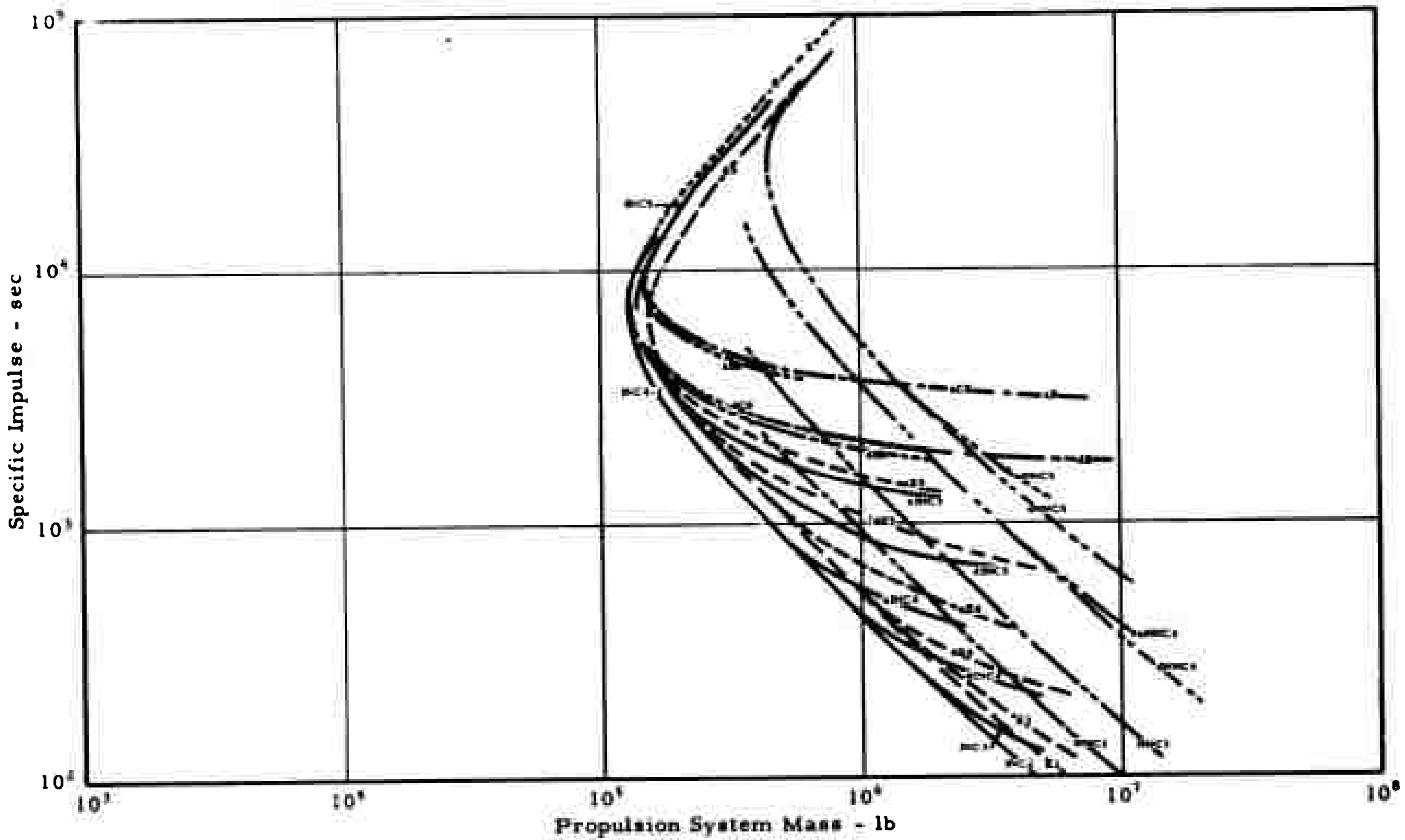

Figure 18. Total Propulsion System Mass for 10 lb-f and 10,000 hr with Power Supply Specific Mass = 40 lb/kwe

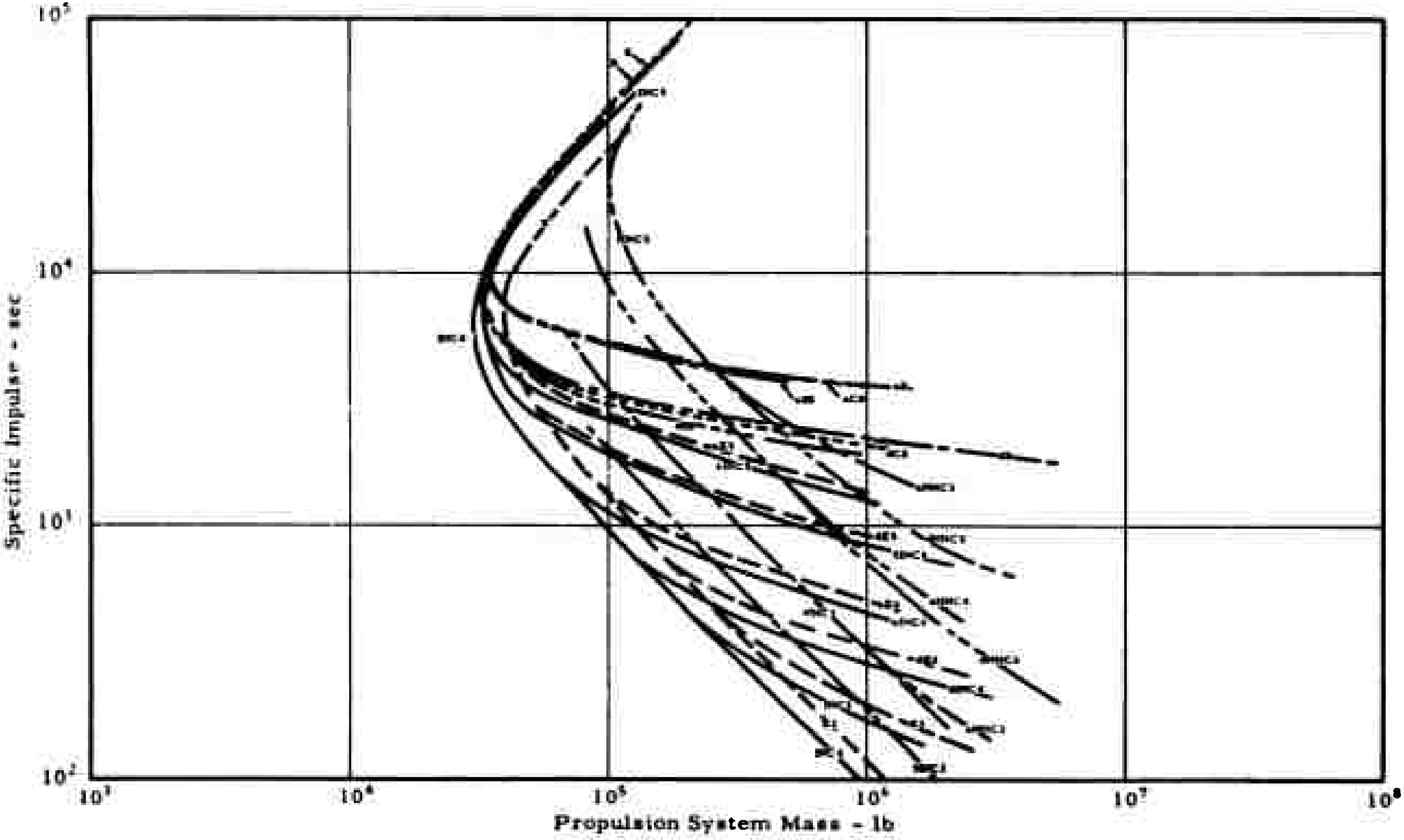

Figure 19. Total Propulsion System Mass for 10 lb-f and 2,000 hr with Power Supply Specific Mass = 10 lb/kwe

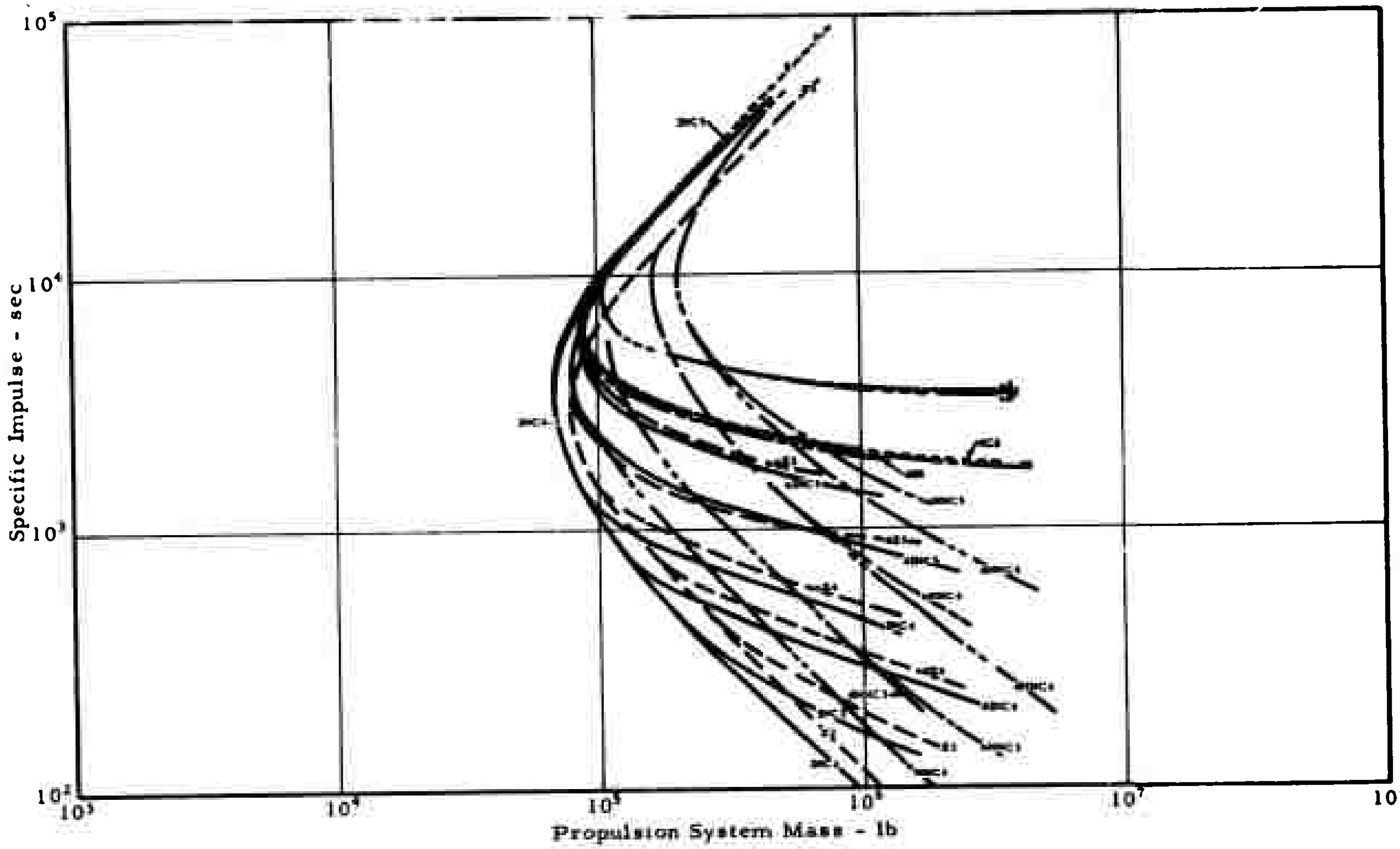

Figure 20. Total Propulsion System Mass for 10 lb-f and 2,000 hr with Power Supply Specific Mass = 40 lb/kwe

TABLES OF CALCULATED RESULTS

BLANK PAGE

TABLE I. ELECTROSTATIC PROPULSION ENGINE CHARACTERISTICS

A. ATOMIC ION ENGINES

1. Surface Contact Engines

q/m (coul/kg)	V* (v)	I_s (sec)	d (cm)	J (amp/cm²)	P_b/A_b (watts/cm²)	F/A_b (lbs-f/cm²)	F/P_b (lbs-f/watt)	$\eta = P_b/P_{in}$	F/P_{in} (lbs-f/watt)	P_m (kwe)
	1×10^3	4,000 1,980	0.20	0.37×10^{-2}	0.0037×10^3 0.00092	0.043×10^{-3} 0.022	11.6×10^{-6} 23.	0.50 0.20	5.8×10^{-6} 4.6	1.73×10^3 2.2
	5×10^3	8,800 4,400	0.20	4.2	0.21 0.052	1.07 0.54	5.2 10.3	0.83 0.56	4.3 5.8	2.3 1.75
	1×10^4	12,500 6,300	0.20	11.7	1.17 0.29	4.3 2.2	3.7 7.3	0.91 0.72	3.3 5.2	3.0 1.91
7.54×10^5	2×10^4	17,900 9,000	0.22	26.	5.3 1.32	13.7 6.8	2.6 5.2	0.95 0.83	2.5 4.3	4.1 2.3
	3×10^4	22,000 10,900	0.34	20.	6.1 1.52	13.0 6.5	2.1 4.3	0.97 0.88	2.0 3.8	4.9 2.6
	5×10^4	28,000 14,000	0.60	14.7	7.3 1.83	12.0 6.0	1.63 3.3	0.98 0.93	1.6 3.0	6.2 3.3
	1×10^5	40,000 19,800	1.28	9.0	9.0 2.3	10.5 5.2	1.16 2.3	0.99 0.96	1.14 2.2	8.7 4.5
	1×10^6	125,000 63,000	24.	0.83	8.3 2.1	3.0 1.52	0.37 0.73	1.00 1.00	0.36 0.73	27. 13.7

2. Bombardment Engines

q/m (coul/kg)	V* (v)	I_s (sec)	d (cm)	J (amp/cm²)	P_b/A_b (watts/cm²)	F/A_b (lbs-f/cm²)	F/P_b (lbs-f/watt)	$\eta = P_b/P_{in}$	F/P_{in} (lbs-f/watt)	P_m (kwe)
	1×10^3	3,200 1,610	0.20	0.30×10^{-2}	0.003×10^3 0.00075	0.043×10^{-3} 0.022	14.3×10^{-6} 29.	0.54 0.24	7.8×10^{-6} 6.8	1.28×10^3 1.48
	5×10^3	7,300 3,600	0.20	3.4	0.168 0.042	1.07 0.54	6.4 12.8	0.84 0.60	5.3 7.6	1.88 1.31
	1×10^4	10,400 5,200	0.20	9.5	0.95 0.24	4.3 2.2	4.5 9.0	0.89 0.74	4.0 6.6	2.5 1.51
5×10^5	2×10^4	14,600 7,300	0.20	27.	5.4 1.36	17.2 8.6	3.2 6.4	0.93 0.83	2.9 5.3	3.4 1.89
	3×10^4	18,000 9,000	0.25	32.	9.6 2.4	25. 12.6	2.6 5.3	0.94 0.87	2.5 4.6	4.0 2.2
	5×10^4	23,000 11,900	0.40	26.	13.1 3.3	27. 13.4	2.0 4.0	0.95 0.90	1.90 3.6	5.3 2.8
	1×10^5	32,000 16,100	0.84	16.9	16.9 4.2	24. 12.1	1.43 2.9	0.96 0.93	1.36 2.6	7.3 3.8
	1×10^6	104,000 52,000	20.	0.94	9.4 2.4	4.2 2.1	0.45 0.90	0.96 0.96	0.43 0.86	23. 11.6

V is the accelerating voltage for the ion source. The upper set of results calculated for each value of V represents the parameters and characteristics of a straight accel engine. The second set of results corresponding to each value of V represents an accel-decel engine with a 4:1 accel-decel ratio.

TABLE I. ELECTROSTATIC PROPULSION ENGINE CHARACTERISTICS (Continued)

B. CONDENSATION COLLOIDAL ION ENGINES

q/m (coul/kg)	V° (v)	I_s (sec)	d (cm)	J (amp/cm²)	P_b/A_b (watts/cm²)	F/A_b (lbs-f/cm²)	F/P_b (lbs-f/watt)	$\eta = P_b/P_{in}$	F/P_{in} (lbs-f/watt)	P_w (kwe)
	1×10^3	1,440 720	0.20	0.135×10^{-2}	0.00135×10^3 0.00034	0.043×10^{-3} 0.022	3.2×10^{-5} 6.4	0.150 0.043	4.8×10^{-6} 2.7	2.1×10^3 3.7
	1×10^4	4,600 2,300	0.20	4.3	0.43 0.107	4.3 2.2	1.00 2.0	0.60 0.30	6.0 6.0	1.66 1.66
1×10^5	2×10^4	6,500 3,200	0.20	12.1	2.4	17.2 8.6	0.71 1.42	0.72 0.45	5.0 7.0	2.0 1.44
	3×10^4	8,000 4,000	0.25	14.4	4.4 1.09	25. 12.6	0.58 1.15	0.77 0.54	4.5 6.2	2.2 1.60
	1×10^5	14,400 7,200	0.84	7.6	7.6 1.89	24. 12.1	0.32 0.64	0.86 0.75	2.7 4.8	3.7 2.1
	1×10^6	46,000 23,000	20.	0.42	4.2 1.05	4.2 2.1	0.100 0.20	0.90 0.88	0.90 1.78	11.1 5.6
	1×10^3	460 230	0.20	0.043×10^{-2}	0.0043×10^2 0.00106	0.043×10^{-3} 0.022	10.0×10^{-5} 20.	0.150 0.043	1.51×10^{-5} 0.86	0.66×10^3 1.16
	1×10^4	1,440 720	0.20	1.35	1.35 0.34	4.3 2.2	3.2 6.4	0.60 0.30	1.91 1.91	0.52 0.52
1×10^4	2×10^4	2,100 1,030	0.20	3.6	7.3 1.82	17.2 8.6	2.4 4.7	0.72 0.45	1.70 2.1	0.59 0.47
	3×10^4	2,600 1,280	0.25	4.5	13.6 3.4	25. 12.6	1.85 3.7	0.77 0.54	1.43 2.0	0.70 0.50
	1×10^5	4,600 2,300	0.84	2.4	24. 6.0	24. 12.1	1.00 2.0	0.86 0.75	0.86 1.51	1.12 0.66
	1×10^6	14,400 7,200	20.	0.133	13.3 3.3	4.2 2.1	0.32 0.64	0.90 0.88	0.28 0.56	3.5 1.78

TABLE I. ELECTROSTATIC PROPULSION ENGINE CHARACTERISTICS (Continued)

B. CONDENSATION COLLOIDAL ION ENGINES (Continued)

q/m (coul/kg)	V (v)	I_s (sec)	d (cm)	j (amp/cm²)	P_b/A_b (watts/cm²)	F/A_b (lbs-f/cm²)	F/P_b (lbs-f/watt)	$\eta = P_b/P_{in}$	F/P_{in} (lbs-f/watt)	P_{in} (kwe)
1×10^3	1×10^3	144	0.20	0.0135×10^{-2}	0.135	0.0043×10^{-2}	$32. \times 10^{-5}$	0.150	4.8×10^{-5}	0.21×10^3
		72			0.034	0.0022	64.	0.043	2.7	0.37
	1×10^4	460	0.20	0.43	43.	0.43	10.0	0.60	6.0	0.166
		230			10.7	0.22	20.	0.30	6.0	0.166
	2×10^4	650	0.20	1.21	240.	1.72	7.1	0.72	5.0	0.20
		320			60.	0.86	14.2	0.45	7.0	0.144
	3×10^4	800	0.25	1.44	430.	2.5	5.8	0.77	4.5	0.22
		400			107.	1.26	11.6	0.54	6.2	0.160
	5×10^4	1,020	0.40	1.19	600.	2.7	4.5	0.82	3.7	0.27
		510			149.	1.34	9.0	0.64	5.8	0.172
	1×10^5	1,440	0.84	0.76	760.	2.4	3.2	0.86	2.7	0.37
		720			190.	1.21	6.4	0.75	4.8	0.21
	1×10^6	4,600	20.	0.042	420.	0.42	1.00	0.90	0.90	1.11
		2,300			105.	0.21	2.0	0.88	1.78	0.56
2×10^2	1×10^3	64	0.20	0.061×10^{-1}	0.060	0.043×10^{-3}	7.1×10^{-4}	0.150	1.06×10^{-4}	0.094×10^3
		32			0.0151	0.022	14.3	0.043	0.61	0.164
	1×10^4	200	0.20	1.93	18.8	4.3	2.2	0.60	1.35	0.074
		102			4.7	2.2	4.5	0.30	1.35	0.074
	2×10^4	300	0.20	5.4	105.	17.2	1.64	0.72	1.18	0.085
		147			26.	8.6	3.3	0.45	1.47	0.070
	3×10^4	360	0.25	6.4	192.	25.	1.31	0.77	1.01	0.099
		180			48.	12.6	2.6	0.54	1.41	0.071
	1×10^5	640	0.84	3.4	340.	24.	0.71	0.86	0.61	0.164
		320			840.	12.1	1.43	0.75	1.07	0.094
	1×10^6	2,000	20.	0.188	188.	4.2	0.22	0.90	0.20	0.50
		1 020			47.	2.1	0.45	0.88	0.40	0.25

TABLE I. ELECTROSTATIC PROPULSION ENGINE CHARACTERISTICS (Continued)

C. ELECTRICAL ATOMIZATION COLLOIDAL ION ENGINE

q/m (coul/kg)	V (v)	I_s (sec)	d (cm)	J (amp/cm^2)	P_b/A_b (watts/cm^2)	F/A_b (lbs-f/cm^2)	F/P_b (lbs-f/watt)	$\eta = P_b/P_{in}$	F/P_{in} (lbs-f/watt)	P_m (kwe)
1×10^5	1×10^3	1,440 720	0.20	13.5×10^{-4}	1.35 0.34	0.43×10^{-4} 0.22	3.2×10^{-5} 6.4	0.71	2.3×10^{-5} 4.5	0.44×10^3 0.22
	1×10^4	4,600 2,300	0.40	107.	107. 27.	10.8 5.4	1.00 2.0		0.71 1.43	1.40 0.70
	2×10^4	6,500 3,200	0.78	79.	159. 40.	11.3 5.6	0.66 1.32		0.47 0.94	2.1 1.07
	3×10^4	8,000 4,000	1.21	61.	184. 46.	10.5 5.3	0.58 1.15		0.41 0.82	2.4 1.22
	1×10^5	14,400 7,200	4.1	32.	320. 80.	10.2 5.1	0.32 0.64		0.23 0.45	4.4 2.2
	1×10^6	46,000 23,000	51.	6.5	650. 163.	6.6 3.3	0.100 0.20		0.071 0.14	14.0 7.0
1×10^4	1×10^3	460 230	0.20	4.3×10^{-4}	0.43 0.11	0.43×10^{-4} 0.22	10.0×10^{-5} 20.	0.71	7.1×10^{-5} 14.3	0.140×10^3 0.070
	1×10^4	1,440 720	0.40	34.	34. 8.4	10.8 5.4	3.2 6.4		2.3 4.5	0.44 0.22
	2×10^4	2,100 1,030	0.78	25.	50. 12.6	11.3 5.6	2.4 4.7		1.60 3.3	0.63 0.30
	3×10^4	2,600 1,280	1.21	21.	62. 15.4	10.5 5.3	1.85 3.7		1.31 2.6	0.76 0.38
	1×10^5	4,600 2,300	4.1	10.1	101. 25.	10.2 5.1	1.00 2.0		0.71 1.43	1.40 0.70
	1×10^6	14,400 7,200	51.	2.1	210. 52.	6.6 3.3	0.32 0.64		0.23 0.45	4.4 2.2

TABLE I. ELECTROSTATIC PROPULSION ENGINE CHARACTERISTICS (Continued)

C. ELECTRICAL ATOMIZATION COLLOIDAL ION ENGINE (Continued)

q/m (coul/kg)	V (v)	I_s (sec)	d (cm)	J (amp/cm²)	P_b/A_b (watts/cm²)	F/A_b (lbs-f/cm²)	F/P_b (lbs-f/watt)	$\eta = P_b/P_{in}$	F/P_{in} (lbs-f/watt)	P_m (kwe)
	1×10^3	144	0.20	1.35×10^{-4}	0.135	0.43×10^{-4}	$32. \times 10^{-5}$	0.71	$23. \times 10^{-5}$	0.044×10^3
		72			0.034	0.22	64.		45.	0.022
	1×10^4	460	0.40	10.7	10.7	10.8	10.0		7.1	0.140
		230			2.7	5.4	20.		14.3	0.070
	2×10^4	650	0.78	7.9	15.9	11.3	6.9		4.9	0.20
		320			4.0	5.6	13.8		9.8	0.104
1×10^3	3×10^4	800	1.21	6.1	18.4	10.5	5.8		4.1	0.24
		400			4.6	5.3	11.6		8.2	0.122
	5×10^4	1,020	2.0	4.7	23.	10.4	4.5		3.2	0.31
		510			5.8	5.2	9.0		6.4	0.156
	1×10^5	1,440	4.1	3.2	32.	10.2	3.2		2.3	0.44
		720			8.0	5.1	6.4		4.5	0.22
	1×10^6	4,600	51.	0.65	65.	6.6	1.00		0.71	1.40
		2,300			16.3	3.3	2.0		1.43	0.70
	1×10^3	64	0.20	0.60×10^{-4}	0.06	0.43×10^{-4}	$71. \times 10^{-5}$	0.71	$51. \times 10^{-5}$	0.0198×10^3
		32			0.0151	0.22	143.		101.	0.0099
	1×10^4	200	0.40	4.8	4.8	10.8	22.		16.	0.062
		102			1.19	5.4	45.		32.	0.031
2×10^2	2×10^4	300	0.78	3.4	6.7	11.3	16.4		11.6	0.086
		150			1.68	5.6	33.		23.	0.043
	3×10^4	360	1.21	2.8	8.3	10.5	13.1		9.3	0.108
		180			2.1	5.3	26.		18.6	0.054
	1×10^5	640	4.1	1.44	14.4	10.2	7.1		5.1	0.198
		320			3.6	5.1	14.3		10.1	0.099
	1×10^6	2,000	51.	0.29	29.	6.6	2.2		1.60	0.63
		1,020			7.3	3.3	4.5		3.2	0.31

A. ATOMIC ION ENGINES

1. Strip Surface Contact Engine

q/m (coul/kg)	V* (v)	I_s (sec)	M_f/A_b (lbs/10,000 hrs-cm^2)	M_f/F (lbs/lb-f)	A_e/A_b	M_e/A_b (lbs/cm^2)	M_e/F (lbs/lb-f)	A_e/F (cm^2/lb-f)	M_{fs}/F (lbs/lb-f)	$1.1\,(M_e/F + M_{fs}/F)$ (lbs/lb-f)
	1×10^3	4,000	0.40	9.4×10^3	40.	1.22	28,000.	$9,400. \times 10^2$	18,000.	51,000.
		1,980		18.7		1.41	66,000.	18,800.	44,000.	129,000.
	5×10^3	8,800	4.5	4.2	9.4	0.28	260.	87.	40.	330.
		4,400		8.4		0.32	600.	175.	97.	760.
	1×10^4	12,500	12.7	3.0	5.5	0.165	39.	12.7	3.3	47.
		6,300		5.9		0.184	86.	25.	8.2	103.
7.54×10^5	2×10^4	17,900	29.	2.1	3.5	0.106	7.8	2.6	0.41	9.0
		9,000		4.2		0.116	17.0	5.2	1.01	20.
	3×10^4	22,000	22.	1.70	2.9	0.088	6.7	2.2	0.34	8.0
		10,900		3.4		0.094	14.5	4.5	0.84	18.0
	5×10^4	28,000	15.9	1.32	2.4	0.072	6.0	1.98	0.29	7.0
		14,000		2.6		0.076	12.6	4.0	0.72	15.0
	1×10^5	40,000	9.8	0.94	2.0	0.061	5.8	1.90	0.28	7.0
		19,800		1.88		0.063	12.0	3.8	0.65	14.0
	1×10^6	125,000	0.90	0.30	1.60	0.069	23.	5.4	1.07	26.
		63,000		0.59		0.069	45.	10.8	2.6	53.

2. Bombardment Engines

q/m (coul/kg)	V* (v)	I_s (sec)	M_f/A_b (lbs/10,000 hrs-cm^2)	M_f/F (lbs/lb-f)	A_e/A_b	M_e/A_b (lbs/cm^2)	M_e/F (lbs/lb-f)	A_e/F (cm^2/lb-f)	M_{fs}/F (lbs/lb-f)	$1.1\,(M_e/F + M_{fs}/F)$ (lbs/lb-f)
	1×10^3	3,200	0.51	11.9×10^3	260.	6.8	158,000.	$5,900. \times 10^3$	189,000.	380,000.
		1,610		24.		8.0	370,000.	11,900.	460,000.	920,000.
	5×10^3	7,300	5.7	5.3	55.	1.46	1,360.	51.	390.	1,900.
		3,600		10.7		1.71	3,200.	102.	980.	4,600.
	1×10^4	10,400	16.2	3.8	30.	0.80	186.	7.0	29.	240.
		5,200		7.6		0.92	430.	14.0	72.	550.
5×10^5	2×10^4	14,600	46.	2.7	17.5	0.47	27.	1.02	2.4	32.
		7,300		5.4		0.53	62.	2.0	5.9	75.
	3×10^4	18,000	54.	2.2	13.3	0.36	14.1	0.53	1.04	16.0
		9,000		4.3		0.40	32.	1.06	2.6	37.
	5×10^4	23,000	45.	1.66	10.0	0.27	9.9	0.37	0.71	12.0
		11,900		3.3		0.28	21.	0.74	1.15	24.
	1×10^5	32,000	29.	1.19	7.5	0.20	8.3	0.31	0.52	99.
		16,100		2.4		0.21	17.6	0.62	0.98	21.
	1×10^6	104,000	1.60	0.38	5.2	0.192	45.	1.24	3.1	53.
		52,000		0.76		0.193	91.	2.5	5.0	106.

* V is the accelerating voltage for the ion source. The upper set of results calculated for each value of V represents the parameters and characteristics of a straight accel engine. The second set of results corresponding to each value of V represents an accel-decel engine with a 4:1 accel-decel ratio.

set of results corresponding to each value of V represents an accel-decel engine with a 4:1 accel-decel ratio.

TABLE 11. THRUSTOR COMPONENT WEIGHTS (Continued)

A. ATOMIC ION ENGINES (Continued)

3. Sastrugi Surface Contact Engine

q/m (coul/kg)	V (v)	I_s (sec)	M_f/A_b (lbs/10,000 hrs-cm²)	M_f/F (lbs/lb-f)	A_e/A_b	M_e/A_b (lbs/cm²)	M_e/F (lbs/lb-f)	A_e/F (cm²/lb-f)	M_{fs}/F (lbs/lb-f)	$1.1\,(M_e/F + M_{fs}/F)$ (lbs/lb-f)
	1×10^3	4,000 1,980	0.40	9.4×10^3 18.7	27.	0.80 0.93	18,600. 43,000.	$6{,}200. \times 10^2$ 12,400	9,930. 25,000.	31,000. 74,000.
	5×10^3	8,800 4,400	4.5	4.2 8.4	6.6	0.198 0.22	185. 420.	62. 123.	25. 62.	230. 530.
	1×10^4	12,500 6,300	12.7	3.0 5.9	4.1	0.123 0.136	29. 63.	9.5 19.1	2.2 5.5	34. 75.
$7.54 \times 10^{[illegible]}$	2×10^4	17,900 9,000	29.	2.1 4.2	2.8	0.086 0.102	6.3 15.0	2.1 4.2	0.30 0.75	7.0 18.0
	3×10^4	22,000 10,900	22.	1.7 3.4	2.4	0.073 0.078	5.7 11.9	1.87 3.7	0.27 0.60	7.0 14.0
	5×10^4	28,000 14,000	15.9	1.32 2.6	2.1	0.064 0.066	5.3 11.0	1.74 3.5	0.24 0.60	6.0 13.0
	1×10^5	40,000 19,800	4.8	0.94 1.88	1.85	0.057 0.058	5.4 11.1	1.77 3.5	0.25 0.61	6.0 13.0
	1×10^6	125,000 63,000	[illegible]	0.30 0.59	1.62	0.068 0.068	22. 45.	5.4 10.7	1.06 2.6	25. 53.

B. CONDENSATION COLLOIDAL ION ENGINE

1. Ionic Nucleation

q/m (coul/kg)	V (v)	I_s (sec)	M_f/A_b (lbs/10,000 hrs-cm²)	M_f/F (lbs/lb-f)	A_e/A_b	M_e/A_b (lbs/cm²)	M_e/F (lbs/lb-f)	A_e/F (cm²/lb-f)	M_{fs}/F (lbs/lb-f)	$1.1\,(M_e/F + M_{fs}/F)$ (lbs/lb-f)
	1×10^3	1,440 720	1.19	$28. \times 10^3$ 55.	40.	1.62 1.81	38,000. 84,000.	$9{,}400. \times 10^2$ 18,800.	27,000. 66,000.	71,000. 166,000.
	1×10^4	4,600 2,300	38.	8.8 17.5	5.5	0.22 0.24	51. 111.	12.7 25.	4.9 12.3	62. 136.
1×10^5	2×10^4	6,500 3,200	106.	6.2 12.4	3.5	0.140 0.150	8.3 17.6	2.1 4.1	0.54 7.1	10.0 27.
	3×10^4	8,000 4,000	127.	5.1 10.1	2.9	0.116 0.133	4.6 10.5	1.15 2.3	0.22 0.53	5.0 12.0
	1×10^5	14,400 7,200	67.	2.8 5.5	1.99	0.080 0.082	3.3 6.8	0.82 1.70	0.137 0.34	4.0 8.0
	1×10^6	46,000 23,000	3.7	0.88 1.75	1.64	0.082 0.082	19.4 39.	3.9 7.7	1.04 2.6	22. 46.

TABLE II. THRUSTOR COMPONENT WEIGHTS (Continued)

1. Ionic Nucleation (Continued)

q/m (coul/kg)	V (v)	I_s (sec)	M_f/A_b (lbs/10,000 hrs-cm²)	M_f/F (lbs/lb-f)	A_e/A_b	M_e/A_b (lbs/cm²)	M_e/F (lbs/lb-f)	A_e/F (cm²/lb-f)	M_{fs}/F (lbs/lb-f)	$1.1\ (M_e/F + M_{fs}/F)$ (lbs/lb-f)
	1×10^3	460 230	3.8	8.8×10^4 17.5	40.	1.62 1.81	38,000. 84,000.	$9,400. \times 10^2$ 18,800.	27,000. 66,000.	71,000. 156,000.
	1×10^4	1,440 720	117.	2.8 5.5	5.5	0.22 0.24	51. 111.	12.7 25.	4.9 12.3	62. 136.
1×10^4	2×10^4	2,100 1,030	320.	1.87 3.8	3.5	0.140 0.150	8.3 17.6	2.1 4.1	0.54 7.1	10.0 27.
	3×10^4	2,600 1,280	400.	1.59 3.2	2.9	0.116 0.133	4.6 10.5	1.15 2.3	0.22 0.53	5.0 12.0
	1×10^5	4,600 2,300	210.	0.86 1.73	1.99	0.080 0.082	3.3 6.8	0.82 1.70	0.137 0.34	4.0 8.0
	1×10^6	14,400 7,200	11.2	0.26 0.53	1.64	0.082 0.082	19.4 39.	3.9 7.7	1.04 2.6	22. 46.
	1×10^3	144 72	11.9	$28. \times 10^4$ 55.	40.	1.62 1.81	38,000. 84,000.	$9,400. \times 10^2$ 18,800.	27,000. 66,000.	71,000. 166,000.
	1×10^4	460 230	380.	8.8 17.5	5.5	0.22 0.24	51. 111.	12.7 25.	4.9 12.3	62. 136.
	2×10^4	650 320	1,060.	6.2 12.4	3.5	0.140 0.150	8.3 17.6	2.1 4.1	0.54 7.1	10.0 27.
1×10^3	3×10^4	800 400	1,270.	5.1 10.1	2.9	0.116 0.133	4.6 10.5	1.15 2.3	0.22 0.53	5.0 12.0
	5×10^4	1,020 510	1,050.	4.0 7.8	2.4	0.096 0.100	3.6 7.4	0.88 1.78	0.152 0.38	4.0 9.0
	1×10^5	1,440 720	670.	2.8 5.5	1.99	0.080 0.082	3.3 6.8	0.82 1.70	0.137 0.34	4.0 8.0
	1×10^6	4,600 2,300	37.	0.88 1.75	1.64	0.082 0.082	19.4 39.	3.9 7.7	1.04 2.6	22. 46.

TABLE II. THRUSTOR COMPONENT WEIGHTS (Continued)

1. Ionic Nucleation (Continued)

q/m (coul/kg)	V (v)	I_s (sec)	M_f/A_b (lbs/10,000 hrs-cm²)	M_f/F (lbs/lb-f)	A_e/A_b	M_e/A_b (lbs/cm²)	M_e/F (lbs/lb-f)	A_e/F (cm²/lb-f)	M_{fs}/F (lbs/lb-f)	$1.1\,(M_e/F + M_{fs}/F)$ (lbs/lb-f)
	1×10^3	65	27.	6.3×10^5	40.	1.62	38,000.	$9,400. \times 10^2$	27,000.	71,000.
		32		12.5		1.81	84,000.	18,800.	66,000.	166,000.
	1×10^4	200	850.	1.98	5.5	0.22	51.	12.7	4.9	62.
		102		4.0		0.24	111.	25.	12.3	136.
2×10^2	2×10^4	300	2,400.	1.40	3.5	0.140	8.3	2.1	0.54	10.0
		147		2.8		0.150	17.6	4.1	7.1	27.
	3×10^4	360	2,800.	1.12	2.9	0.116	4.6	1.15	0.22	5.0
		180		2.2		0.133	10.5	2.3	0.53	12.0
	1×10^5	640	1,490.	0.62	1.99	0.080	3.3	0.82	0.137	4.0
		320		1.23		0.082	6.8	1.70	0.34	8.0
	1×10^6	2,000	83.	0.20	1.64	0.082	19.4	3.9	1.04	22.
		1,020		0.39		0.082	39.	7.7	2.6	46.

2. Neutral Nucleation

q/m (coul/kg)	V (v)	I_s (sec)	M_f/A_b (lbs/10,000 hrs-cm²)	M_f/F (lbs/lb-f)	A_e/A_b	M_e/A_b (lbs/cm²)	M_e/F (lbs/lb-f)	A_e/F (cm²/lb-f)	M_{fs}/F (lbs/lb-f)	$1.1\,(M_e/F + M_{fs}/F)$ (lbs/lb-f)
	$1 \quad 10^3$	1,440	13.6	3.2×10^5	40.	1.62	38,000.	$9,400. \times 10^2$	18,000.	61,000.
		720		6.3		1.81	84,000.	18,800.	44,000.	141,000.
	1×10^4	4,600	430.	1.00	5.5	0.22	51.	12.7	3.3	60.
		2,300		2.0		0.24	111.	25.	8.2	131.
1×10^5	2×10^4	6,500	1,220.	0.71	3.5	0.140	8.3	2.1	0.36	9.0
		3,200		1.42		0.150	17.6	4.1	4.7	22.
	3×10^4	8,000	1,450.	0.58	2.9	0.116	4.6	1.15	0.143	5.0
		4,000		1.15		0.133	10.5	2.3	0.35	12.0
	1×10^5	14,400	760.	0.32	1.99	0.080	3.3	0.82	0.092	4.0
		7,200		0.63		0.082	6.8	1.70	0.23	8.0
	1×10^6	46,000	42.	0.100	1.64	0.082	19.4	3.9	0.69	22.
		23,000		0.20		0.082	39.	7.7	1.72	45.

TABLE 11. THRUSTOR COMPONENT WEIGHTS (Continued)

2. Neutral Nucleation (Continued)

q/m (coul/kg)	V (v)	I_s (sec)	M_f/A_b (lbs/10,000 hrs-cm^2)	M_f/F (lbs/lb-f)	A_e/A_b	M_e/A_b (lbs/cm^2)	M_e/F (lbs/lb-f)	A_e/F (cm^2/lb-f)	M_{fs}/F (lbs/lb-f)	$1.1\,(M_e/F + M_{fs}/F)$ (lbs/lb-f)
	1×10^3	460	29.	6.8 $\times 10^5$	40.	1.62	38,000.	9,400. $\times 10^2$	18,000.	61,000.
		230		13.5		1.81	84,000.	18,800.	44,000.	141,000.
	1×10^4	1,440	920.	2.2	5.5	0.22	51.	12.7	3.3	60.
		720		4.3		0.24	111.	25.	8.2	131.
1×10^4	2×10^4	2,100	2,500.	1.45	3.5	0.140	8.3	2.1	0.36	9.0
		1,030		2.9		0.150	17.6	4.1	4.7	22.
	3×10^4	2,600	3,100.	1.23	2.9	0.116	4.6	1.15	0.143	5.0
		1,280		2.4		0.133	10.5	2.3	0.35	12.0
	1×10^5	4,600	1,640.	0.68	1.99	0.080	3.3	0.82	0.092	4.0
		2,300		1.36		0.082	6.8	1.70	0.23	8.0
	1×10^6	14,400	91.	0.21	1.64	0.082	19.4	3.9	0.69	22.
		7,200		0.43		0.082	39.	7.7	1.72	45.
	1×10^3	144	43.	10.0 $\times 10^5$	40.	1.62	38,000.	9,400. $\times 10^2$	18,000.	61,000.
		72		20.		1.81	84,000.	18,800.	44,000.	141,000.
	1×10^4	460	1,360	3.2	5.5	0.22	51.	12.7	3.3	60.
		230		6.3		0.24	111.	25.	8.2	131.
	2×10^4	650	3,800.	2.2	3.5	0.140	8.3	2.1	0.36	9.0
		320		4.5		0.150	17.6	4.1	4.7	22.
1×10^3	3×10^4	800	4,600.	1.82	2.9	0.116	4.6	1.15	0.143	5.0
		400		3.6		0.133	10.5	2.3	0.35	12.0
	5×10^4	1,020	3,800.	1.40	2.4	0.096	3.6	0.88	0.101	4.0
		510		2.8		0.100	7.4	1.78	0.25	8.0
	1×10^5	1,440	2,400.	1.00	1.99	0.080	3.3	0.82	0.092	4.0
		720		1.99		0.082	6.8	1.70	0.23	8.0
	1×10^6	4,600	133.	0.32	1.64	0.082	19.4	3.9	0.69	22.
		2,300		0.63		0.082	39.	7.7	1.72	45.

TABLE II. THRUSTOR COMPONENT WEIGHTS (Continued)

2. Neutral Nucleation (Continued)

q/m (coul/kg)	V (v)	I_s (sec)	M_f/A_b (lbs/10,000 hrs-cm^2)	M_f/F (lbs/lb-f)	A_e/A_b	M_e/A_b (lbs/cm^2)	M_e/F (lbs/lb-f)	A_e/F (cm^2/lb-f)	M_{fs}/F (lbs/lb-f)	1.1 $(M_e/F + M_{fs}/F)$ (lbs/lb-f)
	1×10^3	65	57.	13.2×10^5	40.	1.62	38,000.	$9,400. \times 10^2$	18,000.	61,000.
		32		26.		1.81	84,000.	18,800.	44,000.	141,000.
	1×10^4	200	1,790.	4.2	5.5	0.22	51.	12.7	3.3	60.
		102		8.4		0.24	111.	25.	8.2	131.
2×10^2	2×10^4	300	5,100.	2.9	3.5	0.140	8.3	2.1	0.36	9.0
		147		5.9		0.150	17.6	4.1	4.7	22.
	3×10^4	360	5,900.	2.4	2.9	0.116	4.6	1.15	0.143	5.0
		180		4.7		0.133	10.5	2.3	0.35	12.0
	1×10^5	640	3,100.	1.30	1.99	0.080	3.3	0.82	0.092	4.0
		320		2.6		0.082	6.8	1.70	0.23	8.0
	1×10^6	2,000	174.	0.41	1.64	0.082	19.4	3.9	0.69	22.
		1,020		0.82		0.082	39.	7.7	1.72	45.

C. ELECTRICAL ATOMIZATION COLLOIDAL ION ENGINE

q/m (coul/kg)	V (v)	I_s (sec)	M_f/A_b (lbs/10,000 hrs-cm^2)	M_f/F (lbs/lb-f)	A_e/A_b	M_e/A_b (lbs/cm^2)	M_e/F (lbs/lb-f)	A_e/F (cm^2/lb-f)	M_{fs}/F (lbs/lb-f)	1.1 $(M_e/F + M_{fs}/F)$ (lbs/lb-f)
	1×10^3	1,440	1.48	$34. \times 10^3$	101.	2.0	$470. \times 10^2$	$2,400. \times 10^3$	57,000.	115,000.
		720		69.		2.5	1,180.	4,700.	142,000.	290,000.
	1×10^4	4,600	11.7	10.9	11.3	0.23	2.1	10.5	50.	290.
		2,300		22.		0.28	5.2	21.	125.	710.
1×10^5	2×10^4	6,500	8.7	7.7	6.3	0.129	1.14	5.6	22.	150.
		3,200		15.4		0.154	2.7	11.2	55.	360.
	3×10^4	8,000	6.7	6.4	4.7	0.096	0.91	4.4	16.5	118.
		4,000		12.8		0.113	2.1	8.9	40.	280.
	1×10^5	14,400	3.5	3.4	2.3	0.051	0.50	2.3	6.9	63.
		7,200		6.9		0.056	1.10	4.6	17.1	140.
	1×10^6	46,000	0.72	1.09	1.43	0.065	0.99	2.2	6.5	116.
		23,000		2.1		0.066	1.99	4.3	15.7	240.

TABLE II. THRUSTOR COMPONENT WEIGHTS (Continued)

C. ELECTRICAL ATOMIZATION COLLOIDAL ION ENGINE (Continued)

q/m (coul/kg)	V (v)	I_s (sec)	M_f/A_b (lbs/10,000 hrs-cm²)	M_f/F (lbs/lb-f)	A_e/A_b	M_e/A_b (lbs/cm²)	M_e/F (lbs/lb-f)	A_e/F (cm²/lb-f)	M_{fs}/F (lbs/lb-f)	$1.1\,(M_e/F + M_{fs}/F)$ (lbs/lb-f)
1×10^4	1×10^3	460 230	4.7	10.9×10^4 22.	101.	2.0 2.5	470. $\times 10^2$ 1,180.	2,400. $\times 10^3$ 4,700.	57,000. 142,000.	115,000. 290,000.
	1×10^4	1,440 720	37.	3.4 6.9	11.3	0.23 0.28	2.1 5.2	10.5 21.	50. 125.	290. 710.
	2×10^4	2,100 1,030	28.	2.4 4.9	6.3	0.129 0.154	1.14 2.7	5.6 11.2	22. 55.	150. 360.
	3×10^4	2,600 1,280	23.	2.1 4.3	4.7	0.096 0.113	0.91 2.1	4.4 8.9	16.5 40.	118. 280.
	1×10^5	4,600 2,300	11.1	1.09 2.2	2.3	0.051 0.056	0.50 1.10	2.3 4.6	6.9 17.1	63. 140.
	1×10^6	14,400 7,200	2.3	0.34 0.69	1.43	0.065 0.066	0.99 1.99	2.2 4.3	6.5 15.7	116. 240.
1×10^3	1×10^3	144 72	14.8	34. $\times 10^4$ 69.	101.	2.0 2.5	470. $\times 10^2$ 1,180.	2,400. $\times 10^3$ 4,700.	57,000. 142,000.	115,000. 290,000.
	1×10^4	460 230	117.	10.9 22.	11.3	0.23 0.28	2.1 5.2	10.5 21.	50. 125.	290. 710.
	2×10^4	650 320	87.	7.7 15.5	6.3	0.129 0.154	1.14 2.7	5.6 11.2	22. 55.	150. 360.
	3×10^4	800 400	67.	6.4 12.8	4.7	0.096 0.113	0.91 2.1	4.4 8.9	16.5 40.	118. 280.
	5×10^4	1,020 510	51.	4.9 9.9	3.3	0.070 0.080	0.67 1.54	3.2 6.4	10.7 26.	86. 200.
	1×10^5	1,440 720	35.	3.4 6.9	2.3	0.051 0.056	0.50 1.10	2.3 4.6	6.9 17.1	63. 140.
	1×10^6	4,600 2,300	7.2	1.09 2.2	1.43	0.065 0.066	0.99 1.99	2.2 4.3	6.5 15.7	116. 240.

TABLE 11. THRUSTOR COMPONENT WEIGHTS (Continued)

C. ELECTRICAL ATOMIZATION COLLOIDAL ION ENGINE (Continued)

q/m (coul/kg)	V (v)	I_s (sec)	M_f/A_b (lbs/10,000 hrs-cm^2)	M_f/F (lbs/lb-f)	A_e/A_b	M_e/A_b (lbs/cm^2)	M_e/F (lbs/lb-f)	A_e/F (cm^2/lb-f)	M_{fs}/F (lbs/lb-f)	$1.1\,(M_e/F + M_{fs}/F)$ (lbs/lb-f)
	1×10^3	64	33.	7.7×10^3	101.	2.0	$470. \times 10^2$	$2,400. \times 10^3$	57,000.	115,000.
		32		15.4		2.5	1,180.	4,700.	142,000.	290,000.
	1×10^4	200	260.	2.4	11.3	0.23	2.1	10.5	50.	290.
		102		4.9		0.28	5.2	21.	125.	710.
2×10^2	2×10^4	300	184.	1.63	6.3	0.129	1.14	5.6	22.	150.
		147		3.3		0.154	2.7	11.2	55.	360.
	3×10^4	360	152.	1.45	4.7	0.096	0.91	4.4	16.5	118.
		180		2.9		0.113	2.1	8.9	40.	280.
	1×10^5	640	79.	0.77	2.3	0.051	0.50	2.3	6.9	63.
		320		1.54		0.056	1.10	4.6	17.1	140.
	1×10^6	2,000	16.0	0.24	1.43	0.065	0.99	2.2	6.5	116.
		1,020		0.49		0.066	1.99	4.3	15.7	240.

TABLE III. TOTAL PROPULSION SYSTEM WEIGHTS FOR TEN POUNDS OF THRUST FOR TEN THOUSAND HOURS OF ENGINE OPERATION

A. ATOMIC ION ENGINES

1. Strip Surface Contact Engine

q/m (coul/kg)	V* (v)	I_s (sec)	M_p/P_e = 10 lbs/kwe: M_p (lbs)	M_p/P_e = 10 lbs/kwe: M_{tot} (lbs)	M_p/P_e = 20 lbs/kwe: M_p (lbs)	M_p/P_e = 20 lbs/kwe: M_{tot} (lbs)	M_p/P_e = 30 lbs/kwe: M_p (lbs)	M_p/P_e = 30 lbs/kwe: M_{tot} (lbs)	M_p/P_e = 40 lbs/kwe: M_p (lbs)	M_p/P_e = 40 lbs/kwe: M_{tot} (lbs)
	1×10^3	4,000	17.3×10^3	640×10^3	$35. \times 10^3$	660×10^3	$52. \times 10^3$	680×10^3	$69. \times 10^3$	690×10^3
		1,980	22.	1,530	43.	1,550	65.	1,570	86.	1,590
	5×10^3	8,800	23.	75	46.	98	70.	121	93.	145
		4,400	17.5	122	35.	140	52.	157	70.	174
	1×10^4	12,500	30.	65	60.	95	90.	125	120.	155
		6,300	19.1	88	38.	107	57.	126	76.	145
7.54×10^5	2×10^4	17,900	41.	65	81.	106	122.	146	162.	187
		9,000	23.	72	46.	95	70.	118	93.	142
	3×10^4	22,000	49.	69	98.	118	147.	167	196.	220
		10,900	26.	66	53.	92	80.	119	106.	146
	5×10^4	28,000	62.	78	125.	140	188.	200	250.	270
		14,000	33.	64	65.	97	99.	129	132.	163
	1×10^5	40,000	87.	98	175.	185	260.	270	350.	360
		19,800	45.	67	90.	112	135.	157	180.	200
	1×10^6	125,000	270.	280	550.	550	810.	830	1,100.	1,100
		63,000	137.	140	270.	280	410.	420	550.	550

2. Bombardment Engine

q/m (coul/kg)	V* (v)	I_s (sec)	M_p/P_e = 10 lbs/kwe: M_p (lbs)	M_p/P_e = 10 lbs/kwe: M_{tot} (lbs)	M_p/P_e = 20 lbs/kwe: M_p (lbs)	M_p/P_e = 20 lbs/kwe: M_{tot} (lbs)	M_p/P_e = 30 lbs/kwe: M_p (lbs)	M_p/P_e = 30 lbs/kwe: M_{tot} (lbs)	M_p/P_e = 40 lbs/kwe: M_p (lbs)	M_p/P_e = 40 lbs/kwe: M_{tot} (lbs)
	1×10^3	3,200	12.8×10^3	$4,000 \times 10^3$	$26. \times 10^3$	$4,000 \times 10^3$	$39. \times 10^3$	$4,000 \times 10^3$	$51. \times 10^3$	$4,000 \times 10^3$
		1,610	14.8	9,400	30.	9,500	44.	9,500	59.	9,500
	5×10^3	7,300	18.8	98	38.	116	56.	135	75.	154
		3,600	13.1	178	26.	192	39.	200	53.	220
	1×10^4	10,400	25.	70	30.	74	74.	119	99.	144
		5,200	15.1	105	30.	120	45.	136	60.	151
5×10^5	2×10^4	14,600	34.	64	68.	98	102.	132	136.	166
		7,300	18.9	80	38.	99	57.	118	76.	137
	3×10^4	18,000	40.	65	81.	105	121.	146	162.	186
		9,000	22.	71	44.	92	65.	114	87.	136
	5×10^4	23,000	53.	71	105.	124	158.	176	210.	230
		11,900	28.	65	55.	92	83.	120	110.	147
	1×10^5	32,000	73.	88	147.	161	220.	230	290.	310
		16,100	38.	65	75.	102	113.	140	151.	178
	1×10^6	104,000	230.	240	460.	470	700.	700	930.	930
		52,000	116.	126	230.	240	350.	360	460.	470

* V is the accelerating voltage for the ion source. The upper set of results calculated for each value of V represents the parameters and characteristics of a straight accel engine. The second set of results corresponding to each value of V represents an accel-decel engine with a 4:1 accel-decel ratio.

TABLE III. TOTAL PROPULSION SYSTEM WEIGHTS FOR TEN POUNDS OF THRUST FOR TEN THOUSAND HOURS OF ENGINE OPERATION (Continued)

3. Sastrugi Surface Contact Engine

q/m (coul/kg)	V (v)	I_s (sec)	M_p/P_e = 10 lbs/kwe: M_p (lbs)	M_p/P_e = 10 lbs/kwe: $M_{tot\ s}$ (lbs)	M_p/P_e = 20 lbs/kwe: M_p (lbs)	M_p/P_e = 20 lbs/kwe: $M_{tot\ s}$ (lbs)	M_p/P_e = 30 lbs/kwe: M_p (lbs)	M_p/P_e = 30 lbs/kwe: $M_{tot\ s}$ (lbs)	M_p/P_e = 40 lbs/kwe: M_p (lbs)	M_p/P_e = 40 lbs/kwe: $M_{tot\ s}$ (lbs)
	1×10^3	4,000	17.3×10^3	440×10^3	$35. \times 10^3$	460×10^3	$52. \times 10^3$	470×10^3	$69. \times 10^3$	490×10^3
		1,980	22.	980	43.	1,000	65.	1,020	86.	1,050
	5×10^3	8,800	23.	74	46.	97	70.	120	93.	144
		4,400	17.5	120	35.	137	52.	155	70.	172
	1×10^4	12,500	30.	64	60.	95	90.	125	120.	155
		6,300	19.1	88	38.	107	57.	126	76.	145
7.54×10^5	2×10^4	17,900	41.	65	81.	106	122.	146	162.	186
		9,000	23.	72	46.	95	70.	119	93.	142
	3×10^4	22,000	49.	69	98.	118	147.	167	196.	220
		10,900	26.	66	53.	92	80.	119	106.	146
	5×10^4	28,000	62.	78	125.	140	188.	200	250.	260
		14,000	33.	64	66.	96	99.	129	132.	162
	1×10^5	40,000	87.	98	175.	186	260.	270	350.	360
		19,800	45.	67	90.	112	135.	157	180.	200
	1×10^6	125,000	270.	280	550.	550	820.	820	1,100.	1,100
		63,000	137.	144	270.	280	410.	420	550.	560

B. CONDENSATION COLLOIDAL ION ENGINE

1. Ionic Nucleation

q/m (coul/kg)	V (v)	I_s (sec)	M_p/P_e = 10 lbs/kwe: M_p (lbs)	M_p/P_e = 10 lbs/kwe: $M_{tot\ s}$ (lbs)	M_p/P_e = 20 lbs/kwe: M_p (lbs)	M_p/P_e = 20 lbs/kwe: $M_{tot\ s}$ (lbs)	M_p/P_e = 30 lbs/kwe: M_p (lbs)	M_p/P_e = 30 lbs/kwe: $M_{tot\ s}$ (lbs)	M_p/P_e = 40 lbs/kwe: M_p (lbs)	M_p/P_e = 40 lbs/kwe: $M_{tot\ s}$ (lbs)
	1×10^3	1,440	$21. \times 10^3$	$1,030 \times 10^3$	$42. \times 10^3$	$1,050 \times 10^3$	$63. \times 10^3$	$1,070 \times 10^3$	$84. \times 10^3$	$1,090 \times 10^3$
		720	37.	2,300	74	2,300	110.	2,400	147.	2,400
	1×10^4	4,600	16.6	117	33.	134	50.	150	66.	170
		2,300	16.6	210	33.	230	50.	240	66.	260
1×10^5	2×10^4	6,500	20.	91	40.	111	60.	131	81.	152
		3,200	14.4	156	29.	170	43.	185	58.	199
	3×10^4	8,000	22.	80	45.	103	67.	125	90.	147
		4,000	16.0	131	32.	147	48.	163	64.	179
	1×10^5	14,400	37.	68	74.	105	110.	142	147.	178
		7,200	21.	84	42.	105	63.	126	84.	147
	1×10^6	46,000	111.	121	220.	230	330.	343	440.	450
		23,000	56.	76	113.	133	169.	189	230.	240

TABLE III. TOTAL PROPULSION SYSTEM WEIGHTS FOR TEN POUNDS OF THRUST FOR TEN THOUSAND HOURS OF ENGINE OPERATION (Continued)

1. Ionic Nucleation (Continued)

q/m	V	I_s	M_p/P_e = 10 lbs/kwe		M_p/P_e = 20 lbs/kwe		M_p/P_e = 30 lbs/kwe		M_p/P_e = 40 lbs/kwe	
(coul k_g)	(v)	(sec)	M_p (lbs)	$M_{tot\,m}$ (lbs)	M_p (lbs)	$M_{tot\,m}$ (lbs)	M_p (lbs)	$M_{tot\,m}$ (lbs)	M_p (lbs)	$M_{tot\,m}$ (lbs)
	1×10^3	460	6.6×10^3	$1,720 \times 10^3$	13.3×10^3	$1,730 \times 10^3$	19.9×10^3	$1,730 \times 10^3$	$26. \times 10^3$	$1,740 \times 10^3$
		230	11.6	3,700	23.	3,700	35.	3,700	46.	3,700
	1×10^4	1,440	5.2	320	10.5	330	15.7	330	21.	340
		720	5.2	640	10.5	650	15.7	650	21.	660
1×10^4	2×10^4	2,100	5.9	220	11.8	230	17.7	230	24.	240
		1,030	4.7	430	9.5	440	14.2	440	18.9	450
	3×10^4	2,600	7.0	188	14.0	196	21.	200	28.	210
		1,280	5.0	370	10.0	370	15.0	380	20.	380
	1×10^5	4,600	11.2	110	22.	121	33.	132	45.	143
		2,300	6.6	200	13.3	211	19.9	220	27.	220
	1×10^6	14,400	35.	65	70.	101	105.	136	140.	171
		7,200	17.8	79	36.	96	53.	114	71.	132
	1×10^3	144	2.1×10^3	$3,900 \times 10^3$	4.2×10^3	$3,900 \times 10^3$	6.3×10^3	$3,900 \times 10^3$	8.4×10^3	$3,900 \times 10^3$
		72	3.7	8,000	7.3	8,000	11.0	8,000	14.7	8,000
	1×10^4	460	1.66	1,000	3.3	1,000	5.0	1,000	6.6	1,000
		230	1.56	2,000	3.3	2,000	5.0	2,000	6.6	2,000
	2×10^4	650	2.0	710	4.0	710	6.0	710	8.1	720
		320	1.44	1,410	2.5	1,420	4.3	1,420	5.0	1,420
1×10^3	3×10^4	800	2.2	580	4.5	580	6.7	580	9.0	590
		400	1.60	1,150	3.2	1,150	4.8	1,160	6.4	1,160
	5×10^4	1,020	2.7	460	5.4	470	8.1	470	10.8	470
		510	1.72	890	3.4	900	5.2	900	7.0	900
	1×10^5	1,440	3.7	320	7.3	320	11.0	330	14.7	330
		720	2.1	630	4.2	640	6.3	640	8.4	640
	1×10^6	4,600	11.1	110	22.	122	33.	130	44.	144
		2,300	5.6	210	11.3	210	16.9	220	22.	220

TABLE III. TOTAL PROPULSION SYSTEM WEIGHTS FOR TEN POUNDS OF THRUST FOR TEN THOUSAND HOURS OF ENGINE OPERATION (Continued)

1. Ionic Nucleation (Continued)

q/m (coul/kg)	V (v)	I_s (sec)	M_p/P_e = 10 lbs/kwe: M_p (lbs)	M_{tot_w} (lbs)	M_p/P_e = 20 lbs/kwe: M_p (lbs)	M_{tot_w} (lbs)	M_p/P_e = 30 lbs/kwe: M_p (lbs)	M_{tot_w} (lbs)	M_p/P_e = 40 lbs/kwe: M_p (lbs)	M_{tot_w} (lbs)
	1×10^3	65	0.94×10^3	$7,900 \times 10^3$	1.89×10^3	$7,900 \times 10^3$	2.8×10^3	$7,900 \times 10^3$	3.8×10^3	$7,900 \times 10^3$
		32	1.64	16,000	3.3	16,000	4.9	16,000	6.6	16,000
	1×10^4	200	0.74	2,300	1.48	2,300	2.2	2,300	3.0	2,300
		102	0.74	4,500	1.48	4,500	2.2	4,500	3.0	4,500
2×10^2	2×10^4	300	0.85	1,600	1.60	1,600	2.6	1,600	3.2	1,600
		147	0.68	3,200	1.36	3,200	1.94	3,200	2.7	3,200
	3×10^4	360	0.99	1,280	1.98	1,280	3.0	1,280	4.0	1,280
		180	0.71	2,600	1.42	2,600	2.0	2,600	2.8	2,600
	1×10^5	640	1.64	700	3.3	710	4.9	710	6.5	710
		320	0.94	1,400	1.87	1,410	2.8	1,410	3.7	1,410
	1×10^6	2,000	5.0	230	9.9	230	14.9	240	19.9	240
		1,020	2.5	450	5.0	450	7.6	450	10.1	460

2. Neutral Nucleation

q/m (coul/kg)	V (v)	I_s (sec)	M_p/P_e = 10 lbs/kwe: M_p (lbs)	M_{tot_w} (lbs)	M_p/P_e = 20 lbs/kwe: M_p (lbs)	M_{tot_w} (lbs)	M_p/P_e = 30 lbs/kwe: M_p (lbs)	M_{tot_w} (lbs)	M_p/P_e = 40 lbs/kwe: M_p (lbs)	M_{tot_w} (lbs)
	1×10^3	1,440	$21. \times 10^3$	$4,200 \times 10^3$	$42. \times 10^3$	$4,200 \times 10^3$	$63. \times 10^3$	$4,200 \times 10^3$	$84. \times 10^3$	$4,300 \times 10^3$
		720	37.	8,500	74.	8,600	110.	8,600	147.	8,700
	1×10^4	4,600	16.6	1,140	33.	1,160	50.	1,170	66.	1,190
		2,300	16.6	2,300	33.	2,300	50.	2,300	66.	2,300
1×10^5	2×10^4	6,500	20.	820	40.	840	60.	860	81.	880
		3,200	14.4	1,600	29.	1,620	43.	1,630	58.	1,650
	3×10^4	8,000	22.	670	45.	690	67.	720	90.	740
		4,000	[illegible]	1,310	32.	1,320	48.	1,340	64.	1,360
	1×10^5	14,400	37.	390	74.	430	110.	460	147.	500
		7,200	21.	730	42.	750	63.	770	124.	830
	1×10^6	46,000	111.	220	220.	330	330.	440	440.	560
		23,000	56.	280	113.	340	169.	390	230.	450

TABLE III. TOTAL PROPULSION SYSTEM WEIGHTS FOR TEN POUNDS OF THRUST FOR TEN THOUSAND HOURS OF ENGINE OPERATION (Continued)

2. Neutral Nucleation (Continued)

			M_p/P_e = 10 lbs/kwe		M_p/P_e = 20 lbs/kwe		M_p/P_e = 30 lbs/kwe		M_p/P_e = 40 lbs/kwe	
q/m (coul/kg)	V (v)	I_s (sec)	M_p (lbs)	M_{tot_m} (lbs)	M_p (lbs)	M_{tot_m} (lbs)	M_p (lbs)	M_{tot_m} (lbs)	M_p (lbs)	M_{tot_m} (lbs)
	1×10^3	460	6.6×10^3	$8,200 \times 10^3$	13.3×10^3	$8,200 \times 10^3$	19.9×10^3	$8,200 \times 10^3$	$26. \times 10^3$	$8,300 \times 10^3$
		230	11.6	16,600	23.	16,600	35.	16,600	46.	16,700
	1×10^4	1,440	5.2	2,400	10.5	2,400	15.7	2,400	21.	2,400
		720	5.2	4,800	10.5	4,800	15.7	4,800	21.	4,900
1×10^4	2×10^4	2,100	5.9	1,630	11.8	1,640	17.7	1,640	24.	1,650
		1,030	4.7	3,200	9.5	3,200	14.2	3,300	18.9	3,300
	3×10^4	2,600	7.0	1,390	14.	1,390	21.	1,400	28.	1,410
		1,280	5.0	2,800	10.0	2,800	15.0	2,800	20.	2,800
	1×10^5	4,600	11.2	770	22.	780	33.	790	45.	800
		2,300	6.6	1,530	13.3	1,530	19.9	1,540	27.	1,550
	1×10^6	14,400	35.	280	70.	310	105.	340	140.	380
		7,200	17.8	500	36.	520	53.	530	71.	550
	1×10^3	144	2.1×10^3	$11,800 \times 10^3$	4.2×10^3	$11,800 \times 10^3$	6.3×10^3	$11,800 \times 10^3$	8.4×10^3	$11,800 \times 10^3$
		72	3.7	24,000	7.3	24,000	11.0	24,000	14.7	24,000
	1×10^4	460	1.66	3,600	3.3	3,600	5.0	3,600	6.6	3,600
		230	1.66	7,100	3.3	7,100	5.0	7,100	6.6	7,100
	2×10^4	650	2.0	2,500	4.0	2,500	6.0	2,500	8.1	2,500
		320	1.44	5,000	2.5	5,000	4.3	5,000	5.0	5,000
1×10^3	3×10^4	800	2.2	2,000	4.5	2,000	6.7	2,000	9.0	2,000
		400	1.60	4,100	3.2	4,100	4.8	4,100	6.4	4,100
	5×10^4	1,020	2.7	1,580	5.4	1,580	8.1	1,580	10.8	1,580
		510	1.72	3,200	3.4	3,200	5.2	3,200	7.0	3,200
	1×10^5	1,440	3.7	1,120	7.3	1,120	11.0	1,130	14.7	1,130
		720	2.1	2,200	4.2	2,200	6.3	2,200	8.4	2,200
	1×10^6	4,600	11.1	360	22.	380	33.	390	44.	400
		2,300	5.6	710	11.3	720	16.9	720	22.	730

TABLE III. TOTAL PROPULSION SYSTEM WEIGHTS FOR TEN POUNDS OF THRUST FOR TEN THOUSAND HOURS OF ENGINE OPERATION (Continued)

2. Neutral Nucleation (Continued)

			M_p/P_e = 10 lbs/kwe		M_p/P_e = 20 lbs/kwe		M_p/P_e = 30 lbs/kwe		M_p/P_e = 40 lbs/kwe	
q/m (coul/kg)	V (v)	I_s (sec)	M_p (lbs)	M_{tot} (lbs)	M_p (lbs)	M_{tot} (lbs)	M_p (lbs)	M_{tot} (lbs)	M_p (lbs)	M_{tot} (lbs)
	1×10^3	65 32	0.94×10^3 1.64	$15,400 \times 10^3$ 31,000	1.89×10^3 3.3	$15,400 \times 10^3$ 31,000	2.8×10^3 4.9	$15,400 \times 10^3$ 31,000	3.8×10^3 6.6	$15,400 \times 10^3$ 31,000
	1×10^4	200 102	0.74 0.74	4,700 9,400	1.48 1.48	4,700 9,400	2.2 2.2	4,700 9,400	3.0 3.0	4,700 9,400
2×10^2	2×10^4	300 147	0.85 0.68	3,300 6,600	1.60 1.36	3,300 6,600	2.6 1.94	3,300 6,600	3.2 2.7	3,300 6,600
	3×10^4	350 180	0.99 0.71	2,600 5,300	1.98 1.42	2,600 5,300	3.0 2.0	2,600 5,300	4.0 2.8	2,600 5,300
	1×10^5	640 320	1.64 0.94	1,460 2,900	3.3 1.87	1,460 2,900	4.9 2.8	1,460 2,900	6.5 3.7	1,460 2,900
	1×10^6	2,000 1,020	5.0 2.5	470 920	9.9 5.0	470 930	14.9 7.6	480 930	19.9 10.1	480 930

C. ELECTRICAL ATOMIZATION COLLOIDAL ION ENGINE

q/m (coul/kg)	V (v)	I_s (sec)	M_p (lbs)	M_{tot} (lbs)	M_p (lbs)	M_{tot} (lbs)	M_p (lbs)	M_{tot} (lbs)	M_p (lbs)	M_{tot} (lbs)
	1×10^3	1,440 720	4.4×10^3 2.2	$1,530 \times 10^3$ 3,700	8.8×10^3 4.4	$1,530 \times 10^3$ 3,700	13.3×10^3 6.6	$1,540 \times 10^3$ 3,700	17.7×10^3 8.9	$1,540 \times 10^3$ 3,700
	1×10^4	4,600 2,300	14.0 7.0	146 270	28. 14.0	160 280	42. 21.	174 280	56. 28.	188 290
1×10^5	2×10^4	6,500 3,200	21. 10.7	115 198	43. 21.	136 210	64. 32.	157 220	85. 43.	179 230
	3×10^4	8,000 4,000	24. 12.2	101 167	49. 24.	126 179	73. 37.	150 191	98. 49.	175 200
	1×10^5	14,400 7,200	44. 22.	86 106	89. 44.	130 128	133. 67.	174 150	177. 89.	220 172
	1×10^6	46,000 23,000	140. 70.	154 97	280. 140.	290 167	420. 210.	430 240	560. 280.	570 310

TABLE III. TOTAL PROPULSION SYSTEM WEIGHTS FOR TEN POUNDS OF THRUST FOR TEN THOUSAND HOURS OF ENGINE OPERATION (Continued)

C. ELECTRICAL ATOMIZATION COLLOIDAL ION ENGINE (Continued)

q/m (coul/kg)	V (v)	I_s (sec)	M_p/P_e = 10 lbs/kwe: M_p (lbs)	M_p/P_e = 10 lbs/kwe: M_{tot_m} (lbs)	M_p/P_e = 20 lbs/kwe: M_p (lbs)	M_p/P_e = 20 lbs/kwe: M_{tot_m} (lbs)	M_p/P_e = 30 lbs/kwe: M_p (lbs)	M_p/P_e = 30 lbs/kwe: M_{tot_m} (lbs)	M_p/P_e = 40 lbs/kwe: M_p (lbs)	M_p/P_e = 40 lbs/kwe: M_{tot_m} (lbs)
	1×10^3	460 230	1.40×10^3 0.70	$2,400 \times 10^3$ 5,400	2.8×10^3 1.40	$2,400 \times 10^3$ 5,400	4.2×10^3 2.1	$2,400 \times 10^3$ 5,400	$[illegible].6 \times 10^3$ 2.8	$2,400 \times 10^3$ 5,400
	1×10^4	1,440 720	4.4 2.2	420 830	8.9 4.4	420 830	13.3 6.7	420 830	17.7 8.9	430 830
1×10^4	2×10^4	2,100 1,030	6.3 3.0	300 590	12.5 5.9	300 590	18.8 8.9	310 590	25. 11.8	320 600
	3×10^4	2,600 1,280	7.6 3.8	260 520	15.2 7.6	270 520	23. 11.4	280 520	30. 15.2	29. 530
	1×10^5	4,600 2,300	14.0 7.0	144 270	28. 14.0	158 270	42. 21.	172 280	56. 28.	186 290
	1×10^6	14,400 7,200	44. 22.	86 106	89. 44.	131 128	133. 66.	175 150	177. 89.	220 173
	1×10^3	144 72	0.44×10^3 0.22	$5,200 \times 10^3$ 11,000	0.89×10^3 0.44	$5,200 \times 10^3$ 11,000	1.33×10^3 0.67	$5,200 \times 10^3$ 11,000	1.77×10^3 0.89	$5,200 \times 10^3$ 11,000
	1×10^4	460 230	1.40 0.70	1,300 2,600	2.8 1.40	1,300 2,600	4.2 2.1	1,300 2,600	5.6 2.8	1,300 2,600
	2×10^4	650 320	2.0 1.00	920 1,840	4.1 2.1	920 1,840	6.1 3.1	930 1,840	8.2 4.2	930 1,840
1×10^3	3×10^4	800 400	2.4 1.22	760 1,520	4.9 2.4	760 1,520	7.2 3.6	770 1,530	9.7 4.9	770 1,530
	5×10^4	1,020 510	3.1 1.56	590 1,180	6.2 3.1	590 1,180	9.3 4.7	590 1,180	12.5 6.2	600 1,180
	1×10^5	1,440 7[illegible]	4.4 2.2	410 820	8.9 4.4	420 820	13.3 6.6	420 830	17.7 8.8	430 830
	1×10^6	4,600 2,300	14.0 7.0	144 270	28. 14.0	158 270	42. 21.	172 280	56. 28.	186 290

TABLE III. TOTAL PROPULSION SYSTEM WEIGHTS FOR TEN POUNDS OF THRUST FOR TEN THOUSAND HOURS OF ENGINE OPERATION (Continued)

C. ELECTRICAL ATOMIZATION COLLOIDAL ION ENGINE (Continued)

			M_p/P_e = 10 lbs/kwe		M_p/P_e = 20 lbs/kwe		M_p/P_e = 30 lbs/kwe		M_p/P_e = 40 lbs/kwe	
q/m (coul/kg)	V (v)	I_s (sec)	M_p (lbs)	M_{tot_w} (lbs)	M_p (lbs)	M_{tot_w} (lbs)	M_p (lbs)	M_{tot_w} (lbs)	M_p (lbs)	M_{tot_w} (lbs)
	1×10^3	64	0.198×10^3	$10,300 \times 10^3$	0.40×10^3	$10,300 \times 10^3$	0.59×10^3	$10,300 \times 10^3$	0.79×10^3	$10,300 \times 10^3$
		32	0.099	21,000	0.198	21,000	0.30	21,000	0.40	21,000
	1×10^4	200	0.62	2,900	1.25	2,900	1.88	2,900	2.5	2,900
		102	0.31	5,800	0.63	5,800	0.94	5,800	1.25	5,800
2×10^2	2×10^4	300	0.86	1,940	1.72	1,940	2.6	1,940	3.4	1,940
		147	0.43	3,900	0.86	3,900	1.29	3,900	1.72	3,900
	3×10^4	360	1.08	1,720	2.2	1,720	3.2	1,720	4.3	1,720
		180	0.54	3,400	1.08	3,400	1.62	3,400	2.2	3,400
	1×10^5	640	1.98	920	4.0	920	5.9	920	7.9	920
		320	0.99	1,840	1.97	1,800	3.0	1,840	3.9	1,846
	1×10^6	2,000	6.3	300	12.5	300	18.8	310	25.	310
		1,020	3.1	580	6.3	580	9.4	590	12.5	590

TABLE IV. TOTAL PROPULSION SYSTEM WEIGHTS FOR TEN POUNDS OF THRUST FOR TWO THOUSAND HOURS OF ENGINE OPERATION

A. ATOMIC ION ENGINES

1. Strip Surface Contact Engine

q/m (coul/kg)	V* (v)	I_s (sec)	M_p/P_e = 10 lbs/kwe: M_p (lbs)	M_p/P_e = 10 lbs/kwe: $M_{tot_{10}}$ (lbs)	M_p/P_e = 20 lbs/kwe: M_p (lbs)	M_p/P_e = 20 lbs/kwe: $M_{tot_{10}}$ (lbs)	M_p/P_e = 30 lbs/kwe: M_p (lbs)	M_p/P_e = 30 lbs/kwe: $M_{tot_{10}}$ (lbs)	M_p/P_e = 40 lbs/kwe: M_p (lbs)	M_p/P_e = 40 lbs/kwe: $M_{tot_{10}}$ (lbs)
	1×10^3	4,000	17.3×10^3	550×10^3	35×10^3	570×10^3	52×10^3	580×10^3	69×10^3	600×10^3
		1,980	22.	1,350	43	1,370	65	1,390	86	1,410
	5×10^3	8,800	23.	36	46	59	70	82	93	106
		4,400	17.5	45	35	62	52	80	70	98
	1×10^4	12,500	30.	37	60	67	90	97	120	127
		6,300	19.1	34	38	53	57	72	76	91
7.54×10^5	2×10^4	17,900	41.	46	81	87	122	125	162	168
		9,000	23.	33	46	56	70	80	93	103
	3×10^4	22,000	49.	53	98	102	147	151	196	200
		10,900	26.	35	53	62	80	88	106	114
	5×10^4	28,000	62.	66	125	128	188	191	250	250
		14,000	33.	37	66	72	99	105	132	138
	1×10^5	40,000	87.	91	175	178	260	270	350	350
		19,800	45.	49	90	94	135	139	180	184
	1×10^6	125,000	270.	270	550	540	810	820	1,100	1,100
		63,000	137.	139	270	270	410	410	550	550

2. Bombardment Engine

q/m (coul/kg)	V* (v)	I_s (sec)	M_p/P_e = 10 lbs/kwe: M_p (lbs)	M_p/P_e = 10 lbs/kwe: $M_{tot_{10}}$ (lbs)	M_p/P_e = 20 lbs/kwe: M_p (lbs)	M_p/P_e = 20 lbs/kwe: $M_{tot_{10}}$ (lbs)	M_p/P_e = 30 lbs/kwe: M_p (lbs)	M_p/P_e = 30 lbs/kwe: $M_{tot_{10}}$ (lbs)	M_p/P_e = 40 lbs/kwe: M_p (lbs)	M_p/P_e = 40 lbs/kwe: $M_{tot_{10}}$ (lbs)
	1×10^3	3,200	12.8×10^3	$3,800 \times 10^3$	26×10^3	$3,900 \times 10^3$	39×10^3	$3,900 \times 10^3$	51×10^3	$3,900 \times 10^3$
		1,610	14.8	9,200	30	9,200	44	9,300	59	9,300
	5×10^3	7,300	18.8	50	38	69	56	88	75	106
		3,600	13.1	83	26	96	39	109	53	122
	1×10^4	10,400	25.	36	30	40	74	85	99	110
		5,200	15.1	38	30	53	45	68	60	83
5×10^5	2×10^4	14,600	34	40	68	74	102	108	136	142
		7,300	18.9	32	38	51	57	69	76	88
	3×10^4	18,000	40.	46	81	86	121	126	162	167
		9,000	22	32	44	54	65	75	87	97
	5×10^4	23,000	53.	56	105	109	158	162	210	210
		11,900	28.	35	55	63	83	90	110	118
	1×10^5	32,000	73.	77	147	150	220	220	290	300
		16,100	38.	43	75	81	113	119	151	156
	1×10^6	104,000	230.	230	460	460	700	700	930	930
		52,000	116.	119	230	230	350	350	460	470

*V is the accelerating voltage for the ion source. The upper set of results calculated for each value of V represents the parameters and characteristics of a straight accel engine. The second set of results corresponding to each value of V represents an accel-decel engine with a 4:1 accel-decel ratio.

TABLE IV. TOTAL PROPULSION SYSTEM WEIGHTS FOR TEN POUNDS OF THRUST FOR TWO THOUSAND HOURS OF ENGINE OPERATION (Continued)

3. Sastrugi Surface Contact Engine

q/m (coul/kg)	V (v)	I_s (sec)	M_p/P_e = 10 lbs/kwe: M_p (lbs)	M_p/P_e = 10 lbs/kwe: M_{tot_m} (lbs)	M_p/P_e = 20 lbs/kwe: M_p (lbs)	M_p/P_e = 20 lbs/kwe: M_{tot_m} (lbs)	M_p/P_e = 30 lbs/kwe: M_p (lbs)	M_p/P_e = 30 lbs/kwe: M_{tot_m} (lbs)	M_p/P_e = 40 lbs/kwe: M_p (lbs)	M_p/P_e = 40 lbs/kwe: M_{tot_m} (lbs)
	1×10^3	4,000 1,980	17.3×10^3 22.	350×10^3 810	35×10^3 43	370×10^3 830	52×10^3 65	390×10^3 850	69×10^3 86	400×10^3 870
	5×10^3	8,800 4,400	23. 17.5	35 42	46 35	58 60	70 52	82 77	93 70	105 95
	1×10^4	12,500 6,300	30. 19.1	37 34	60 38	67 53	90 57	97 72	120 76	127 91
7.54×10^5	2×10^4	17,900 9,000	41. 23.	46 33	81 46	86 56	122 70	127 80	162 93	167 103
	3×10^4	22,000 10,900	49. 26.	53 34	98 53	102 61	147 80	151 88	196 106	200 114
	5×10^4	28,000 14,000	62. 33.	66 38	125 66	128 71	188 99	191 104	250 132	250 137
	1×10^5	40,000 19,800	87. 45.	90 49	175 90	177 94	260 135	260 139	350 180	350 184
	1×10^6	125,000 63,000	270. 137.	270 139	550 270	550 280	820 410	820 410	1,100 550	1,100 550

B. CONDENSATION COLLOIDAL ION ENGINES

1. Ionic Nucleation

q/m (coul/kg)	V (v)	I_s (sec)	M_p/P_e = 10 lbs/kwe: M_p (lbs)	M_p/P_e = 10 lbs/kwe: M_{tot_m} (lbs)	M_p/P_e = 20 lbs/kwe: M_p (lbs)	M_p/P_e = 20 lbs/kwe: M_{tot_m} (lbs)	M_p/P_e = 30 lbs/kwe: M_p (lbs)	M_p/P_e = 30 lbs/kwe: M_{tot_m} (lbs)	M_p/P_e = 40 lbs/kwe: M_p (lbs)	M_p/P_e = 40 lbs/kwe: M_{tot_m} (lbs)
	1×10^3	1,440 720	$21. \times 10^3$ 37.	790×10^3 1,820	$42. \times 10^3$ 74.	810×10^3 1,860	$63. \times 10^3$ 110.	830×10^3 1,890	$84. \times 10^3$ 147.	850×10^3 1,930
	1×10^4	4,600 2,300	16.6 16.6	37 58	[illegible]	54 75	50. 50.	70 91	66. 66.	87 108
1×10^5	2×10^4	6,500 3,200	20. 14.4	34 43	40. 29.	54 57	60. 43.	75 72	81. 58.	95 86
	3×10^4	8,000 4,000	22. 16.0	34 39	45. 32.	56 55	67. 48.	79 71	90. 64.	101 87
	1×10^5	14,400 7,200	37. 21.	43 34	74. 42.	80 54	110. 63.	116 76	147. 84.	153 97
	1×10^6	46,000 23,000	111. 56.	113 61	220. 113.	220 117	330. 169.	340 170	440. 230.	450 230

TABLE IV. TOTAL PROPULSION SYSTEM WEIGHTS FOR TEN "OUNDS OF THRUST FOR TWO THOUSAND HOURS OF ENGINE OPERATION (Continued)

1. Ionic Nucleation (Continued)

			M_p/P_e = 10 lbs/kwe		M_p/P_e = 20 lbs/kwe		M_p/P_e = 30 lbs/kwe		M_p/P_e = 40 lbs/kwe	
q/m (coul/kg)	V (v)	I_s (sec)	M_p (lbs)	M_{tot_m} (lbs)	M_p (lbs)	M_{tot_m} (lbs)	M_p (lbs)	M_{tot_m} (lbs)	M_p (lbs)	M_{tot_m} (lbs)
	1×10^3	460	6.6×10^3	920×10^3	13.3×10^3	930×10^3	19.9×10^3	930×10^3	$26. \times 10^3$	940×10^3
		230	11.6	2,100	23.	2,100	35.	2,100	46.	2,100
	1×10^4	1,440	5.2	69	10.5	74	15.7	79	21.	85
		720	5.2	133	10.5	138	15.7	143	21.	149
1×10^4	2×10^4	2,100	5.9	49	11.8	55	17.7	60	24.	66
		1,030	4.7	90	9.5	95	14.2	100	18.9	105
	3×10^4	2,600	7.0	43	4.0	50	21.	57	28.	64
		1,280	5.0	77	10.0	82	15.0	87	20.	92
	1×10^5	4,600	11.2	31	22.	42	33.	53	45.	64
		2,300	6.6	46	13.3	53	19.9	59	27.	66
	1×10^6	14,400	35.	41	70.	76	105.	111	140.	146
		7,200	17.8	30	36.	53	53.	66	71.	84
	1×10^3	144	2.1×10^3	$1,340 \times 10^3$	4.2×10^3	$1,340 \times 10^3$	6.3×10^3	$1,350 \times 10^3$	8.4×10^3	$1,350 \times 10^3$
		72	3.7	2,900	7.3	2,900	11.0	2,900	14.7	2,900
	1×10^4	460	1.66	200	3.3	200	5.0	210	6.6	210
		230	1.66	400	3.3	400	5.0	410	6.6	410
	2×10^4	650	2.0	144	4.0	146	6.0	148	8.1	150
		320	1.44	280	2.5	285	4.3	290	5.0	290
1×10^3	3×10^4	800	2.2	118	4.5	120	6.7	122	9.0	124
		400	1.60	230	3.2	230	4.8	240	6.4	240
	5×10^4	1,020	2.7	95	5.4	98	8.1	100	10.8	103
		510	1.72	180	3.4	182	5.2	184	6.9	185
	1×10^5	1,440	3.7	67	7.3	71	11.0	74	14.7	78
		720	2.1	128	4.2	130	6.3	132	8.4	135
	1×10^6	4,600	11.1	31	22.	42	33.	53	44.	65
		2,300	5.6	46	11.3	51	16.9	57	22.	62

TABLE IV. TOTAL PROPULSION SYSTEM WEIGHTS FOR TEN POUNDS OF THRUST FOR TWO THOUSAND HOURS OF ENGINE OPERATION (Continued)

1. Ionic Nucleation (Continued)

q/m (coul/kg)	V (v)	I_s (sec)	M_p/P_e = 10 lbs/kwe: M_p (lbs)	M_p/P_e = 10 lbs/kwe: M_{tot_m} (lbs)	M_p/P_e = 20 lbs/kwe: M_p (lbs)	M_p/P_e = 20 lbs/kwe: M_{tot_m} (lbs)	M_p/P_e = 30 lbs/kwe: M_p (lbs)	M_p/P_e = 30 lbs/kwe: M_{tot_m} (lbs)	M_p/P_e = 40 lbs/kwe: M_p (lbs)	M_p/P_e = 40 lbs/kwe: M_{tot_m} (lbs)
	1×10^3	65	0.94×10^3	$2,100 \times 10^3$	1.89×10^3	$2,100 \times 10^3$	2.8×10^3	$2,100 \times 10^3$	3.8×10^3	$2,100 \times 10^3$
		32	1.64	4,500	3.3	4,500	4.9	4,500	6.6	4,500
	1×10^4	200	0.74	450	1.48	460	2.2	460	3.0	460
		102	0.74	910	1.48	910	2.2	910	3.0	910
2×10^2	2×10^4	300	0.85	320	1.60	320	2.6	322	3.2	320
		147	0.68	640	1.36	640	1.94	641	2.7	640
	3×10^4	360	0.99	260	1.98	260	3.0	260	4.0	260
		180	0.71	510	1.42	512	2.1	510	2.8	510
	1×10^5	640	1.64	142	3.3	144	4.9	146	6.5	147
		320	0.94	280	1.87	283	2.8	280	3.7	280
	1×10^6	2,000	5.0	50	9.9	55	14.9	60	19.9	65
		1,020	2.5	92	5.0	94	7.6	97	10.1	99

2. Neutral Nucleation

q/m (coul/kg)	V (v)	I_s (sec)	M_p/P_e = 10 lbs/kwe: M_p (lbs)	M_p/P_e = 10 lbs/kwe: M_{tot_m} (lbs)	M_p/P_e = 20 lbs/kwe: M_p (lbs)	M_p/P_e = 20 lbs/kwe: M_{tot_m} (lbs)	M_p/P_e = 30 lbs/kwe: M_p (lbs)	M_p/P_e = 30 lbs/kwe: M_{tot_m} (lbs)	M_p/P_e = 40 lbs/kwe: M_p (lbs)	M_p/P_e = 40 lbs/kwe: M_{tot_m} (lbs)
	1×10^3	1,440	$21. \times 10^3$	$1,300 \times 10^3$	$42. \times 10^3$	$1,400 \times 10^3$	$63. \times 10^3$	$1,400 \times 10^3$	$84. \times 10^3$	$1,400 \times 10^3$
		720	37.	2,900	74.	2,900	110.	2,900	147.	3,000
	1×10^4	4,600	16.6	240	33.	260	50.	270	66.	290
		2,300	16.6	470	33.	480	50.	500	66.	520
1×10^5	2×10^4	6,500	20.	179	40.	199	60.	220	81.	240
		3,200	14.4	330	29.	350	43.	360	58.	380
	3×10^4	8,000	22.	152	45.	175	67.	197	90.	220
		4,000	16.0	270	32.	290	48.	310	64	320
	1×10^5	14,400	37.	108	74.	144	110.	181	147.	218
		7,200	21.	163	42.	184	63.	200	84.	220
	1×10^6	46,000	111.	134	220.	240	330.	360	440.	470
		23,000	56.	102	113.	158	169.	210	230.	270

TABLE IV. TOTAL PROPULSION SYSTEM WEIGHTS FOR TEN POUNDS OF THRUST FOR TWO THOUSAND HOURS OF ENGINE OPERATION (Continued)

2. Neutral Nucleation (Continued)

q/m (coul/kg)	V (v)	I_s (sec)	M_p/P_e = 10 lbs/kwe: M_p (lbs)	M_p/P_e = 10 lbs/kwe: $M_{tot_{10}}$ (lbs)	M_p/P_e = 20 lbs/kwe: M_p (lbs)	M_p/P_e = 20 lbs/kwe: $M_{tot_{10}}$ (lbs)	M_p/P_e = 30 lbs/kwe: M_p (lbs)	M_p/P_e = 30 lbs/kwe: $M_{tot_{10}}$ (lbs)	M_p/P_e = 40 lbs/kwe: M_p (lbs)	M_p/P_e = 40 lbs/kwe: $M_{tot_{10}}$ (lbs)
	1×10^3	460	6.6×10^3	$2,100 \times 10^3$	13.3×10^3	$2,100 \times 10^3$	19.9×10^3	$2,200 \times 10^3$	$26. \times 10^3$	$2,200 \times 10^3$
		230	11.6	4,500	23.	4,500	35.	4,500	46.	4,500
	1×10^4	1,440	5.2	490	10.5	490	15.7	500	21.	500
		720	5.2	970	10.5	980	15.7	980	21.	990
1×10^4	2×10^4	2,100	5.9	330	11.8	330	17.7	340	24.	350
		1,030	4.7	660	9.5	660	14.2	660	18.9	670
	3×10^4	2,600	7.0	280	14.0	290	21.	300	28.	300
		1,280	5.0	550	10.0	560	15.0	560	20.	570
	1×10^5	4,600	11.2	163	22.	174	33.	186	45.	197
		2,300	6.6	310	13.3	320	19.9	320	27.	330
	1×10^6	14,400	35.	83	70.	118	105.	153	140.	188
		7,200	17.8	114	36.	132	53.	150	71.	168
	1×10^3	144	2.1×10^3	$2,900 \times 10^3$	4.2×10^3	$2,900 \times 10^3$	6.3×10^3	$2,900 \times 10^3$	8.4×10^3	$2,900 \times 10^3$
		72	3.7	5,900	7.3	5,900	11.0	5,900	14.7	5,900
	1×10^4	460	1.66	730	3.3	730	5.0	730	6.6	730
		230	1.66	1,440	3.3	1,440	5.0	1,440	6.6	1,440
	2×10^4	650	2.0	500	4.0	500	6.0	510	8.1	510
		320	1.44	1,000	2.5	1,000	4.3	1,010	5.0	1,010
1×10^3	3×10^4	800	2.2	410	4.5	410	6.7	420	9.0	420
		400	1.60	820	3.2	820	4.8	820	6.4	820
	5×10^4	1,020	2.7	320	5.4	320	8.1	320	10.8	320
		510	1.72	630	3.4	640	5.2	640	6.9	640
	1×10^5	1,440	3.7	230	7.3	230	11.0	230	14.7	230
		720	2.1	450	4.2	450	6.3	450	8.4	450
	1×10^6	4,600	11.1	82	22.	93	33.	104	44.	115
		2,300	5.6	147	11.3	153	16.9	158	22.	164

TABLE IV. TOTAL PROPULSION SYSTEM WEIGHTS FOR TEN POUNDS OF THRUST FOR TWO THOUSAND HOURS OF ENGINE OPERATION (Continued)

2. Neutral Nucleation (Continued)

q/m (coul/kg)	V (v)	I_s (sec)	M_p/P_e = 10 lbs/kwe: M_p (lbs)	M_p/P_e = 10 lbs/kwe: M_{tot_p} (lbs)	M_p/P_e = 20 lbs/kwe: M_p (lbs)	M_p/P_e = 20 lbs/kwe: M_{tot_p} (lbs)	M_p/P_e = 30 lbs/kwe: M_p (lbs)	M_p/P_e = 30 lbs/kwe: M_{tot_p} (lbs)	M_p/P_e = 40 lbs/kwe: M_p (lbs)	M_p/P_e = 40 lbs/kwe: M_{tot_p} (lbs)
	1×10^3	64	0.94×10^3	$3,600 \times 10^3$	1.89×10^3	$3,600 \times 10^3$	2.8×10^3	$3,600 \times 10^3$	3.8×10^3	$3,600 \times 10^3$
		32	1.64	7,300	3.3	7,300	4.9	7,300	6.6	7,300
	1×10^4	200	0.74	940	1.48	940	2.2	940	3.0	940
		102	0.74	1,880	1.48	1,880	2.2	1,880	3.0	1,880
2×10^2	2×10^4	300	0.85	660	1.60	660	2.6	660	3.2	660
		147	0.68	1,320	1.36	1,320	1.94	1,320	2.7	1,320
	3×10^4	360	0.99	530	1.98	530	3.0	530	4.0	530
		180	0.71	1,060	1.42	1,060	2.1	1,060	2.8	1,060
	1×10^5	640	1.64	290	3.3	290	4.9	300	6.5	300
		320	0.94	580	1.87	580	2.8	580	3.7	580
	1×10^6	2,000	5.0	98	9.9	102	14.9	107	19.9	112
		1,020	2.5	187	5.0	190	7.6	192	10.1	195

C. ELECTRICAL ATOMIZATION COLLOIDAL ION ENGINES

q/m (coul/kg)	V (v)	I_s (sec)	M_p/P_e = 10 lbs/kwe: M_p (lbs)	M_p/P_e = 10 lbs/kwe: M_{tot_p} (lbs)	M_p/P_e = 20 lbs/kwe: M_p (lbs)	M_p/P_e = 20 lbs/kwe: M_{tot_p} (lbs)	M_p/P_e = 30 lbs/kwe: M_p (lbs)	M_p/P_e = 30 lbs/kwe: M_{tot_p} (lbs)	M_p/P_e = 40 lbs/kwe: M_p (lbs)	M_p/P_e = 40 lbs/kwe: M_{tot_p} (lbs)
	1×10^3	1,440	4.4×10^3	$1,200 \times 10^3$	8.8×10^3	$1,210 \times 10^3$	13.3×10^3	$1,210 \times 10^3$	17.7×10^3	$1,220 \times 10^3$
		720	2.2	3,000	4.4	3,000	6.6	3,000	8.9	3,000
	1×10^4	4,600	14.0	43	28.	57	42.	71	56.	85
		2,300	7.0	66	14.0	73	21.	80	28.	87
1×10^4	2×10^4	6,500	21	41	43.	62	64.	84	85.	105
		3,200	10.7	51	21.	62	32.	72	43.	83
	3×10^4	8,000	24.	41	49	65	73.	90	98.	115
		4,000	12.2	45	24.	58	37.	70	49.	82
	1×10^5	14,400	44	53	89.	97	133.	142	177.	186
		7,200	22.	40	44.	62	67.	84	89.	106
	1×10^6	46,000	140.	144	280.	280	420.	420	560.	560
		23,000	70.	77	140.	148	210.	220	280.	290

TABLE IV. TOTAL PROPULSION SYSTEM WEIGHTS FOR TEN POUNDS OF THRUST FOR TWO THOUSAND HOURS OF ENGINE OPERATION (Continued)

C. ELECTRICAL ATOMIZATION COLLOIDAL ION ENGINES (Continued)

q/m (coul/kg)	V (v)	I_s (sec)	M_p/P_e = 10 lbs/kwe: M_p (lbs)	M_p/P_e = 10 lbs/kwe: M_{tot_w} (lbs)	M_p/P_e = 20 lbs/kwe: M_p (lbs)	M_p/P_e = 20 lbs/kwe: M_{tot_w} (lbs)	M_p/P_e = 30 lbs/kwe: M_p (lbs)	M_p/P_e = 30 lbs/kwe: M_{tot_w} (lbs)	M_p/P_e = 40 lbs/kwe: M_p (lbs)	M_p/P_e = 40 lbs/kwe: M_{tot_w} (lbs)
1×10	1×10^3	460	1.40×10^3	$1,410 \times 10^3$	2.8×10^3	$1,410 \times 10^3$	4.2×10^3	$1,410 \times 10^3$	5.6×10^3	$1,410 \times 10^3$
		230	0.70	3,400	1.40	3,400	2.1	3,400	2.8	3,400
	1×10^4	1,440	4.4	89	8.9	93	13.3	98	17.7	102
		720	2.2	173	4.4	175	6.7	177	8.9	179
	2×10^4	2,100	6.3	66	12.5	72	18.8	78	25.	84
		1,030	3.0	122	5.9	125	8.9	128	11.8	131
	3×10^4	2,600	7.6	60	15.2	67	23.	75	30.	82
		1,280	3.8	109	7.6	112	11.4	116	15.2	120
	1×10^5	4,600	14.0	40	28.	54	42.	68	56.	82
		2,300	7.0	60	14.0	67	21.	74	28.	81
	1×10^6	14,400	44.	54	89.	98	133.	142	177.	186
		7,200	22.	41	44.	63	66.	85	89.	107
1×10	1×10^3	144	0.44×10^3	$1,970 \times 10^3$	0.89×10^3	$2,000 \times 10^3$	1.33×10^3	$1,970 \times 10^3$	1.77×10^3	$1,970 \times 10^3$
		72	0.22	4,500	0.44	4,500	0.67	4,500	0.89	4,500
	1×10^4	460	1.40	270	2.8	270	4.2	270	5.6	280
		230	0.70	520	1.40	520	2.1	520	2.8	520
	2×10^4	650	2.0	187	4.1	189	6.1	191	8.2	193
		320	1.00	370	2.1	370	3.1	370	4.2	380
	3×10^4	800	2.4	155	4.9	158	7.3	160	9.7	163
		400	1.22	310	2.4	310	3.6	310	4.9	310
	5×10^4	1,020	3.1	121	6.2	124	9.3	127	12.5	130
		510	1.56	240	3.1	240	4.7	240	6.2	240
	1×10^5	1,440	4.4	87	8.9	91	13.3	96	17.7	100
		720	2.2	168	4.4	170	6.6	172	8.8	174
	1×10^6	4,600	14.0	41	28.	55	42.	69	56.	83
		2,300	7.0	61	14.0	68	21.	75	28	82

TABLE IV. TOTAL PROPULSION SYSTEM WEIGHTS FOR TEN POUNDS OF THRUST FOR TWO THOUSAND HOURS OF ENGINE OPERATION (Continued)

C. ELECTRICAL ATOMIZATION COLLOIDAL ION ENGINES (Continued)

			M_p/P_e = 10 lbs/kwe		M_p/P_e = 20 lbs/kwe		M_p/P_e = 30 lbs/kwe		M_p/P_e = 40 lbs/kwe	
q/m (coul/kg)	V (v)	I_s (sec)	M_p (lbs)	M_{tot} (lbs)	M_p (lbs)	M_{tot} (lbs)	M_p (lbs)	M_{tot} (lbs)	M_p (lbs)	M_{tot} (lbs)
	1×10^3	64	0.198×10^3	$3,000 \times 10^3$	0.40×10^3	$3,000 \times 10^3$	0.59×10^3	$3,000 \times 10^3$	0.79×10^3	$3,000 \times 10^3$
		32	0.099	6,500	0.198	6,500	0.30	6,500	0.40	6,500
	1×10^4	200	0.62	580	1.25	580	1.88	580	2.5	580
		102	0.31	1,160	0.63	1,160	0.94	1,160	1.25	1,160
2×10^2	2×10^4	300	0.86	390	1.72	390	2.6	390	3.4	390
		150	0.43	780	0.86	780	1.29	780	1.72	780
	3×10^4	360	1.08	350	2.2	350	3.2	350	4.3	350
		180	0.54	690	1.08	690	1.62	690	2.2	690
	1×10^5	640	1.98	186	4.0	187	5.9	190	7.9	191
		320	0.99	370	1.97	370	3.0	370	3.9	370
	1×10^6	2,000	6.3	65	12.5	71	18.8	78	25.	94
		1,020	3.1	121	6.3	124	9.4	127	12.5	130

TABLE V. PAYLOAD CAPABILITIES FOR SPECIFIC MISSIONS

Engine	Mission A M_{pay}/M_1	Mission A t (hrs)	Mission B M_{pay}/M_1	Mission B t (hrs)	Mission C M_{pay}/M_1	Mission C t (hrs)	Mission D M_{pay}/M_1	Mission D t (hrs)	Mission E M_{pay}/M_1	Mission E t (hrs)
A. ATOMIC ION ENGINES										
1. Cs Contact (acc-dec)	NM*	1.87×10^3	NM	7.0×10^2	0.27	1.89×10^4	0.006	8.5×10^3	0.45	1.33×10^4
2. Hg Bombardment (acc-dec)	NM	1.79×10^3	NM	7.7×10^2	0.29	1.78×10^4	0.002	8.1×10^3	0.46	1.25×10^4
3. Cs Sastrugi (acc-dec)	0.21	1.87×10^3	NM	7.0×10^2	0.27	1.89×10^4	0.026	8.5×10^3	0.45	1.33×10^4
B. CONDENSATION COLLOIDAL ION ENGINES										
1. Ionic Nucleation										
$q/m = 10^5$	0.57 (0.070)**	1.72×10^3	NM	6.4×10^2	0.25	1.70×10^4	0.056	7.9×10^3	0.43	1.19×10^4
$q/m = 10^4$	0.66 (0.38)	1.72×10^3	0.50 (0.128)	6.4×10^2	0.27	1.70×10^4	0.120	7.9×10^3	0.43	1.19×10^4
$q/m = 10^3$	0.66 (0.40)	1.72×10^3	0.54 (0.27)	6.4×10^2	0.27	1.70×10^4	0.120	7.9×10^3	0.42	1.19×10^4
$q/m = 2 \times 10^2$	0.66 (0.40)	1.72×10^3	0.54 (0.27)	6.4×10^2	0.24	1.70×10^4	0.031	7.9×10^3	0.35	1.19×10^4
2. Neutral Nucleation										
$q/m = 10^5$	NM	1.51×10^2	NM	0.55×10^2	NM	1.51×10^3	NM	6.8×10^2	NM	1.06×10^3
$q/m = 10^4$	NM	2.3×10^2	NM	0.86×10^2	NM	2.3×10^3	NM	1.02×10^2	NM	1.60×10^3
$q/m = 10^3$	0.36	4.8×10^2	0.20	1.79×10^2	NM	4.9×10^3	NM	2.2×10^3	NM	3.4×10^3
$q/m = 2 \times 10^2$	0.53	8.3×10^2	0.39	3.1×10^2	0.016	8.5×10^3	NM	3.7×10^3	NM	5.8×10^3

* No mission.

** Values in parentheses indicate payload ratios with a power supply specific weight of 40 lb/kwe instead of 10 lb/kwe as assumed for the other calculated payload ratios. No entry signifies no payload with the higher power supply specific weight.

TABLE V. PAYLOAD CAPABILITIES FOR SPECIFIC MISSIONS (Continued)

Engine	Mission A M_{pay}/M_i	Mission A t (hrs)	Mission B M_{pay}/M_i	Mission B t (hrs)	Mission C M_{pay}/M_i	Mission C t (hrs)	Mission D M_{pay}/M_i	Mission D t (hrs)	Mission E M_{pay}/M_i	Mission E t (hrs)
C. ELECTRICAL ATOMIZATION COLLOIDAL ION ENGINES										
$q/m = 10^5$	0.54 (0.14)	1.42×10^3	NM	5.3×10^2	0.144	1.42×10^4	NM	6.4×10^3	0.25	9.9×10^3
$q/m = 10^4$	0.58 (0.18)	1.42×10^3	0.41 (0.002)	5.3×10	0.145	1.42×10^4	NM	6.4×10^3	0.25	9.9×10^3
$q/m = 10^3$	0.58 (0.18)	1.42×10^3	0.44 (0.034)	5.3×10^2	0.139	1.42×10^4	NM	6.4×10^3	0.24	9.9×10^3
$q/m = 2 \times 10^2$	0.57 (0.17)	1.42×10^3	0.43 (0.028)	5.3×10^2	0.125	1.42×10^4	NM	6.4×10^3	0.16	9.9×10^3

Mission A Round trip from Earth orbit to Moon orbit. $\Delta v = 7.62 \times 10^3$ m/sec, $I_s = 3200$ sec, $G = 10^{-4}$ (Reference 3)

Mission B Round trip from Earth orbit to Moon orbit. $\Delta v = 6.1 \times 10^3$ m/sec, $I_s = 1600$ sec, $G = 2 \times 10^{-4}$ (Reference 3)

Mission C Round trip from Earth orbit to Mars orbit. $\Delta v = 5.68 \times 10^4$ m/sec, $I_s = 8100$ sec, $G = 6 \times 10^{-5}$ (Reference 3)

Mission D Round trip from Earth orbit to Mars orbit. $\Delta v = 4.91 \times 10^4$ m/sec, $I_s = 4800$ sec, $G = 10^{-4}$ (Reference 3)

Mission E One way from Earth orbit to Jupiter orbit. $\Delta v = 4 \times 10^4$ m/sec, $I_s = 12,000$ sec, $G = 7.15 \times 10^{-5}$ (Reference 27)

BLANK PAGE

REFERENCES

1. Pinkel, B., "Electrical Propulsion for Space Missions: Planning Considerations", AIAA Paper No. 64-715, September 1-4, 1964

2. Mickelsen, W. R., "Effect of Thrustor Characteristics on Electric Spacecraft Missions", AIAA Paper No. 64-676, August 31 - September 2, 1964

3. Cox, A. L., "Heavy Ions for Electrical Propulsion", Proceedings of the IRE National Aeronautical Electronics Conference, 483-490, May 2-4, 1960

4. Cox, A. L., "Molecular and Colloidal Ions for Electrical Propulsion", ASME Paper No. 61-AV-62, March 12-16, 1961

5. Cox, A. L., "Toward Colloid Propulsion", Astronautics, 1, No. 6, 56-59, 1962

6. Cox, A. L., "Condensation Colloidal Ion Source", ASD-TDR-63-825, June 12, 1964

7. Cox, A. L., "The Principle of Operation and Applications of a Skimmer Nozzle", Brown Engineering Company, Inc. Technical Note R-90, March 1964

8. Hunter, R. E., "Theoretical Consideration of Nonuniformly Charged Expellant Beams", ARL TN 60-138, October 1960

9. Cox, A. L. and S. E. Graybill, "A Study of the Particle Distribution Produced by a Colloidal Ion Source", Ion Physics Corporation Report 312-TR-121, December 1963

10. Norgren, C. T., "Onboard Colloidal Particle Generator for Electrostatic Engines", ARS Paper No. 2380-62, March 14-16, 1962

11. Goldin, D. S. and C. T. Norgren, "Thrust Measurements of Colloidal Particles as an Indication of Particle Size and Thrustor Operation", AIAA Paper No. 63050-63, March 11-13, 1963

12. Norgren, C. T. and D. S. Goldin, "Experimental Analysis of the Exhaust Beam from a Colloid Thrustor", AIAA Paper No. 64-674, August 31-September 2, 1964

13. Cohen, E., "Research on Charged Colloid Generation", APL TDR 64-75, June 1964

14. Peterson, C. R., "Feeding, Deagglomerating, and Charging Solid Particles for Colloid Propulsion", Thesis, Massachusetts Institute of Technology, 1963

15. Singer, S., N. G. Kim, and M. Farber, "An Experimental Study of Colloidal Propulsion Using Sub-Micron Solid Particles", AIAA Paper No. 63052-63, March 11-13, 1963

16. Strayer, R. W., C. J. Bennette, E. C. Cooper, and L. W. Swanson, "Investigation of the Pre-Breakdown Gap Currents Leading to Electrical Breakdown Between Clean and Cesium-Coated Tungsten Electrodes", AIAA Paper No. 64-694, August 31-September 2, 1964

17. Cranberg, L., Journal of Applied Physics, 23, 518, 1952

18. Olendzkaya, N. F., "Vacuum Breakdown with Transfer of Conducting Particles between Electrodes", paper presented at the Tenth Conference on Cathode Electronics, Tashkent, November 1961

19. Teem, J. M. and G. C. Szego, "Electric Propulsion and Power", Astronautics and Aerospace Engineering, 1, No. 10, 98-103, November 1963

20. Brewer, G. R., R. L. Zimmerman, D. Berman, and H. J. King, "Design Criteria and Performance of a Cesium Contact Ion Engine", AIAA Paper No. 64-710, August 31-September 2, 1964

21. Moeckel, W. E., "Electric Propulsion", Science, 142, 172-178, 1963

22. Reader, P. D., "Experimental Performance of a 50 Centimeter Diameter Electron-Bombardment Ion Rocket", AIAA Paper No. 64-689, August 31-September 2, 1964

23. Eilenberg, S. L., W. Seitz, and E. Caplinger, "Ion Optics of Sastrugi Ion Engines", AIAA Paper No. 64-695, August 31-September 2, 1964

24. Brown, H. and H. E. Nicoll, Jr., "Electrical Propulsion Capabilities for Lunar Exploration", AIAA Journal, 1, 314-319, 1963

25. Cox, A. L. and R. W. Blanton, Jr., "Parametric Study of Rankine-Cycle Space Nuclear Power Systems", Brown Engineering Company, Inc. Technical Note R-113, August 1964

26. Stuhlinger, E., "Ion Propulsion for Space Flight", McGraw-Hill Book Company, New York, 1964

27. Beale, R. J., E. W. Speiser, and J. R. Womack, "The Electric Space Cruiser for High-Energy Missions", JPL Technical Report No. 32-404, June 8, 1963

BLANK PAGE

DOCUMENT CONTROL DATA - R&D

(Security classification of title, body of abstract and indexing annotation must be entered when the overall report is classified)

1 ORIGINATING ACTIVITY (Corporate author) Research Laboratories Brown Engineering Company, Inc.	2a REPORT SECURITY CLASSIFICATION Unclassified 2b GROUP N/A

3 REPORT TITLE

"A Comparative Analysis of the Performance Capabilities of Various Types of Electrostatic Propulsion Engines"

4 DESCRIPTIVE NOTES (Type of report and inclusive dates)

Technical Note, March, 1965

5 AUTHOR(S) (Last name, first name, initial)

Cox, Dr. A. Lucile

6. REPORT DATE	7a. TOTAL NO. OF PAGES	7b. NO. OF REFS
March, 1965	116	27

8a CONTRACT OR GRANT NO. Company-sponsored b. PROJECT NO. N/A c d	9a. ORIGINATOR'S REPORT NUMBER(S) TN R-136 9b. OTHER REPORT NO(S) (Any other numbers that may be assigned this report) None

10 AVAILABILITY/LIMITATION NOTICES

None

11. SUPPLEMENTARY NOTES	12. SPONSORING MILITARY ACTIVITY
None	None

13 ABSTRACT

The operating characteristics of three types of atomic ion engines and three types of colloidal ion engines are evaluated. The major theoretical factors which will limit payload capacity are brought out for each type of engine. Total propulsion system masses for the production of ten pounds of thrust for 2,000 hours and for 10,000 hours of engine operation are compared. Examination of the payload capacities of the various engines for several lunar and planetary missions shows that the colloidal ion engines have a superior payload capacity for lunar missions and may be competitive with atomic ion engines for planetary missions. The specific mass of the power supply system is shown to be a much more dominant factor in determining the payload capacities of the atomic ion engines than for the colloidal ion engines.

14. KEY WORDS

colloidal ion engine
atomic ion engine
electrostatic propulsion
space payload capacity
electric engine characteristics
space mission vehicles